

**SYNTHESIS OF ARYLPIPERAZINYL ANALOGUES OF
CHELATE GD(III)-DTPA FOR MRI APPLICATIONS**

BY

Abdullah Omar Obaid Basalem

A Thesis Presented to the
DEANSHIP OF GRADUATE STUDIES

KING FAHD UNIVERSITY OF PETROLEUM & MINERALS

DHAHRAN, SAUDI ARABIA

In Partial Fulfillment of the
Requirements for the Degree of

MASTER OF SCIENCE

In

CHEMISTRY

April 2015

KING FAHD UNIVERSITY OF PETROLEUM & MINERALS

DHAHRAN- 31261, SAUDI ARABIA

DEANSHIP OF GRADUATE STUDIES

This thesis, written by **Abdullah Omar Obaid Basalem** under the direction his thesis advisor and approved by his thesis committee, has been presented and accepted by the Dean of Graduate Studies, in partial fulfillment of the requirements for the degree of **MASTER OF SCIENCE IN CHEMISTRY**.



Dr. Abdulaziz Al-saadi
Department Chairman



Dr. Salam A. Zummo
Dean of Graduate Studies

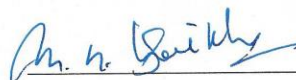


12/5/15

Date



Dr. Nisar Ullah
(Advisor)



Dr. M. Nasiruzzaman Shaikh
(Member)



Dr. Mohammed Wazeer
(Member)

© Abdullah Omar Obaid Ba-salem
2015

Dedicated to my parents, wife, children and
siblings.

ACKNOWLEDGMENTS

First, all praise and thanks be to Allah the almighty and magnificent for providing me with a great opportunity and patience to accomplish this research endeavor. I could have never done it without the help and blessing of Allah (SWT).

My parents, wife and children, deserve my deepest appreciations for the support I had enjoyed in the course of this research work. You have been always there for me when I was of need and advice. You are the best family I could imagine.

My special thanks and gratitude goes to my thesis advisor Dr. Nisar Ullah for his great effort, encouragement and patience with me. He has been my teacher and mentor for the past four years. His words and advice helped me greatly both personally and professionally.

I would like to thank my thesis committee members Dr. Nasiruzzaman Sk. and Dr. Mohammed Wazer for their valuable contributions.

My appreciation and thanks also go to Dr. Khalid Alhooshani for his advice and support throughout my KFUPM studies.

Thanks to the chemistry department, Chairman and faculty members for their support and guidance when needed.

I would like to thank my friends and brothers Mr. Abdullah Alahmadi, Mr. Noktan Alyami and Mr. Ayman Almajed for their support and advice.

Finally, my special thanks go to my friends for their encouragement and support. Thanks to Rayan, Abdurrahman and Mohsen.

Table of Contents

ACKNOWLEDGMENTS	v
LIST OF FIGURES	ix
LIST OF TABLES	x
LIST OF ABBREVIATIONS	xi
ABSTRACT.....	xiv
ملخص الرسالة.....	xiii
CHAPTER 1 INTRODUCTION AND LITERATURE REVIEW	1
1.1.Introduction.....	1
1.2.MRI Working Mechanism.....	3
1.3.Relaxation Mechanism.....	5
1.4.Gadolinium based MR contrast agents.....	6
CHAPTER 2 OBJECTIVES AND WORK PLAN	8
2.1. Present State of the Problem.....	9
CHAPTER 3 RESULTS AND DISCUSSION.....	10
3.1.Synthesis of the Chelates.....	10
3.1.1.Synthesis of Complex 1.....	11
3.1.2.Synthesis of Complexes 2 and 3.....	13
3.1.3.Synthesis of Complexes 4 and 5.....	15
3.2.XPS Analysis.....	17
3.2.1.XPS Analysis for Complex 2.....	17
3.2.2.XPS Analysis for Complex 3.....	18
3.2.3.XPS Analysis for Complex 4.....	20
3.2.4.XPS Analysis for Complex 5.....	21
3.3.T ₁ Measurements in MRI.....	22
3.4.Cytotoxicity Studies.....	23
CHAPTER 4 EXPERIMENTAL PART	24

4.1. Materials Used.....	24
4.2. Product Identification.....	24
4.3. Synthesis of Gd-Complexes.....	25
4.3.1. Synthesis of phenyl(piperazin-1-yl)methanone (8).....	25
4.3.2. Synthesis of 2-(bis(2-(2,6-dioxomorpholino)ethyl)amino)acetic acid (10).....	26
4.3.3. Synthesis of 4-bromo-2-nitrobenzonitrile (15).....	27
4.3.4. Synthesis of 4-(4-benzoylpiperazin-1-yl)-2-nitrobenzonitrile (16).....	28
4.3.5. Synthesis of 2-Amino-4-(4-benzoylpiperazin-1-yl)benzonitrile (17).....	29
4.3.6. Synthesis of 2,2'-(2,2'-(carboxymethylazanediy)bis(ethane-2,1-diy)bis((2-(5-(4benzoylpiperazin-1-yl)-2-cyanophenylamino)-2-oxoethyl)azanediy))diacetic acid (18).....	30
4.3.7. Synthesis of 4-fluoro-2-methoxy-1-nitrobenzene (20).....	31
4.3.8. Synthesis of 4-fluoro-2-(methoxymethoxy)-1-nitrobenzene (21).....	31
4.3.9. Synthesis of (4-(3-methoxy-4-nitrophenyl)piperazin-1-yl)(phenyl)methanone (22)....	32
4.3.10. Synthesis of (4-(3-(methoxymethoxy)-4-nitrophenyl) piperazin-1-yl)(phenyl)methanone (23).....	33
4.3.11. Synthesis of (4-(4-Amino-3-methoxyphenyl)piperazin-1-yl)(phenyl)methanone (24)	34
4.3.12. Synthesis of (4-(4-amino-3-(methoxymethoxy)phenyl) piperazin-1-yl)(phenyl)methanone (25).....	35
4.3.13. Synthesis of 2,2'-(2,2'-(carboxymethylazanediy) bis(ethane-2,1-diy)bis((2-(4-(4-benzoylpiperazin-1-yl)-2-methoxyphenylamino)-2-oxoethyl)azanediy))-diacetic acid (26) .	36
4.3.14. Synthesis of 2,2'-(2,2'-(carboxymethylazanediy) bis(ethane-2,1-diy)bis((2-(4-(4-benzoylpiperazin-1-yl)-2-(methoxymethoxy)phenylamino)-2-oxoethyl)azanediy)) diacetic acid (27).....	37
4.3.15. Synthesis of complex (2).....	38
4.3.16. Synthesis of complex (3).....	39
4.3.17. Synthesis of 1-(3-Methoxy-4-nitrophenyl)piperazine (28).....	39
4.3.18. Synthesis of 1-(3-(Methoxymethoxy)-4-nitrophenyl) piperazine (29).....	40
4.3.19. Synthesis of 3-(4-(3-Methoxy-4-nitrophenyl)piperazin-1-yl)propanenitrile (30).....	41
4.3.20. Synthesis of 3-(4-(3-(Methoxymethoxy)-4-nitrophenyl) piperazin-1-yl)propanenitrile (31).....	42

4.3.21. Synthesis of 3-(4-(4-Amino-3-methoxyphenyl)piperazin-1-yl)propanenitrile (32)....	43
4.3.22. Synthesis of 3-(4-(4-amino-3-(methoxymethoxy)phenyl) piperazin-1-yl)propanenitrile (33).....	44
4.3.23. Synthesis of 2,2'-(2,2'-(carboxymethylazanediyl)bis (ethane-2,1-diyl)bis((2-(4-(4-(2-cyanoethyl)piperazin-1-yl)-2-methoxyphenylamino)-2-oxoethyl)-azanediyl))diacetic acid (34)	45
4.3.24. Synthesis of 2,2'-(2,2'-(carboxymethylazanediyl)bis (ethane-2,1-diyl)bis((2-(4-(4-(2-cyanoethyl)piperazin-1-yl)-2-(methoxymethoxy)phenylamino)-2-oxoethyl)azanediyl))diacetic acid (35)	46
4.3.25.Synthesis of complex (4).....	47
4.3.26.Synthesis of complex (5).....	48
4.4.X-ray Photoelectron Spectroscopy.....	48
4.5.Cytotoxicity Study Assay.....	49
CHAPTER 5 CONCLUSION AND FUTURE WORK	50
References.....	51
Appendices.....	54
Vitae.....	81

LIST OF FIGURES

Figure 1: Effect of MR contrast agent	2
Figure 2: Protons without (a) and (b) with external magnetic field.....	4
Figure 3: Representation of net magnetization vector (M_0).....	5
Figure 4: Commercially available Gd ³⁺ chelate MR agents.....	7
Figure 5: Structure of the Gd-complexes (1-5).....	8
Figure 6: The Gd (III) attempted to synthesize.....	11
Figure 7: XPS survey scan for complex 2.	17
Figure 8: XPS spectrum of chelate 2.	17
Figure 9: XPS survey scan for chelates 3.	18
Figure 10: XPS spectrum of chelate 3.	19
Figure 11: XPS survey scan for chelates 4.	20
Figure 12: XPS spectrum of chelate 4.	20
Figure 13: XPS survey scan for chelates 5.	21
Figure 14: XPS spectrum of chelate 5.	22

LIST OF TABLES

Table 1: Water content in different human tissues	3
Table 2: T1 values of some tumorous and normal human tissues	6
Table 3:T1 of chelates (2-5).....	23
Table 4: cytotoxicity data of chelate (2-5).....	23

LIST OF ABBREVIATIONS

δ	Chemical shift in ppm
bs	Broad singlet
BOC	terf-Butyloxycarbonyl
Bz	benzyloxycarbonyl
CA	Contrast Agent
d	Doublet
DCM	Dichloromethane
dd	Doublet of doublets
DMF	N,N-Dimethylformamide
DMSO	Dimethylsulfoxide
DTPA	Diethylenetriaminepentaacetic acid
FABMS	Fast atomic bombardment mass spectrometry
HPLC	High Performance Liquid Chromatography
Hz	Hertz
m	Multiplet
Me	Methyl
mM	Millimolar
MRI	Magnetic resonance imaging
MS	Mass spectrometry
MTT	3-(4, 5-dimethylthiazol-2-yl)-2, 5-diphenyltetrazolium bromide
NMR	Nuclear magnetic resonance
ppm	Parts per million
R1	Longitudinal relaxations rate
r1	Longitudinal relaxivity

s	Singlet
t	Triplet
T1	Longitudinal relaxation time
T2	Transversal relaxation time
Tert-butyl	1,1-dimethylethyl
TFA	Trifluoroacetic acid
THF	Tetrahydrofuranone
TLC	Thin layer chromatography
q	Quartet
XPS	X-ray photoelectron spectroscopy

ABSTRACT

Full Name: Abdullah Omar Obaid Basalem
Thesis Title: Synthesis of Arylpiperazinyl Analogous of Chelate Gd(III)-DTPA for MRI Applications
Major Field: Master of Chemistry
Date of Degree: April, 2015

Four new DTPA-bis(amide) based ligands conjugated with the arylpiperazinyl moiety were synthesized and subsequently transformed into their corresponding Gd(III) complexes **2**, **3**, **4** and **5** of the type $[\text{Gd}(\text{L})\text{H}_2\text{O}]\cdot 4\text{H}_2\text{O}$. The relaxivity (R_1) of these complexes was measured and compared with that of Omniscan[®], a commercially available MRI contrast agent. The cytotoxicity studies of these complexes indicated that they are non-toxic, which reveals their potential and physiological suitability as MRI contrast agents. All the synthesized ligands and complexes were characterized with the aid of analytical and spectroscopic methods, including elemental analysis, ¹H-NMR, FT-IR, XPS and fast atom bombardment (FAB) mass spectrometry.

Master of Science in Chemistry
King Fahd University of Petroleum and Minerals
Dhahran, Saudi Arabia
May 2015

ملخص الرسالة

الإسم بالكامل: عبدالله عمر عبيد باسالم

عنوان الرسالة: تصنيع مركبات من الجادلونيوم (3) لتطبيقات في مجال التصوير بالرنين المغناطيسي

التخصص: ماجستير العلوم في الكيمياء

أبريل 2015

تاريخ التخرج:

تم صناعة أربع ليجندات DTPA-bis(amide) مرتبطة مع arylpiperazinyl وبعد تم مفاعلتها مع الجادلونيوم (III) المركبات 2 و 3 و 4 و 5 التي تم تصنيعها من النوع $[Gd(L)H_2O] \cdot 4H_2O$. تم قياس معدل الاستقرار (R1) لهذه المركبات ومقارنتها مع Omniscan® وهو معامل تباين للتصوير بالرنين المغناطيسي متوفر بالأسواق. وأشارت الدراسات السمية الخلوية أن هذه المركبات غير سامة، و هذا يكشف عن مدى ملاءمتها المحتملة والفسولوجية كي تكون معاملات تباين للتصوير بالرنين المغناطيسي. وتم تحليل و دراسة تركيب هذه المواد بمساعدة الأساليب التحليلية والتحليل الطيفي، بما في ذلك تحليل العناصر، الرنين النووي المغناطيسي، مطيافية الأشعة تحت الحمراء، مطياف الكتلة ذو القصف النووي السريع (FABMS) و XPS.

ماجستير العلوم في الكيمياء
جامعة الملك فهد للبترول و المعادن
الظهران – المملكة العربية السعودية
أبريل 2015

CHAPTER 1

INTRODUCTION AND LITERATURE REVIEW

1.1. Introduction

In the year 1946, two physicists Felix Bloch and Edward Purcell developed the concept of Nuclear Magnetic Resonance (NMR) in liquid and solid [1, 2]. This landmark discovery earned them the Noble Prize in 1952. NMR was later applied in the medical field for imaging and named Magnetic Resonance Imaging (MRI). In 1970, Dr. Raymond Damadian discovered that the key to utilize NMR concept for human body imaging is the abundance of water molecules in the body. The first human MRI scan was produced in 1975 by Peter Mansfield [3]. To date, 11 contrast agents have been approved by the US Food and Drug Administration for intravenous use.

In the early period between 1950s and the 1980s, MRI developed from building on previously known NMR techniques to evaluate relaxation of ^1H and other nuclei in vivo. However, the current MRI uses field gradients to create millimeter thick slices, which allow for the detailed acquisition of 2D and 3D images. With the fundamental technology based on NMR, MRI uses a radio frequency as the source of excitation during imaging.

MRI is at present one of the most powerful and efficient non-invasive imaging modality in clinical diagnosis. In addition, MRI is considered the safest diagnostic technique due to no use of harmful high-energy radiation compared to competing radio-diagnostic methods, which use ionizing radiation such as in computer tomography (CT) scans or radioactive material in positron emission tomography (PET) scans. Currently many different types of contrast inducing species have been investigated, ranging from paramagnetic nanoparticles over metal complexes of Mn^{2+} , Eu^{2+} and Gd^{3+} ; as well as other lanthanides in the case of

saturation transfer contrast agents. Since the approval of Gd-DTPA (Magnevist®) for clinical use, lanthanides complexes have been the subject of extensive research [4, 5]. The paramagnetic properties Gd-complexes inherit from the presence of gadolinium, having seven unpaired electrons, revealing strong relaxation effects [6, 7].

MRI has emerged as an important diagnostic tools due to its exquisite anatomical resolution, routinely down to 0.5-1 mm. Now commonplace in the clinic, paramagnetic or superparamagnetic metal ions are administered in 40-50% of the 7-10 million MR examinations per year [8]. MRI-CA are diagnostic magneto-pharmaceuticals used to enhance the image contrast by increasing the water proton relaxation rate in the body, which allow enhanced tissue contrast and identification of lesions (Figure 1).

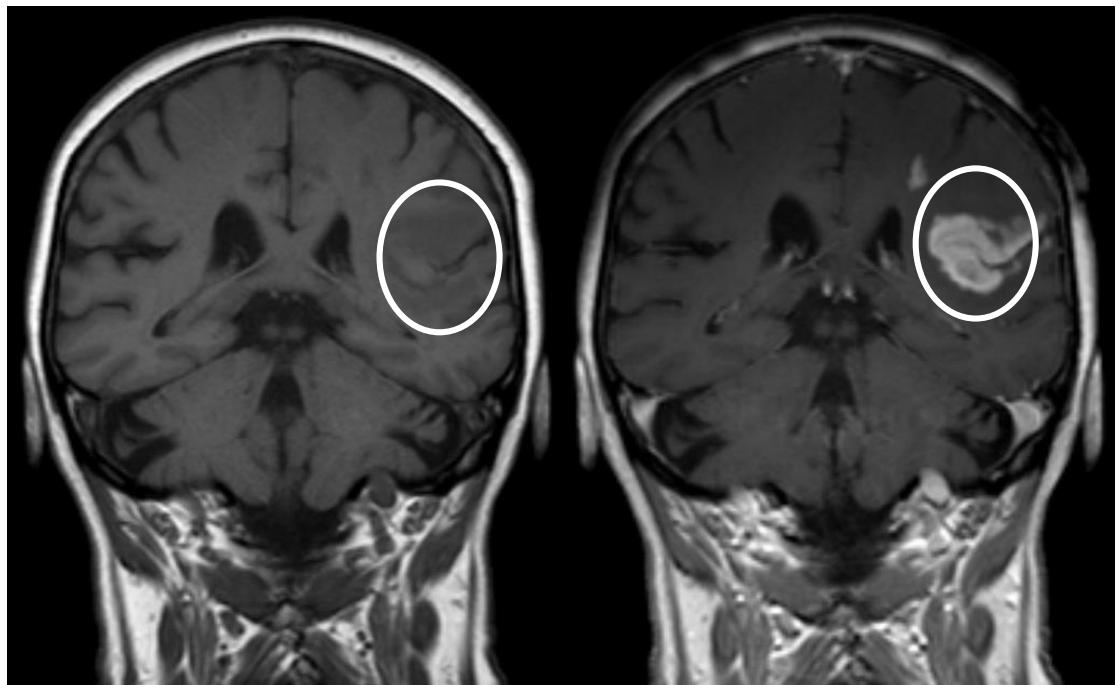


Figure 1: Effect of MR contrast agent

With the fundamental technology based on NMR, MRI contrast can be described by the two NMR processes of spin relaxation, T_1 (longitudinal), and T_2 (transverse) [9].

1.2. MRI Working Mechanism

The key to MRI is the abundance of water in the human body (Table 1). Hydrogen (H^1) has a 99.985% natural abundance and very sensitive NMR signal [10].

Tissue	Water content
Kidney	81 %
Liver	71 %
Teeth/Bones	10%

Table 1: Water content in different human tissues [11]

The protons of the hydrogen atom is spinning around constantly producing a magnetic field. In nature (no applied external magnetic field) protons' magnetic moments are aligned in a random manner. Because of that, the net magnetization is considered to be zero. By applying an external magnetic field (B_0), these magnetic moments will align themselves either align or opposite to the direction of B_0 . There tend to be more in the aligned than in the opposite direction of B_0 and therefore the net magnetization (M_0) remains in the direction of B_0 (Figure 2) [10].

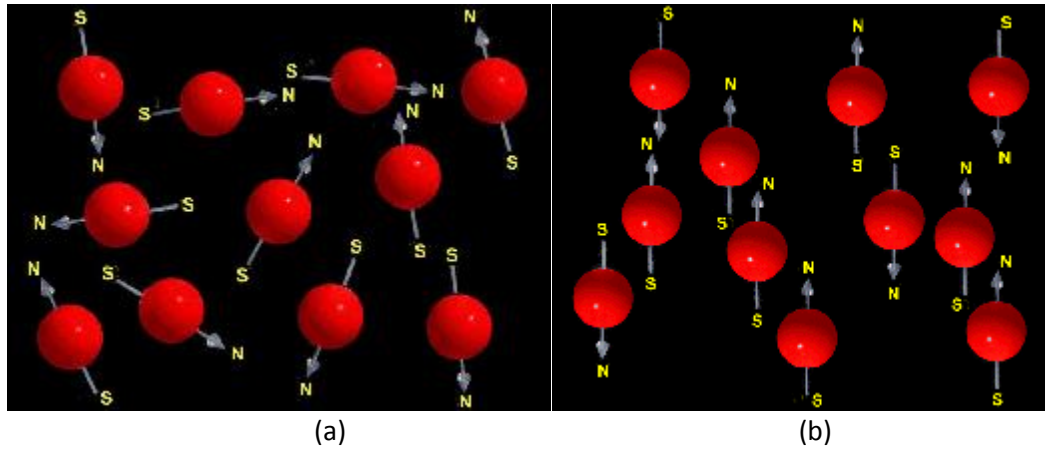


Figure 2: Protons without (a) and (b) with external magnetic field

In reality, the hydrogen atom rotates around the axis of B_0 rather than aligning with it and this phenomena is known as precession. The frequency needed for precession to occur is called Larmor Frequency. It is also the frequency where the protons will absorb energy [10]. The following equation describes the precession frequency (ω_0):

$$\omega_0 = \gamma \times B_0$$

Where γ is the gyromagnetic ratio of H^1 in NMR.

Irradiation at the Larmor frequency using a Rf pulse (B_0) will move M_0 away from the z axis and onto either the x or y axis, where the receiver is situated to measure the energy released during relaxation (Figure 3).

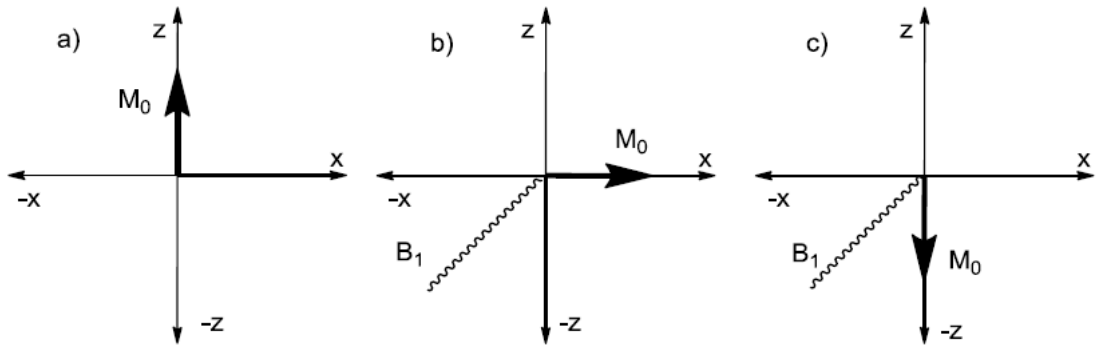


Figure 3: Representation of net magnetization vector (M_0) a) at equilibrium before a B_0 is applied ($M_0 = M_z$). b) After a $90^\circ B_0$ is applied ($M_0 = M_x$). c) After a $180^\circ B_0$ is applied ($M_0 = -M_z$).

As the ^1H nucleus begin to relax, their frequency of precession can be measured as the excess energy is released.

1.3. Relaxation Mechanism

The signal-to-noise ratios in MRI rely on the amount of protons present in the region of interest and the degree of polarization of the nuclear spin states. When placed in a magnetic field, a small population excess of protons will align in the direction of the magnetic field and precess at a Larmor resonance frequency related to the strength of the magnetic field [12]. When the frequency of the electric field component of the incoming radiation is equal to the frequency of the electric field generated by the precessing nucleus, energy is absorbed, causing a spin change. The processes by which excited nuclei return to their ground state, establishing Boltzmann equilibrium are called relaxation processes [13]. Relaxation is calculated in two ways, longitudinal and transverse. Longitudinal or spin-lattice relaxation is defined by the time constant T_1 and occurs in the direction of the applied magnetic field. In this case the spins lose their energy by transferring it to the surrounding *the lattice* as thermal energy. Transverse or spin-spin relaxation corresponds to vector dephasing in the plane perpendicular to the

main magnetic field and is characterized by T_2 . T_1 represents the time required for the magnetization vector to be restored to 63% of its original magnitude, and T_2 represents a 37% decrease in net signal [14]. In addition, T_2 is always equal to or shorter than T_1 . Earlier, it was discovered that T_1 of tumorous tissues in the human body are longer than those of normal tissues (Table 2).

Tissue	T_1 tumor (s)	T_1 normal (s)
Bone	1.027	0.554
Breast	1.080	0.367
Lung	1.110	0.788
Skin	1.047	0.616

Table 2: T1 values of some tumorous and normal human tissues [11]

1.4. Gadolinium based MR contrast agents

Due to its 7 unpaired 4f electrons, the metal ion Gd^{3+} (atomic number = 64, MW = 157.25) is by far the most paramagnetic metal ion used for MRI. Advances in MRI for faster scans and higher resolution have required more rapid pulsing and thus have favored T_1 -weighted imaging and use of contrast enhancers such as Gd^{3+} . In the quantities required for clinical use, free gadolinium ions Gd^{3+} are extremely toxic. $Gd(III)$ is comparable to $Ca(II)$ in size ($Gd(III)$ $r = 1.05-1.11 \text{ \AA}$, $Ca(II)$ $r = 1.00-1.06 \text{ \AA}$), bonding, coordination, and donor atom preference [15]. In addition, when present inside the body, gadolinium ion of the complex can be replaced with protons or endogenous metal ions such as Cu^{2+} , Zn^{2+} or Ca^{2+} , during spontaneous dissociation, or transmetalation *via* competitive reactions [16].

To eliminate the toxicity associated with free $Gd(III)$ ion, many chelates have been developed to synthesize $Gd(III)$ -complexes (Figure 4). These highly stable

complexation cages have a greater affinity for Gd(III) than other metals commonly present *in vivo* such as Zn(II), Ca(II), or Cu(II) (Fig. 5). Moreover, after complexation, renal elimination rises by 550 folds as compared to free Gd(III) metal ion [17].

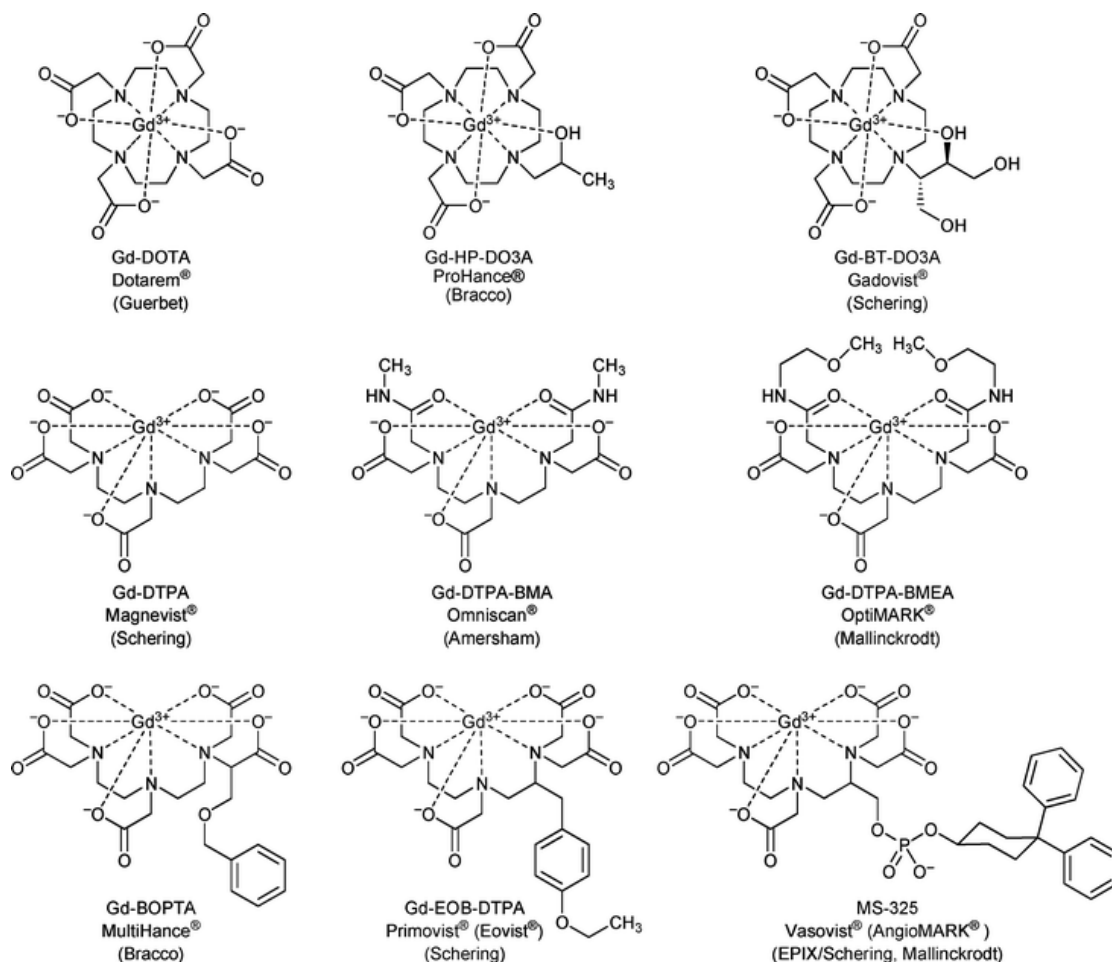


Figure 4: Commercially available Gd³⁺ chelate MR agents.

CHAPTER 2

OBJECTIVES AND WORK PLAN

Following are the objectives of our proposed study:

- (1) The short term objectives of this research are to accomplish the synthesis of Gd based complexes (1-5).
- (2) Long term objectives are
 - (a) Study the relaxation properties of complexes (1-5) by NMR.
 - (b) Application of complexes (1-5) in the MRI.

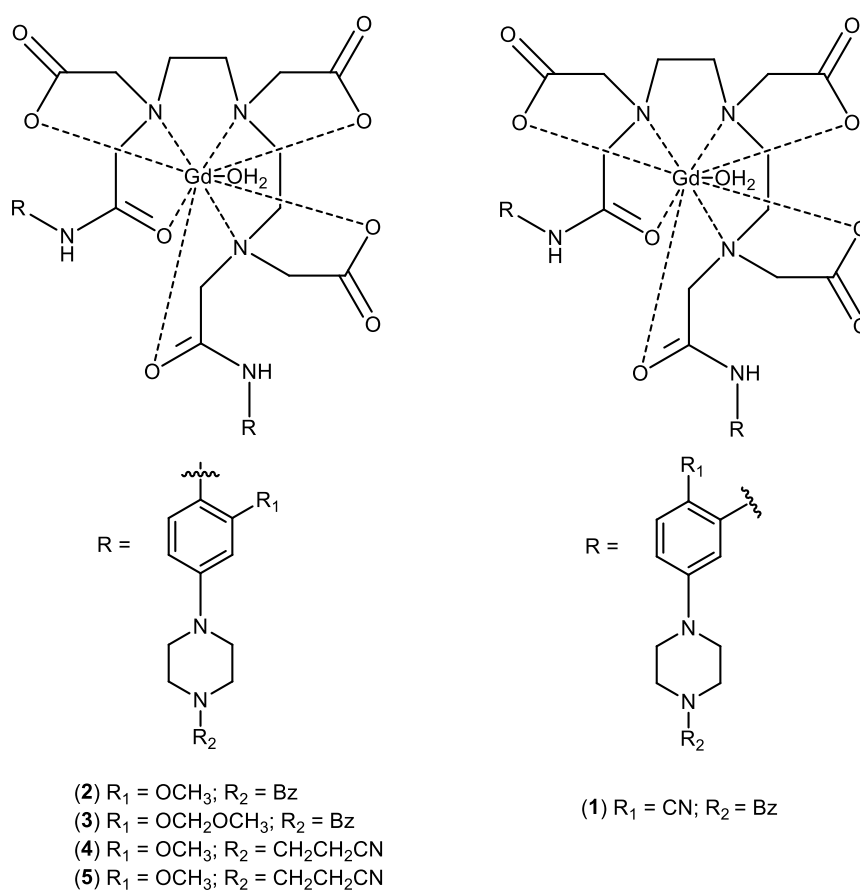


Figure 5: Structure of the Gd-complexes (1-5)

2.1. Present State of the Problem

One of the most important properties of contrast agents is the safety of their usage. In the quantities required for clinical use, free gadolinium ions Gd^{3+} are highly toxic. In order to reduce its toxicity, gadolinium ion must be transformed into Gd-complex with appropriate organic chelates or ligands [18,19]. In addition, contrast agents should also be able to display an effective impact on selected organs. Gd-DTPA (Magnevist®) is a well-established contrast agent in the clinical use for MRI applications due to its high relaxivity, high chemical stability and low toxicity. However, its passive and nonspecific distribution in vivo limits its utility in focal lesion detection and, in addition, its ionic characteristic leads to some side effects associated with its hyperosmolality at clinical dose. Apart from poor sensitivity, the existing contrast agents also suffer from fast renal elimination, which extremely shorten the time frame for MR imaging [20].

In attempts to decrease the side effects and improve the tissue and/or organ-specificity, we aim to synthesize new ligands derived from suitably substituted arylpiperazinyl and diethylene triamine pentaacetic acid (DTPA) and condense them with gadolinium to produce gadolinium complexes (**1-5**) (Figure 5). Based on charge law, it is expected that non-ion complexes will be formed from the complexation of our proposed ligands with Gd^{3+} ion, which, in turn, is expected to contribute towards low osmotic pressure and organ-specificity [21].

CHAPTER 3

RESULTS AND DISCUSSION

3.1. Synthesis of the Chelates

The development of an optimum MRI contrast agent would necessitate consideration of high relaxivity, non-cytotoxicity and high water solubility of the targeted complexes. As suggested by earlier report, suitable modification of the ligand for instance introduction of polar groups to the alkyl substituents on the amide N-atoms of DTPA-bis (amide) can lead to the formation of water soluble Gd-complexes [22]. Therefore, we intended to synthesize Gd-complexes with different arylpiperazine ligands having different functionalities in the aryl moiety (Figure 6).

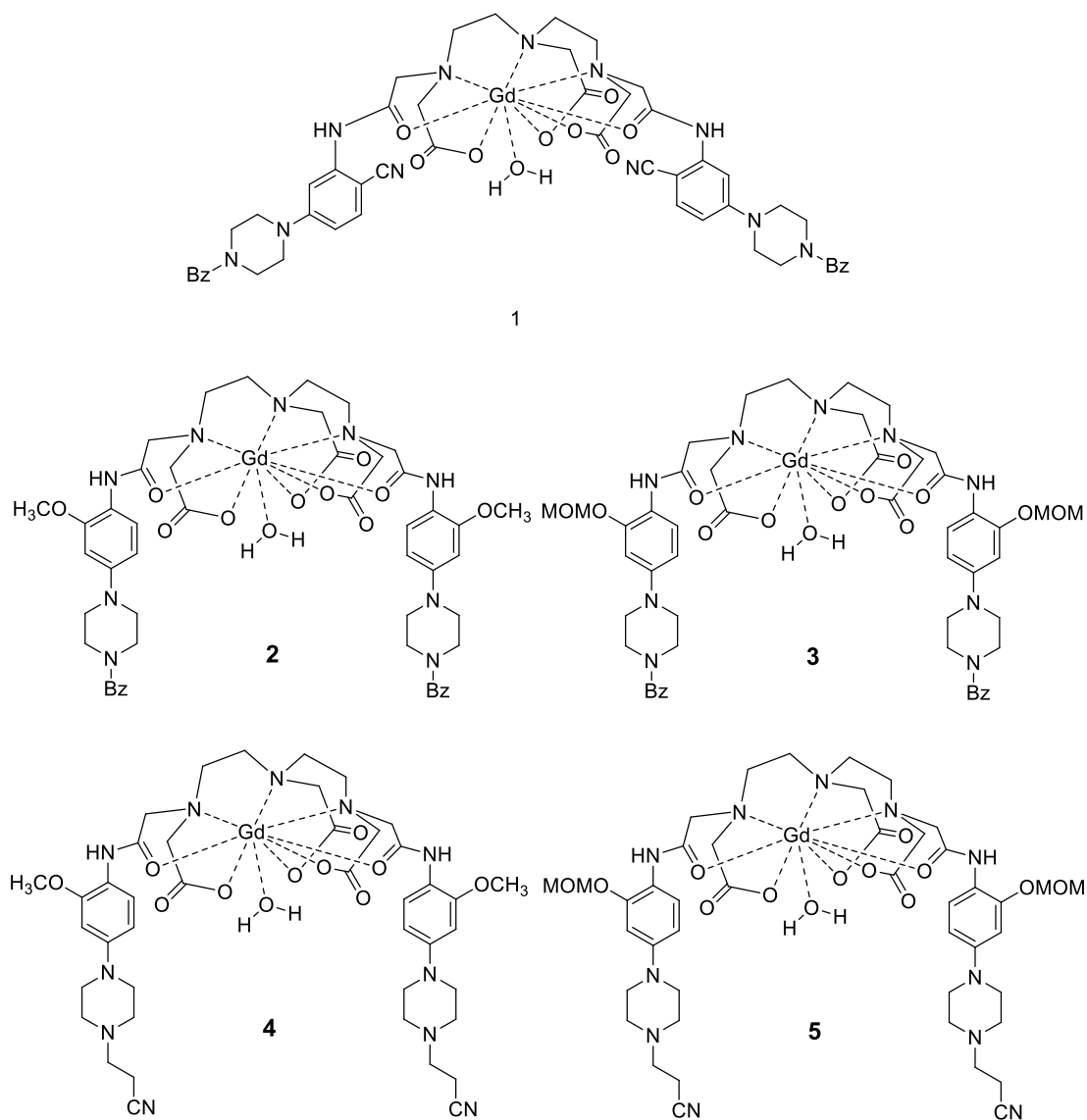
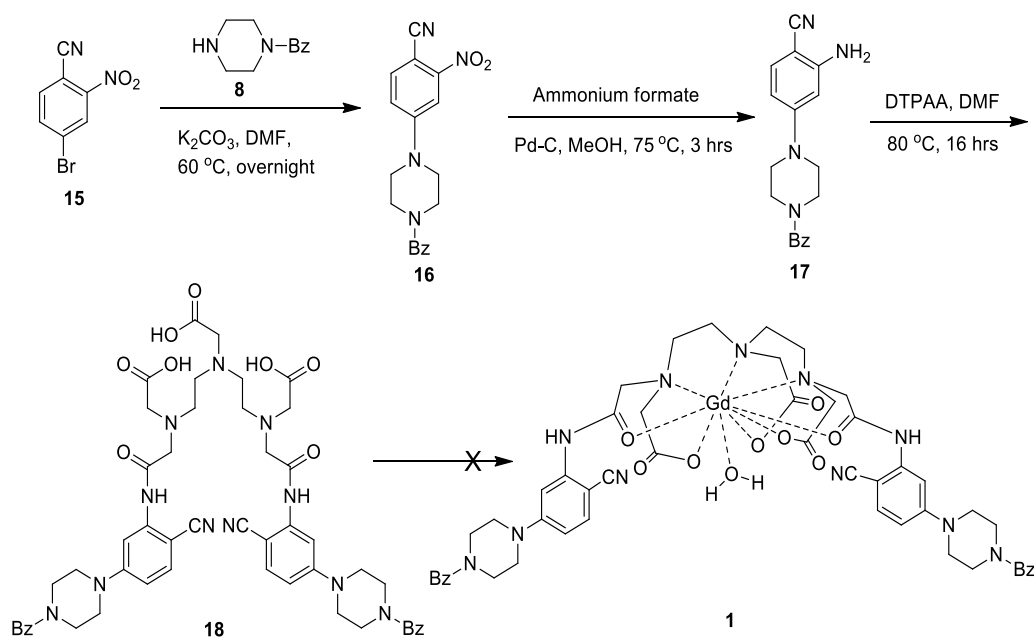


Figure 6: The Gd (III) attempted to synthesize.

3.1.1. Synthesis of Complex 1

The synthesis of complex **1** was envisioned from condensation of ligand **18** (Scheme 1), bearing nitrile group in the aryl moiety, with GdCl_3 or $\text{Gd}(\text{OAc})_3$. The synthesis of **18**, in turn, was commenced as outlined in scheme 1. Condensation of benzonitrile **15** [23] with benzoylpiperazine **8** in DMF generated the coupled product **16** in an excellent yield. Reduction of the nitro group of intermediate **16**, using Pd-C or Ra-Ni as catalysts was problematic and led to complex mixture of products, which were

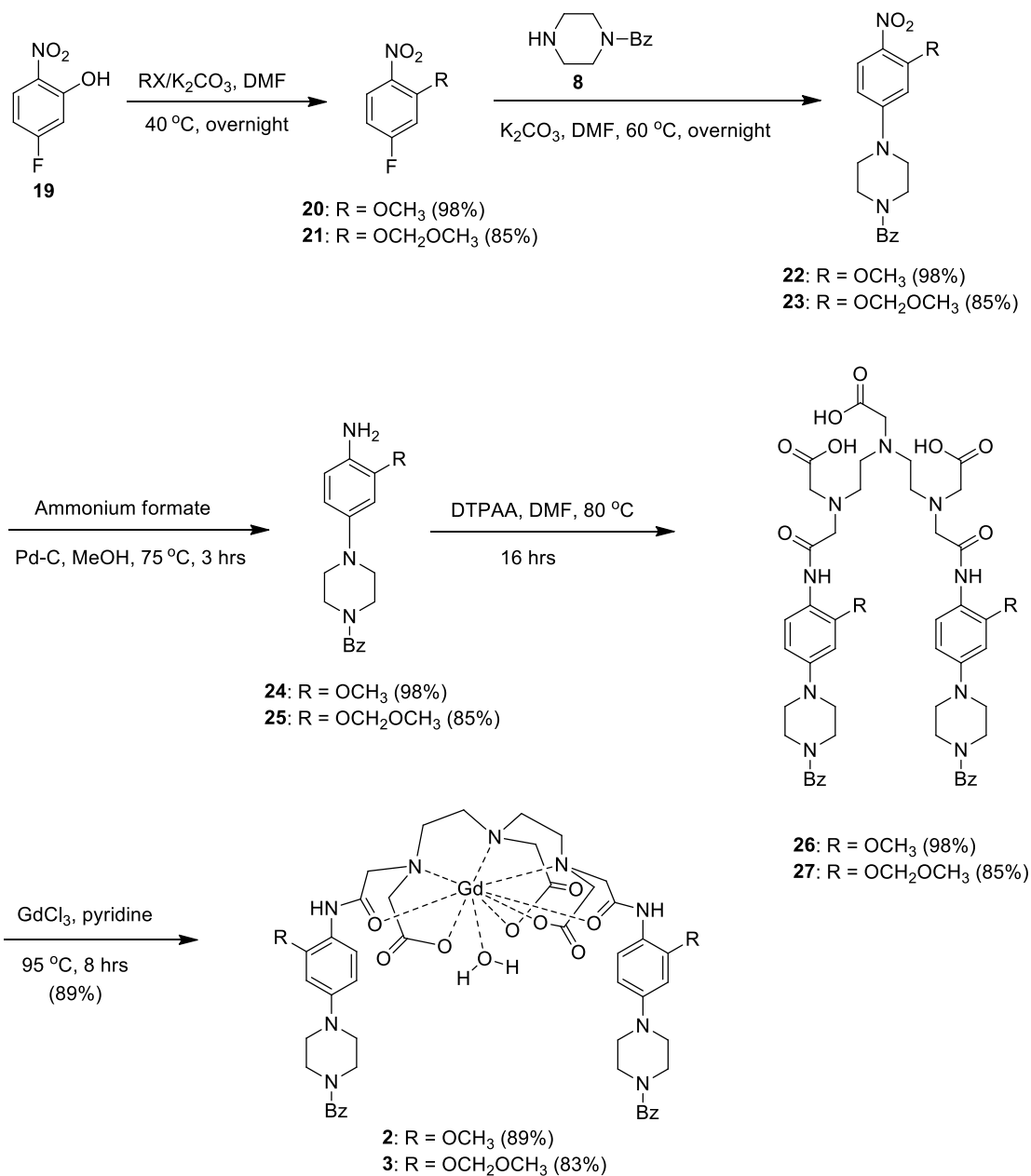
difficult to resolve by column chromatographic purifications. Hence, the reduction of nitro group was conceived via transfer hydrogenation with ammonium formate in methanol and Pd-C as catalyst to produce the corresponding intermediates **17** in high yield. Finally, reaction of aryl amines **17** with diethylene triamine pentaacetic acid dianhydride (DTPAA) [24] in DMF produced the desired ligands **18**. We next moved on to the synthesis of the final Gd-complex from the reaction of ligand **18**. Unfortunately, the reaction of ligand **18** either with GdCl₃ or Gd(OAc)₃ in pyridine were unsuccessful, leading to the recovery of **18** only. The nitrile group in aryl ring might be playing a role in the decreased reactivity of **18** towards complexation (Scheme 1).



Scheme 1: The reaction scheme for chelate 1

3.1.2. Synthesis of Complexes 2 and 3

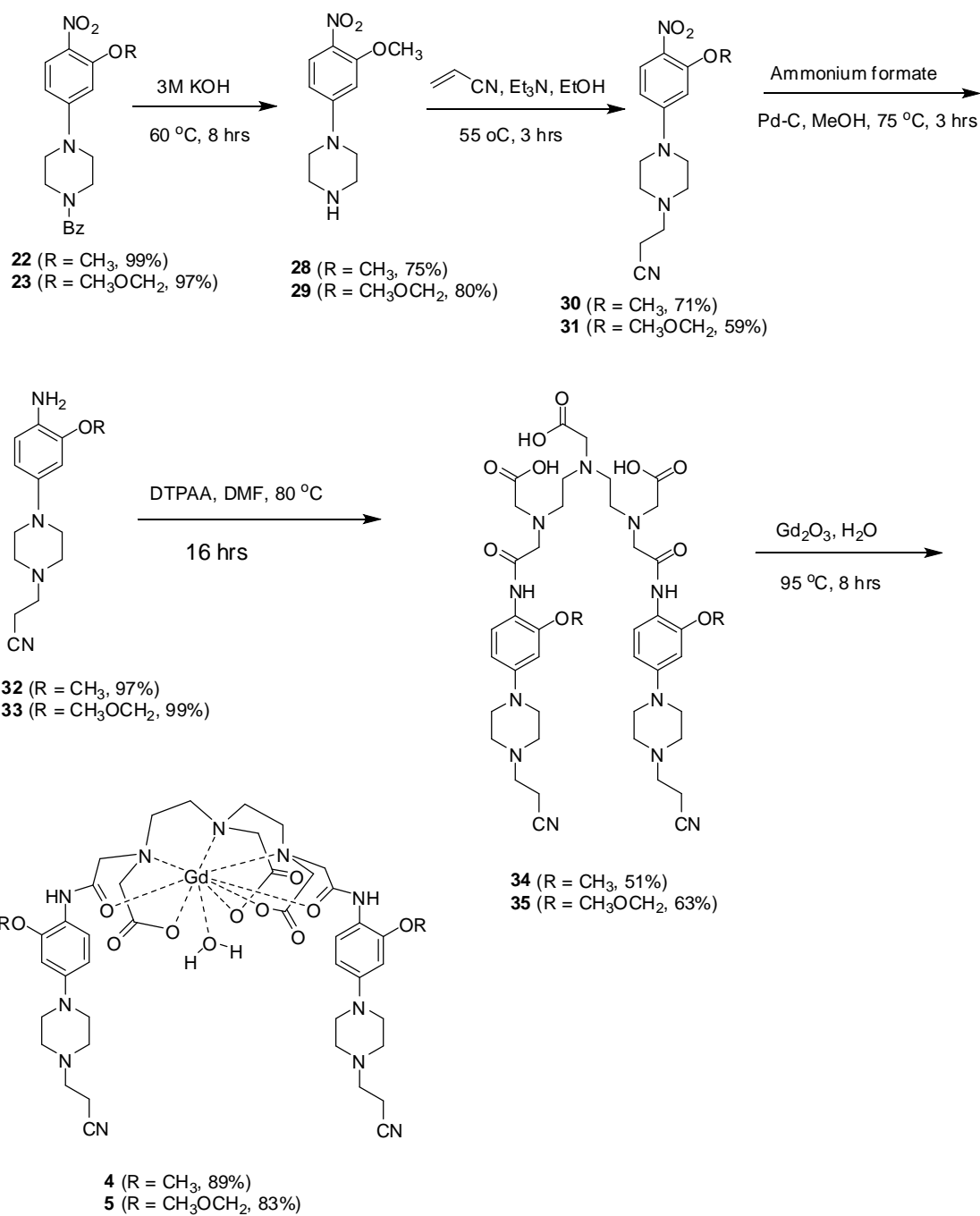
Because of the failure to synthesize Gd-complex from ligand **18**, we decided to synthesize ligands **26** and **27**, which bear methoxy and methoxymethyl substituents in the aryl moiety (Scheme 2). Reaction of phenol **19** with appropriate alkyl halide in DMF rendered **20** [25] and **21** [26]. Treatment of intermediates **20** and **21** with piperazine **8** produced intermediates **22** and **23**, respectively (Scheme 2). Reduction of the nitro group of intermediates **22** and **23** with ammonium formate in methanol, using Pd-C as catalysts generated the corresponding aryl amines **24** and **25** in high yield. Condensation of amines **24** and **25** with DTPAA constructed the desired ligands **26** and **27**, respectively. Finally, heating of ligands **26** and **27** with GdCl₃ in pyridine produced the desired complexes **2** and **3** in good yield (Scheme 2).



Scheme 2: The reaction scheme for chelates 2 and 3.

3.1.3. Synthesis of Complexes 4 and 5

Synthesis of complexes **4** and **5** started with basic hydrolysis of compounds **22** and **23** to produce compounds **28** and **29**, respectively. Michael addition of amine **28** and **29** with acrylonitrile produced intermediate **30** and **31**. The reduction of nitro group of **30** and **31** by hydrogenation using Pd-C or Ra-Ni as catalysts was problematic, leading to complex mixture of products, which were difficult to resolve. Therefore, the reduction of nitro group was conceived via transfer hydrogenation in methanol with ammonium formate and Pd-C as catalyst to produce aminonitrile **32** and **33** in high yield. DTPAA [24] was condensed with **32** and **33** to construct intermediate **34** and **35**, which in turn was heated with Gadolinium(III) oxide to produce complex **4** and **5** respectively (Scheme 3).



Scheme 3: The reaction scheme for chelates 4 and 5.

3.2. XPS Analysis

3.2.1. XPS Analysis for Complex 2

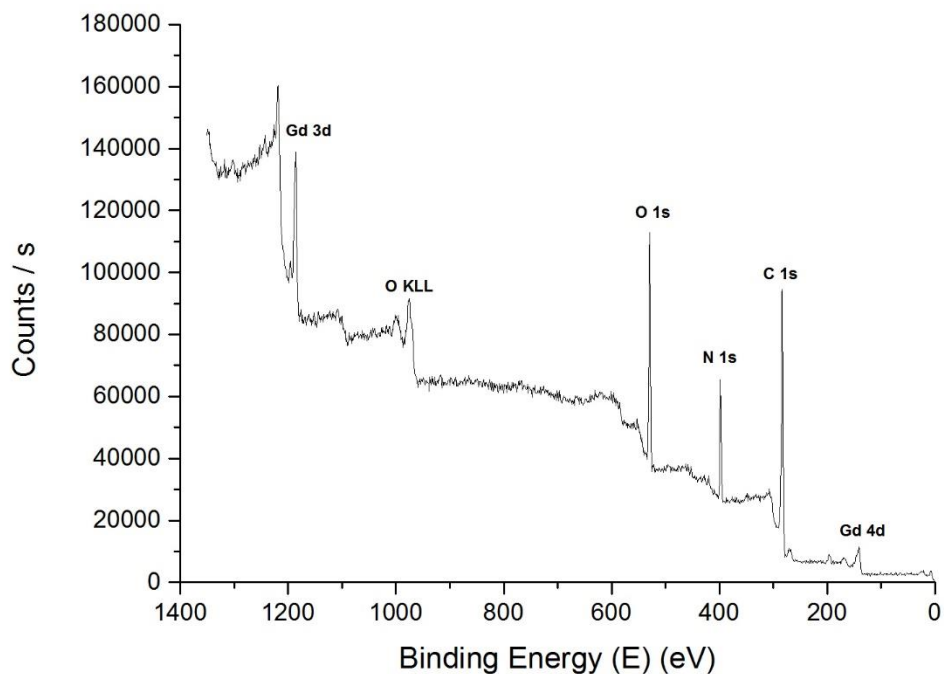


Figure 7: XPS survey scan for complex 2.

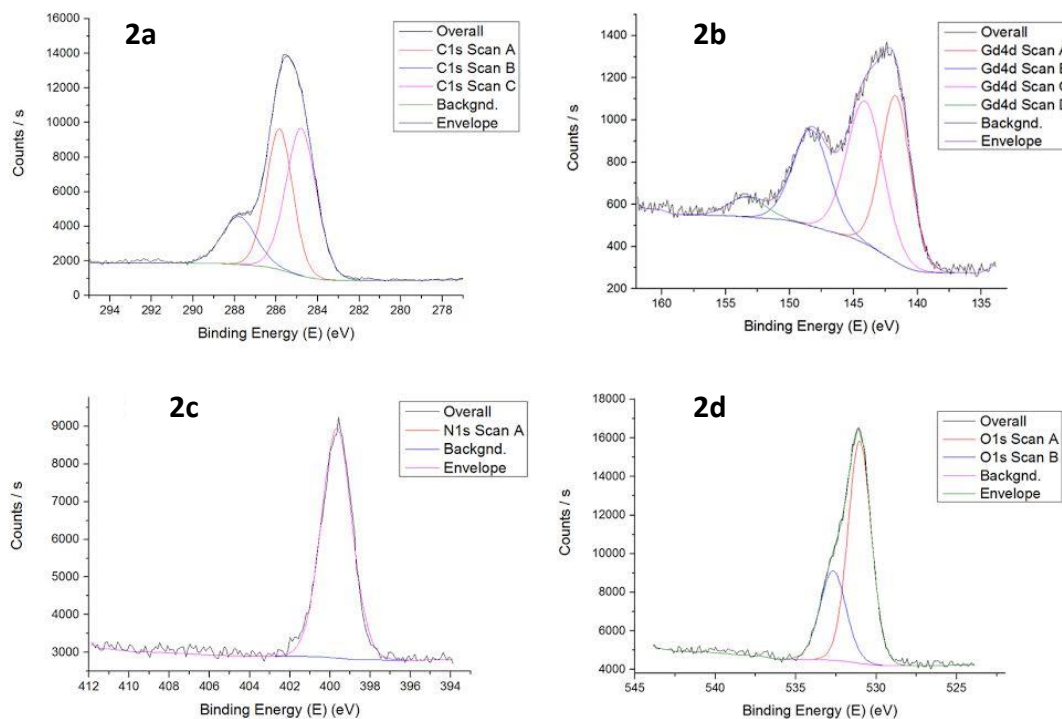


Figure 8: XPS spectrum of chelate 2.

(a) C 1s region fitted with 3 peaks. The peak at 284.8 eV is assigned to C-C, the peak at 286.0 eV is assigned to C-N and C-O, and the peak at 288.2 eV is assigned to C=C and C=O. (b) Gd 4d region fitted with 4 peaks, showing multiplet structure. (c) N 1s region fitted with one peak. (d) O 1s region fitted with 2 peaks. The peak at 531.4 eV is assigned to C-O, and the peak at 532.9 eV is assigned to C=O [27].

3.2.2. XPS Analysis for Complex 3

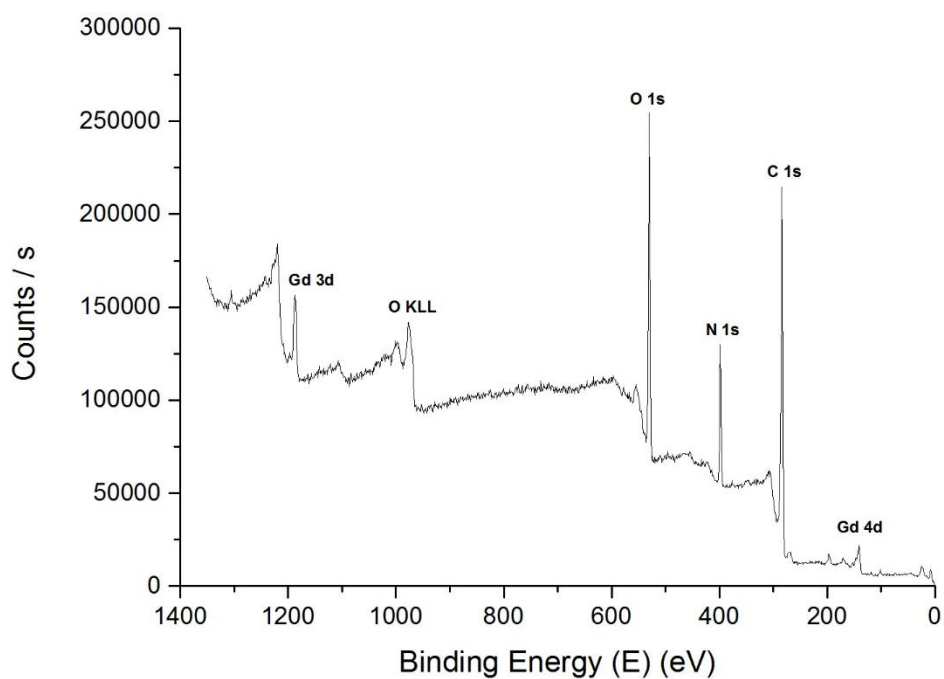


Figure 9: XPS survey scan for chelates 3.

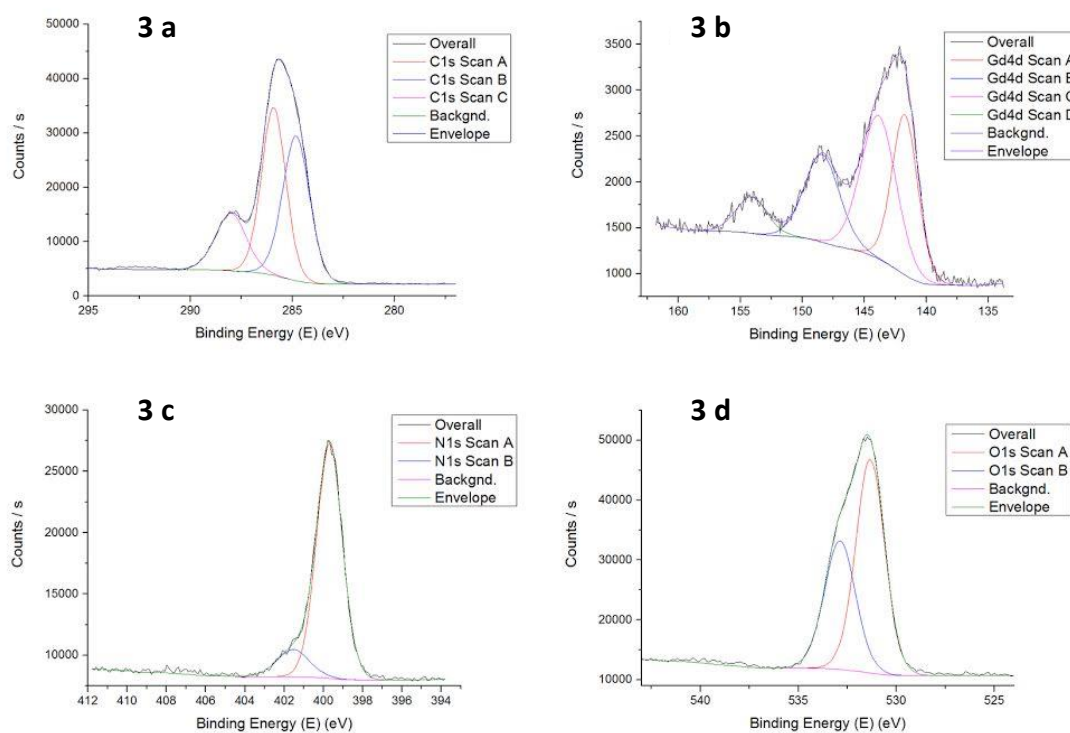


Figure 10: XPS spectrum of chelate 3.

(a) C 1s region fitted with 3 peaks. The peak at 284.8 eV is assigned to C-C, the peak at 286.1 eV is assigned to C-N and C-O, and the peak at 288.4 eV is assigned to C=C and C=O [4]. (b) Gd 4d region fitted with 4 peaks, showing multiplet structure. (c) N 1s region fitted with two peaks. (d) O 1s region fitted with 2 peaks. The peak at 531.5 eV is assigned to C-O, and the peak at 532.6 eV is assigned to C=O [27].

3.2.3. XPS Analysis for Complex 4

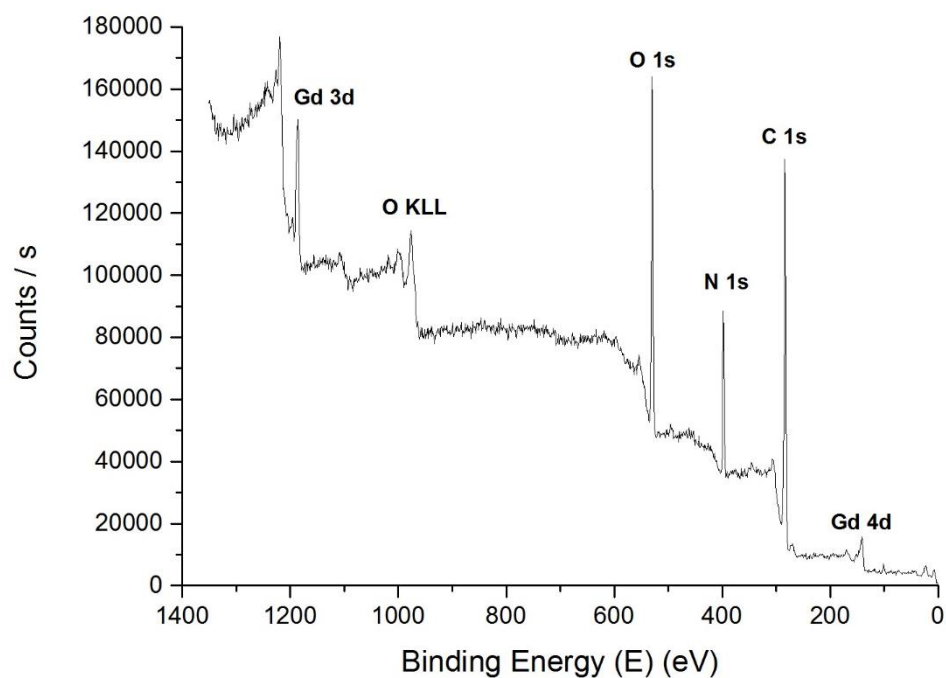


Figure 11: XPS survey scan for chelates 4.

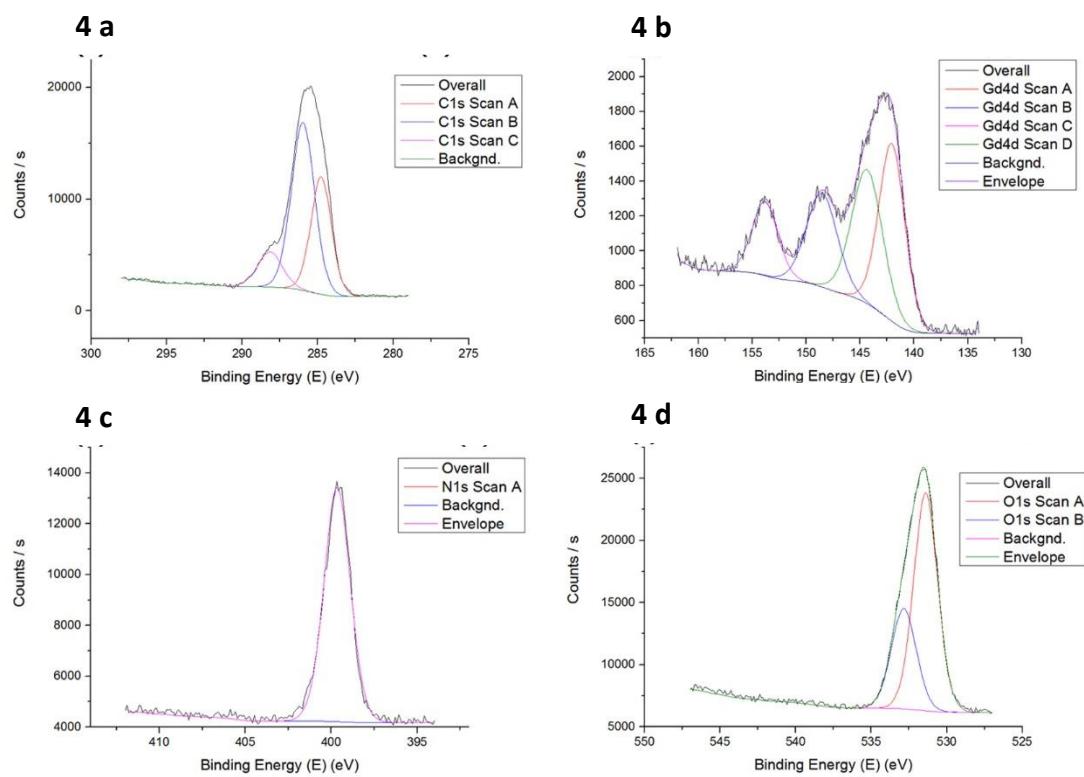


Figure 12: XPS spectrum of chelate 4.

(a) C 1s region fitted with three peaks (eV) at 284.8 (C-C), 285.8 (C-N, C-O) and 287.7 (C=C, C=O). (b) Gd 4d region was fitted with four peaks, showing multiplet structure. (c) N 1s region was fitted with one peak at 399.7 eV. (d) O 1s region was fitted with peaks (eV) at 531.0 (C-O) and 532.7 (C=O) [27].

3.2.4. XPS Analysis for Complex 5

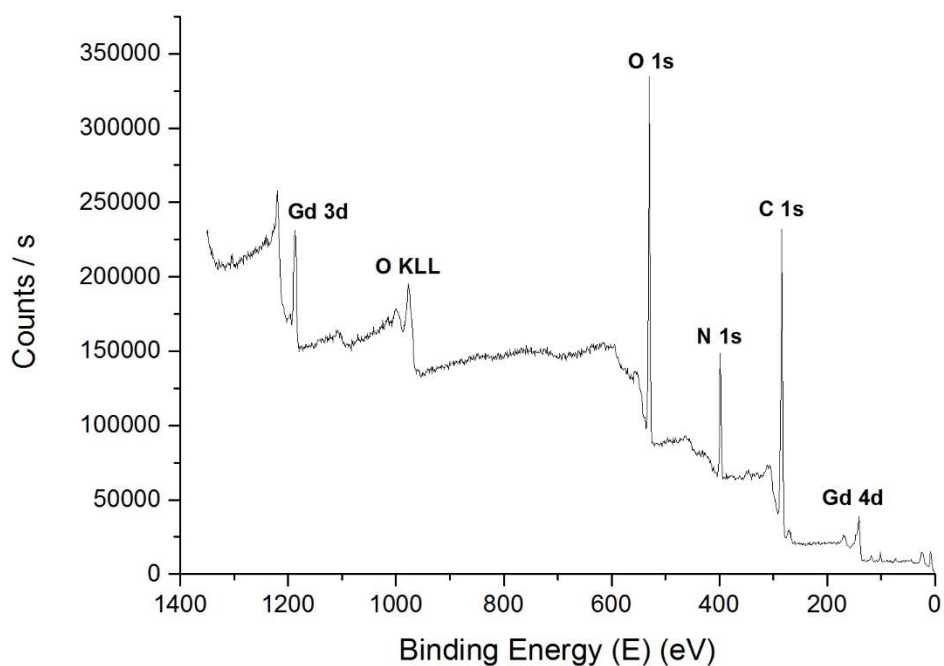


Figure 13: XPS survey scan for chelates 5.

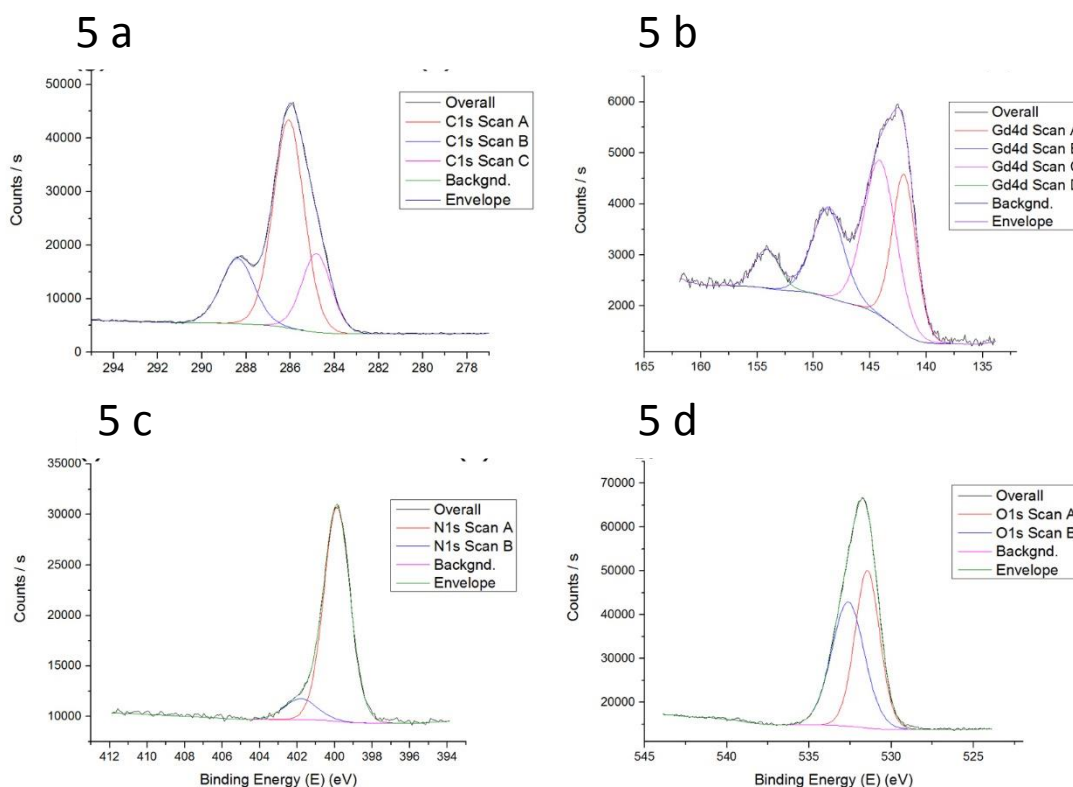


Figure 14: XPS spectrum of chelate 5.

(a) C 1s region fitted with three peaks (eV) at 284.8 (C-C), 285.8 (C-N, C-O) and 287.7 (C=C, C=O). (b) Gd 4d region was fitted with four peaks, showing multiplet structure. (c) N 1s region was fitted with one peak at 399.7 eV. (d) O 1s region was fitted with peaks (eV) at 531.0 (C-O) and 532.7 (C=O) [27].

3.3. T_1 Measurements in MRI

Relaxivity measurements of (2-5): Longitudinal relaxation (T_1) measurements of complexes (2-5) were performed in water at 298K on 3 Tesla MRI machine. The magnetic resonance images were taken at 17 different repetition time (TR) values, ranging from 20 to 1500 msec and T_1 values were obtained from non-linear least-square fit measured at each T_1 values. Relaxivities (R_1) were calculated as an inverse of relaxation times per mM [28].

CA	T ₁ (msec)	R ₁ (mM ⁻¹ sec ⁻¹)
1	415.72±2.32	2.40
2	360.93±1.56	2.77
3	293.51±1.21	3.40
4	235.67±1.01	4.24
Omniscan® ^a	312.50	3.2

Table 3:T1 of chelates (2-5).

3.4. Cytotoxicity Studies

Compounds were evaluated for their toxicity using 3T3 fibroblast cell line by MTT cytotoxicity assay, where all tested compounds were found to be nontoxic. The half maximal inhibitory concentration (IC₅₀) is a measure of how effective a substance is in suppressing a specific biological or biochemical function.

Compound	Cytotoxicity on 3T3 fibroblast cells (IC ₅₀ µg/mL)
2	>50
3	>50
4	>50
5	>50
Cyclohexamide	0.13 ± 0.02

Table 4: cytotoxicity data of chelate (2-5)

CHAPTER 4

EXPERIMENTAL PART

4.1. Materials Used

Chemicals were purchased from commercial sources, and they were used without any further purification unless otherwise specified. All solvents were of reagent grade. Specially dried (anhydrous) solvents were used where necessary. Glassware for moisture-sensitive reactions were oven dried at 120-140 °C for at least three hours and cooled in a desiccators prior to use. Some of the reactions were run in an inert atmosphere of nitrogen or argon as stated.

Purification of the products was carried out either by recrystallization or by flash column chromatography. The column was packed with silica gel 100 from Fluka Chemie AG (Buchs, Switzerland).

4.2. Product Identification

The following techniques were used to identify our products:

I. NMR Spectroscopy: ^1H NMR and ^{13}C NMR spectra were recorded on JEOL Lambda 500 MHz spectrometer. Chemical shifts were reported in ppm (δ) relative to tetramethyl silane (TMS) by using (CDCl_3), (DMSO) or D_2O as deuterated solvents. Multiplicities were reported as singlet (s), doublet (d), triplet (t), quartet (q) or multiplet (m), and coupling constants (J) were reported in hertz (Hz).

II. IR Spectroscopy: IR Spectra were recorded on a Nicolet™ 6700 FT-IR spectrometer from a thermo-electron by making KBr pallets for solids and using NaCl disks for liquids.

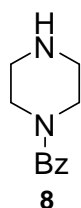
III. Elemental Analyzer "CHN": Elemental analysis was carried out on a EuroVector Elemental Analyzer Model EA3000.

IV. FABMS: Mass was determined by using JEOL JMS-600H.

V. Thin Layer Chromatography: TLC was frequently used to monitor reactions and to give qualitative determination of sample purity. TLC analyses were performed on silica gel Merck 60 F254 plates, and spots were visualized under a spectroline UV lamp. Visualization was improved by using iodine chamber.

4.3. Synthesis of Gd-Complexes

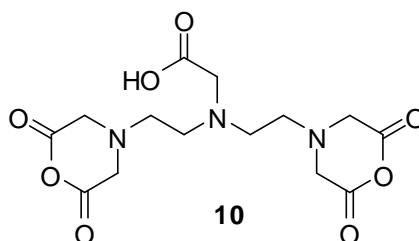
4.3.1. Synthesis of phenyl(piperazin-1-yl)methanone (8)



This compound was synthesized as per the literature procedures [29]. In a flask (1.36g, 20 mmol) of imidazole was dissolved in (50 ml) of DCM. (1.40g, 10 mmol) of benzoyl chloride **6** was added to this solution and left to stir at 0 °C for two hours. After that a white precipitate of imidazole hydrochloride was filtered off. The organic layer was concentrated in rotavap and reconstituted in (25 ml) ethanol. In another flask, (2.06g, 13 mmol) of piperazine dihydrochloride was dissolved in (25 ml) of water. The ethanolic solution was slowly added over a 10 minutes period to the water solution and left to stir at room temperature for six hours. The solution was reduced to 1/4 of its original volume using rotavap. The remaining solution was washed with DCM (4x25 ml) to remove the dialcylated product. (10 ml) of concentrated NaOH was added to the aqueous layer and then washed with (4x25 ml) of DCM. Finally, the organic layer was

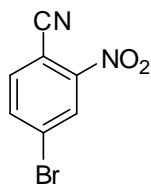
dried over anhydrous CaSO₄ and dried to afford a pale yellow liquid **8** (1.66g, 67.3%). IR (Film): 3522, 3297, 2999, 2914, 2822, 2744, 2361, 1966, 1636, 1577, 1525, 1495, 1433, 1365, 1162, 1140, 1062, 1016, 925, 867, 820, 787, 733, 708, 665, 635, 592, 545 cm⁻¹. ¹H NMR (500 MHz, CDCl₃) δ: 1.99 (br s, 1H), 2.77 (d, 4H, J= 69.55 Hz), 3.37 (br s, 2H), 3.73 (br s, 2H), 7.39 (m, 5H). ¹³C NMR (125 MHz, CDCl₃) δ: 42.92, 45.60, 49.65, 126.64, 128.14, 129.26, 135.60, 170.07.

4.3.2. Synthesis of 2-(bis(2-(2,6-dioxomorpholino)ethyl)amino)acetic acid (**10**)



This compound was synthesized as per the literature procedures [30] the synthesis is as follows. **9** (10.00 g, 25.42 mmol) was suspended in pyridine (15 ml). After that acetic anhydride (10.80 ml, 114.40 mmol) was added and left stirring at 55 °C for 48 hours. At the end of the reaction, the color of the solvents will change from colorless to brown. The product was filtered off and then washed with DCM until a uniform color was seen. **10** was obtained as a creamy powder (7.68 g, 84.57%).

4.3.3. Synthesis of 4-bromo-2-nitrobenzonitrile (**15**)

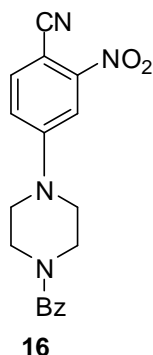


15

This compound was synthesized as per the literature procedures [23]. To a cold solution of trifluoroacetic acid (18 mL) at 0 °C was added compound **15a** (4.5 g, 22.8 mmol). After being stirred for 10 minutes, a solution of 33% hydrogen peroxide (7 mL, 67.8 mmol) was added and the mixture was stirred at room temperature for 0.5 h followed by stirring at 50 °C for 2 h. The mixture was poured into ice water and the solid obtained was filtered and washed with cold water to afford 3.64 g (70%) of compound **15** as an off-white solid, m.p. 84-85 °C; IR (KBr) ν max. cm^{-1} : 3042 (Ar-H), 2252 (CN), 1520, 1412 (C=C). ^1H NMR (500 MHz, DMSO- d_6) δ = 8.15 (dd, 1H, J = 2.4, 8.5 Hz, H-5); 8.25 (d, 1H, J = 8.4 Hz, H-6); 8.46 (d, 1H, J = 2.4 Hz, H-3); ^{13}C NMR (125.7 MHz, DMSO- d_6) δ = 108.88 (C-1), 114.54 (CN), 127.43 (C-3), 128.75 (C-4), 137.57 (C-5/C-6), 138.10 (C-5/C-6), 147.59 (C-2). Calculated (%) for $\text{C}_7\text{H}_3\text{BrN}_2\text{O}_2$ (225.94); C: 37.03, H: 1.33, N: 12.34, found (%); C: 37.00, H: 1.37, N: 12.27.

4.3.4. Synthesis of 4-(4-benzoylpiperazin-1-yl)-2-nitrobenzonitrile

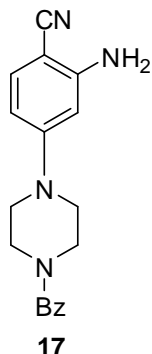
(16)



To a solution of amine **8** (1.82 g, 9.56 mmol) in DMF (20 mL) at 0 °C was added K_2CO_3 (3.61 g, 26.13 mmol) followed by the addition of compound **15** (1.96 g, 8.67 mmol) and the reaction was stirred overnight at 60 °C. After completion of the reaction (TLC analysis), the mixture was cooled to room temperature and diluted with ethyl acetate (75 ml). The solution was washed with H_2O (30 mL x 3), brine (20 ml x 2) and the organic layer was separated, dried over Na_2SO_4 and evaporated under vacuum to afford the title compound **5** as as light yellow amorphous solid (2.16 g, 74%), m.p. 196-197 °C. IR (KBr): 3063, 2999, 2929, 2233, 1670, 1622, 1596, 1578, 1457, 1430, 1389, 1341, 1294, 1249, 1155, 1094, 1072 cm^{-1} . 1H -NMR (500 MHz, $CDCl_3$): δ 3.47 (br. s, 4H, $-CH_2NCH_2-$), 3.79 (br. s, 4H, $-CH_2NCH_2-$), 6.99 (dd, 1H, $J = 2.6, 9.4$ Hz, Ar-H), 7.14 (d, 1H, $J = 2.7$ Hz, Ar-H), 7.40-7.48 (m, 5H, Ar-H), 8.19 (d, 1H, $J = 9.5$ Hz, Ar-H). ^{13}C -NMR (125 MHz, $CDCl_3$): δ 46.44, 46.84, 110.05, 115.66, 118.89, 126.93, 127.10, 127.79, 128.67, 130.33, 134.69, 137.79, 153.10, 170.61. Anal. Calcd for $C_{18}H_{16}N_4O_3$: C, 64.28; H, 4.79; and N, 16.66. Found: C, 64.22; H, 4.84; and N, 16.60.

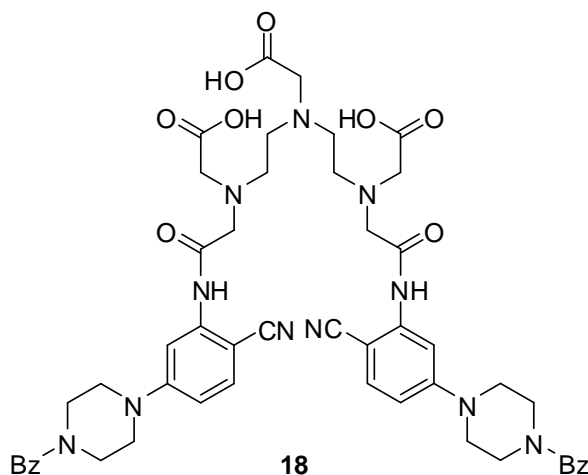
4.3.5. Synthesis of 2-Amino-4-(4-benzoylpiperazin-1-yl)benzonitrile

(17)



To a solution of compound **16** (2.93 g, 7.12 mmol) in anhydrous methanol (50 mL) was sequentially added Pd-C (10% wet basis, 0.25 g) and ammonium formate (2.25 g, 35.63 mmol) and the mixture was refluxed for 3 hours. The reaction mixture was filtered through a pad of celite and the filtrate was concentrated under vacuum. Column chromatography of the dark purple oily material eluting with MeOH:CH₂Cl₂ (1:9) afforded the title compound **6** as a light brown thick oil (1.77 g, 81%). IR (KBr): 3455, 3348, 3060, 2916, 2821, 2213, 1669, 1631, 1577, 1505, 1437, 1388, 1313, 1284, 1241, 1158, 1095 cm⁻¹. ¹H-NMR (500 MHz, CDCl₃): δ 2.86 (br. s, 4H, -CH₂NCH₂-), 3.49 (br. s, 2H, -CH₂N), 3.83 (br. s, 2H, -CH₂N), 4.32 (br. s, 2H, -NH₂), 6.61 (d, 1H, *J* = 8.6 Hz, Ar-H), 6.79 (d, 1H, *J* = 2.4, Ar-H), 6.94 (dd, 1H, *J* = 2.4, 8.6 Hz, Ar-H), 7.34(m, 5H, Ar-H). ¹³C-NMR (125 MHz, CDCl₃): δ 41.81, 47.34, 50.62, 53.32, 95.69, 116.52, 117.54, 119.43, 125.63, 126.76, 128.28, 129.61, 135.19, 142.64, 144.71, 170.09. Anal. Calcd for C₁₈H₁₈N₄O: C, 70.57; H, 5.92; and N, 18.29. Found: C, 70.50; H, 5.97; and N, 18.22.

4.3.6. Synthesis of 2,2'-(2,2'-(carboxymethylazanediy)bis(ethane-2,1-diy)bis((2-(5-(4-benzoylpiperazin-1-yl)-2-cyanophenylamino)-2-oxoethyl)azanediy))diacetic acid (18)



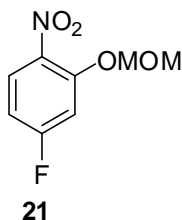
To a solution of DTPAA (0.175 g, 0.49 mmol) in DMF (10 mL) was added compound **6** (0.30 g, 0.98 mmol) and the reaction mixture was stirred at 80 °C for 16 hours. The mixture was cooled to ~40 °C, filtered through a pad of silica gel and the filtrate was concentrated under reduced pressure. The residue was added drop wise to cold acetone (50 ml) and the precipitated product was filtered by suction, dried under reduced pressure to afford compound **7** as an off-white powder (0.31 g, 65%), m.p. 158-160 °C. IR (KBr): 3467, 2917, 2509, 2362, 2228, 1690, 1627, 1517, 1437, 1389, 1284, 1241, 1160, 1048, 1011, 962, 829, 788, 708, 633, 559, 493, 424 cm⁻¹. ¹H-NMR (500 MHz, DMSO-d₆): δ 2.90-3.20 (m, 10H), 3.43-3.72 (m, 24H), 7.22-7.26 (m, 4H, Ar-H), 7.45-7.49 (m, 14H, Ar-H), 10.03 (s, 2H). ¹³C NMR (125 MHz, DMSO-d₆): δ 41.21, 48.05, 51.13, 52.46, 55.07, 57.89, 107.65, 117.08, 118.42, 121.01, 125.85, 127.02, 128.49, 129.68, 121.57, 135.72, 147.91, 169.10, 170.01, 172.63. Anal. Calcd for C₅₀H₅₅N₁₁O₁₀•H₂O: C, 60.78; H, 5.81; and N, 15.59. Found: C, 60.72; H, 5.85; and N, 15.52. FAB-MS (*m/z*): calcd for C₅₀H₅₅N₁₁O₁₀, 969.4 ([MH]⁺). Found: 969.3 ([MH]⁺).

4.3.7. Synthesis of 4-fluoro-2-methoxy-1-nitrobenzene (**20**)



19 (1.00 g, 6.4 mmol) was dissolved in DMF (15 ml) and stirred at 0 °C for 5 minutes and then K₂CO₃ (1.33 g, 9.6 mmol). The suspension left to stir at 0 °C for 15 minutes. After that CH₃I (0.6 ml, 9.6 mmol) was added and left stirring at 40 °C overnight. TLC was used to check the completion of the reaction. The reaction was cooled and ether (25 ml) was added and the solution was transferred to a separation funnel. The solution was washed with H₂O (20 ml x 3), 10% HCl (10 ml x 1) and brine (10 ml x 1). The organic layer was collected, dried over CaSO₄ and dried under vacuum to afford **20** as yellowish white solid (1.08 g, 98%). MP: 41-43 °C. IR (KBr): 2442, 1890, 1626, 1524, 1445, 1350, 1284, 1192, 1162, 1136, 1090, 1020, 954, 841, 748, 688, 631, 577, 532 cm⁻¹. ¹H NMR (500 MHz, CDCl₃) δ: 3.95 (s, 3H), 6.73 (m, 1H), 6.75 (dd, 1H, J1= 12.82 Hz, J2 = 6.41 Hz), 7.96 (dd, 1H, J1 = 10.07 Hz, J2 = 5.04). ¹³C NMR (125 MHz, CDCl₃) δ: 65.76, 101.56, 107.52, 128.23, 155.37, 164.91, 166.34.

4.3.8. Synthesis of 4-fluoro-2-(methoxymethoxy)-1-nitrobenzene (**21**)

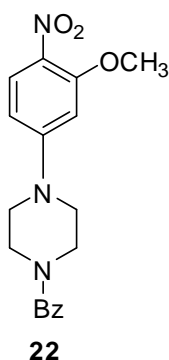


19 (2.00 g, 12.7 mmol) was dissolved in DMF (30 ml) and stirred at 0 °C for 5 minutes and then K₂CO₃ (2.63 g, 19.05 mmol). The suspension left to stir at 0 °C for 15 minutes. After that MOMCl (1.00 ml, 12.7 mmol) was added and left stirring at 40

°C overnight. TLC was used to check the completion of the reaction. The reaction was cooled and ether (75 ml) was added and the solution was transferred to a separation funnel. The solution was washed with H₂O (30 ml x 3), 10% HCl (20 ml x 1) and brine (20 ml x 1). The organic layer was collected, dried over CaSO₄ and dried under vacuum to afford **21** as yellow liquid (2.14 g, 83.8%). IR (Film): 3091, 2937, 2837, 2361, 1676, 1621, 1591, 1529, 1490, 1397, 1352, 1280, 1215, 1158, 1079, 994, 936, 846, 822, 752, 660, 606 cm⁻¹. ¹H NMR (500 MHz, CDCl₃) δ: 3.53 (s, 3H), 5.30 (s, 2H), 6.80 (m, 1H), 7.08 (dd, 1H, J₁= 9.46 Hz, J₂= 4.73 Hz), 7.92 (m, 1H). ¹³C NMR (125 MHz, CDCl₃) δ: 56.70, 95.29, 104.55, 108.57, 127.47, 136.66, 152.43, 164.20, 166.23.

4.3.9. Synthesis of (4-(3-methoxy-4-nitrophenyl)piperazin-1-yl)

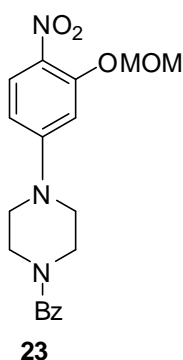
(phenyl)methanone (**22**)



Following the same procedure adopted for the synthesis of **16**, the reaction of amine **8** with compound **20** (1.49 g, 8.71 mmol) afforded the title compound **22** as bright yellow amorphous solid (2.91 g, 98%), m.p. 185-187 °C. IR (KBr): 3021, 1627, 1575, 1488, 1461, 1436, 1383, 1336, 1314, 1245, 1156, 1102, 1080 cm⁻¹. ¹H-NMR (500 MHz, CDCl₃): δ 3.40-3.50 (br. s, 4H, -CH₂NCH₂-), 3.94 (s, 3H, -OCH₃), 4.64 (br. s, 4H, -CH₂NCH₂-), 6.33 (d, 1H, J = 2.4 Hz, Ar-H), 6.43 (dd, 1H, J = 2.4, 9.1 Hz, Ar-H), 7.45 (m, 5H, Ar-H), 8.00 (d, 1H, J = 9.1 Hz, Ar-H). ¹³C-NMR (125 MHz, CDCl₃): δ

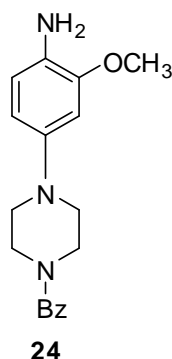
47.01, 56.23, 97.62, 105.75, 127.08, 128.61, 128.74, 130.16, 134.97, 155.23, 156.07, 170.55. Anal. Calcd for C₁₈H₁₉N₃O₄: C, 63.33; H, 5.61; and N, 12.31. Found: C, 63.26; H, 5.66; and N, 12.26.

4.3.10. Synthesis of (4-(3-(methoxymethoxy)-4-nitrophenyl) piperazin-1-yl)(phenyl)methanone (23)



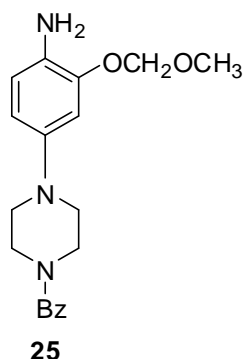
Following the same procedure adopted for the synthesis of **16**, the reaction of amine **8** with compound **21** (4.10 g, 21.39 mmol) afforded the title compound **23** as light yellow solid (7.34 g, 97%), m.p. 189-190 °C. IR (KBr): 3032, 1675, 1620, 1575, 1490, 1461, 1436, 1383, 1336, 1314, 1249, 1150, 1102, 1078, 1035 cm⁻¹. ¹H NMR (500 MHz, CDCl₃): δ 3.31-3.33 (br. s, 4H, -CH₂NCH₂-), 3.45 (s, 3H, -OCH₃), 3.85 (br. s, 4H, -CH₂NCH₂-), 5.21 (s, 2H, -OCH₂O-), 6.42 (dd, 1H, *J* = 2.4, 9.4 Hz, Ar-H), 6.56 (d, 1H, *J* = 2.4, Ar-H), 7.36 (m, 5H, Ar-H), 7.85 (d, 1H, *J* = 9.3 Hz, Ar-H). ¹³C NMR (125 MHz, CDCl₃): δ 46.99, 56.53, 67.02, 95.38, 101.37, 106.83, 126.91, 128.24, 128.42, 129.92, 134.87, 153.48, 154.77, 162.33, 170.28. Anal. Calcd for C₁₉H₂₁N₃O₅: C, 61.45; H, 5.70; and N, 11.31. Found: C, 61.41; H, 5.75; and N, 11.25.

4.3.11. Synthesis of (4-(4-Amino-3-methoxyphenyl)piperazin-1-yl)(phenyl)methanone (**24**)



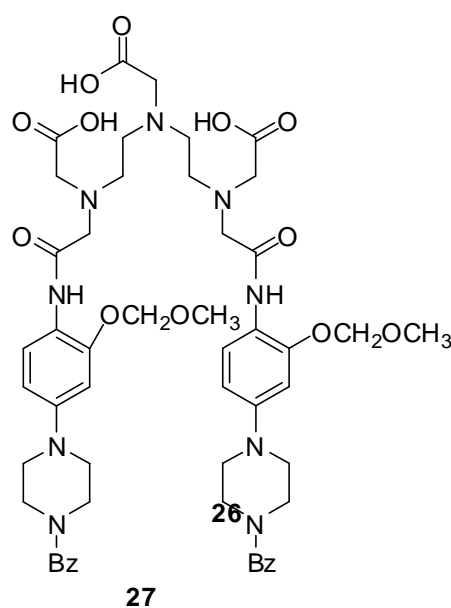
Following the same procedure adopted for the synthesis of **17**, the reduction of the nitro group of compound **22** (2.43 g, 7.12 mmol) afforded compound **24** as a dark brown thick oil (1.84 g, 83%). IR (KBr): 3447, 3346, 3058, 2917, 1673, 1629, 1518, 1438, 1386, 1323, 1282, 1245, 1197, 1170, 1093, 1034, 1015 cm^{-1} . $^1\text{H-NMR}$ (500 MHz, CDCl_3): δ 2.92 (br. s, 2H, $-\text{CH}_2\text{N}$), 3.07 (br. s, 2H, $-\text{CH}_2\text{N}$), 3.53 (br. s, 2H, $-\text{CH}_2\text{N}$), 3.79 (s, 3H, $-\text{OCH}_3$), 3.89 (br. s, 2H, $-\text{CH}_2\text{N}$), 6.37 (dd, 1H, $J = 2.4, 8.2$ Hz, Ar-H), 6.47 (d, 1H, $J = 2.4$, Ar-H), 6.59 (d, 1H, $J = 8.3$, Ar-H), 7.38 (m, 5H, Ar-H). $^{13}\text{C-NMR}$ (125 MHz, CDCl_3): δ 42.23, 47.80, 51.59, 51.81, 53.36, 55.35, 102.74, 109.98, 115.21, 126.96, 128.39, 129.64, 130.85, 135.56, 144.25, 147.85, 170.24. Anal. Calcd for $\text{C}_{18}\text{H}_{21}\text{N}_3\text{O}_2$: C, 69.43; H, 6.80; and N, 13.49. Found: C, 69.36; H, 6.87; and N, 13.42.

4.3.12. Synthesis of (4-(4-amino-3-(methoxymethoxy)phenyl)piperazin-1-yl)(phenyl)methanone (25)



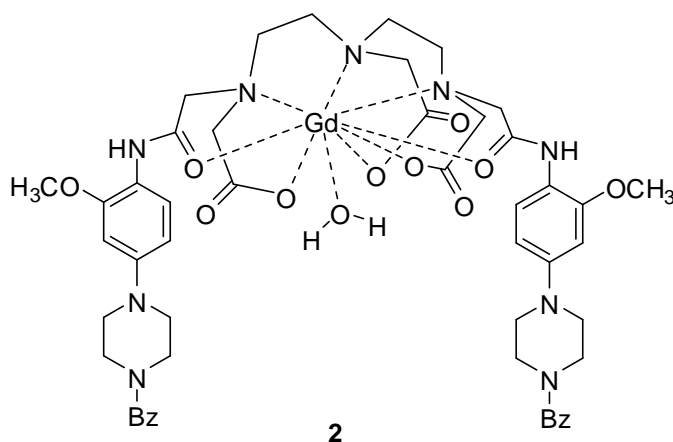
Following the same procedure adopted for the synthesis of **17**, the reduction of the nitro group of compound **23** (1.53 g, 4.12 mmol) afforded compound **25** as a dark purple thick oil (1.13 g, 80%). IR (KBr): 3447, 3352, 3010, 2953, 1671, 1628, 1516, 1436, 1366, 1325, 1284, 1241, 1214, 1150, 1074 cm^{-1} . $^1\text{H-NMR}$ (500 MHz, CDCl_3): δ 2.92 (br. s, 2H, $-\text{CH}_2\text{N}$), 3.08 (br. s, 2H, $-\text{CH}_2\text{N}$), 3.46-3.44 (m, 5H, $-\text{OCH}_3$, $-\text{CH}_2\text{N}$), 3.53 (br. s, 2H, $-\text{CH}_2\text{N}$), 3.89 (br. s, 2H, $-\text{NH}_2$), 5.13 (s, 2H, $-\text{OCH}_2\text{O}-$), 6.44 (dd, 1H, $J = 2.4, 8.3$ Hz, Ar-H), 6.61 (d, 1H, $J = 8.4$, Ar-H), 6.72 (d, 1H, $J = 2.4$ Hz, Ar-H), 7.38 (m, 5H, Ar-H). $^{13}\text{C-NMR}$ (125 MHz, CDCl_3): δ 42.18, 47.69, 51.40, 55.99, 95.25, 106.35, 111.64, 115.81, 126.95, 128.37, 129.63, 131.22, 135.53, 144.12, 145.52, 170.23. Anal. Calcd for $\text{C}_{19}\text{H}_{23}\text{N}_3\text{O}_3$: C, 66.84; H, 6.79; and N, 12.31. Found: C, 66.77; H, 6.86; and N, 12.24.

4.3.14. Synthesis of 2,2'-(2,2'-(carboxymethylazanediy)bis(ethane-2,1-diy)bis((2-(4-(4-benzoylpiperazin-1-yl)-2-(methoxymethoxy)phenylamino)-2-oxoethyl)azanediy))diacetic acid (27)



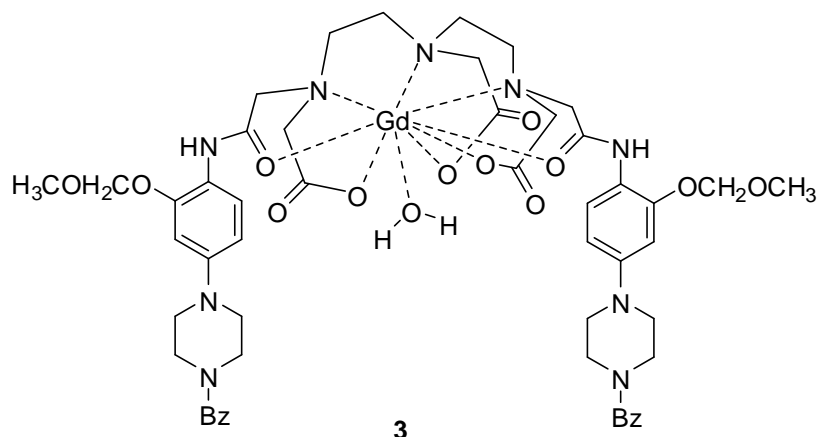
Following the same procedure adopted for the synthesis of **18**, condensation of compound **25** (0.26 g, 0.76 mmol) with DTPAA afforded compound **27** as a white powder (0.15 g, 38%), m.p. 165-167 °C. IR (KBr): 3452, 3021, 2929, 1722, 1626, 1536, 1443, 1389, 1285, 1201, 1153, 1089, 1031, 1015 cm^{-1} . $^1\text{H-NMR}$ (500 MHz, DMSO-d_6): δ 2.74-2.82 (br. s, 4H), 2.95-3.13 (m, 6H), 3.29-3.70 (m, 24H), 3.73 (s, 6H, - OCH_3), 5.19 (s, 4H, - OCH_2O -), 6.54 (dd, 2H, $J = 2.6, 8.6$ Hz, Ar-H), 6.72 (d, 2H, $J = 2.5$, Ar-H), 7.44 (m, 10H, Ar-H), 7.92 (d, 2H, $J = 8.5$ Hz, Ar-H), 9.50 (s, 2H). $^{13}\text{C-NMR}$ (125 MHz, DMSO-d_6): δ 49.09, 52.36, 55.89, 59.00, 94.54, 103.68, 109.01, 120.84, 126.99, 128.45, 129.59, 135.81, 147.10, 169.04. Anal. Calcd for $\text{C}_{52}\text{H}_{65}\text{N}_9\text{O}_{14} \cdot \text{H}_2\text{O}$: C, 59.02; H, 6.38; and N, 11.91. Found: C, 58.96; H, 6.44; and N, 11.85. FAB-MS (m/z): calcd for $\text{C}_{52}\text{H}_{65}\text{N}_9\text{O}_{14}$, 1039.47 ($[\text{MH}]^+$). Found: 1039.3 ($[\text{MH}]^+$).

4.3.15. Synthesis of complex (2)



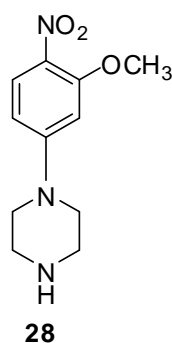
To a solution of compound **26** (0.30 g, 0.31 mmol) in pyridine (15 mL) was added $\text{GdCl}_3 \cdot 6\text{H}_2\text{O}$ (0.11 g, 0.30 mmol) and the reaction mixture was stirred at 90 °C for 8 hours. The mixture was filtered through a pad of celite while hot and the filtrate was concentrated under reduced pressure. The residue was added drop wise to cold acetone (25 ml) and the precipitated product was filtered, dried under reduced pressure to afford compound **1** as a white amorphous solid (0.25 g, 70%), m.p. > 300 °C. IR (KBr): 3426, 3036, 2973, 1641, 1438, 1324, 1251, 1202, 1153, 1092, 1007 cm^{-1} . Anal. Calcd for $\text{C}_{50}\text{H}_{58}\text{GdN}_9\text{O}_{12} \cdot 4\text{H}_2\text{O}$: C, 49.78; H, 5.51; and N, 10.45. Found: C, 49.71; H, 5.57; and N, 10.38. FAB-MS (m/z): calcd for $\text{C}_{50}\text{H}_{58}\text{GdN}_9\text{O}_{12}$, 1134.34 ($[\text{MH}]^+$). Found: 1134.3 ($[\text{MH}]^+$).

4.3.16. Synthesis of complex (3)



Following the same procedure adopted for the synthesis of complex **2**, condensation of ligand **27** (0.15 g, 0.14 mmol) with GdCl₃ • 6H₂O afforded complex **3** as light purple amorphous solid (0.14 g, 82%). m.p. > 300 °C. IR (KBr): 3480, 3042, 2914, 1631, 1437, 1322, 1245, 1153, 1090 cm⁻¹. Anal. Calcd for C₅₂H₆₂GdN₉O₁₄ • 4H₂O: C, 49.32; H, 5.57; and N, 9.95. Found: C, 49.25; H, 5.64; and N, 9.88. FAB-MS (*m/z*): calcd for C₅₂H₆₂GdN₉O₁₄, 1194.37 ([MH]⁺). Found: 1194.3 ([MH]⁺).

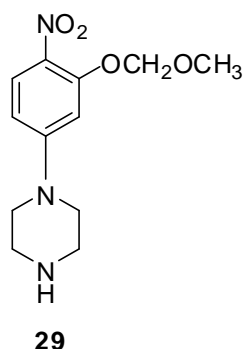
4.3.17. Synthesis of 1-(3-Methoxy-4-nitrophenyl)piperazine (28)



To a solution of compound **22** (2.08 g, 6.10 mmol) in ethanol (20 ml) was added 3M KOH solution (20.33 ml, 61.0 mmol) and mixture was left stirring for 8 hours at 60 °C. After completion of the reaction, the reaction was cooled to room temperature, DCM (30 ml) was added, and the solution was then transferred to a separation funnel.

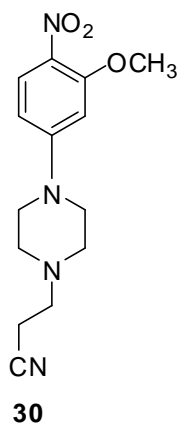
The solution was washed with H₂O (10 ml) and the organic layer was collected, dried over CaSO₄ and evaporated under vacuum to afford **28** as a dark yellow powder (1.09 g, 75.31%). MP: 126-129 °C. IR (KBr): 3429, 3339, 2833, 1908, 1606, 1575, 1509, 1481, 1392, 1335, 1312, 1290, 1250, 1144, 1098, 1019, 972, 817, 747, 655, 612, 571, 528 cm⁻¹. ¹H NMR (500 MHz, CDCl₃) δ: 1.95 (br s, 1H), 3.00 (t, 4H, J = 5.19 Hz), 3.36 (t, 4H, J = 5.21 Hz), 3.93 (s, 3H), 6.30 (s, 1H), 6.39 (dd, 1H, J₁ = 10.38 Hz, J₂ = 5.19), 7.93 (d, 1H, J = 9.16 Hz). ¹³C NMR (125 MHz, CDCl₃) δ: 14.27, 45.31, 46.84, 47.68, 64.74, 96.27, 104.90, 128.12, 128.34, 155.56, 156.02.

4.3.18. Synthesis of 1-(3-(Methoxymethoxy)-4-nitrophenyl) piperazine (**29**)



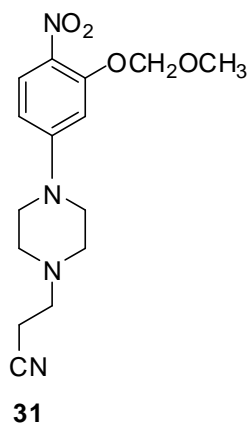
Following the same procedure adopted for the synthesis of compound **28**, hydrolysis of compound **23** (2.23 g, 6.01 mmol) with 3M KOH afford the title compound **29** as a brown paste (1.29 g, 80.39%). IR (KBr): 3429, 2928, 2794, 1898, 1603, 1552, 1487, 1409, 1333, 1245, 1150, 1095, 1046, 1011, 986, 957, 814, 747, 710, 620 cm⁻¹. ¹H NMR (500 MHz, CDCl₃) δ: 2.90 (s, 4H), 3.25 (s, 4H), 3.44 (s, 3H), 5.20 (s, 2H), 6.37 (d, 1H, J = 9.46 Hz), 6.51 (s, 1H), 7.83 (d, 1H, J = 9.16 Hz). ¹³C NMR (125 MHz, CDCl₃) δ: 39.83, 45.32, 47.69, 56.36, 95.29, 100.53, 106.28, 126.79, 127.99, 129.72, 153.55, 155.39.

4.3.19. Synthesis of 3-(4-(3-Methoxy-4-nitrophenyl)piperazin-1-yl)propanenitrile (**30**)



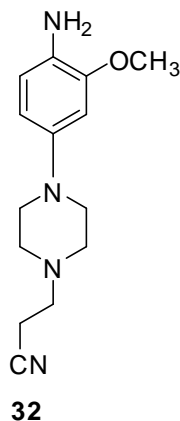
To a solution of compound **28** (1.94 g, 8.2 mmol) in ethanol (30 ml) at 0 °C was added triethylamine (2.50 mL, 18.0 mmol) followed by the addition of acrylonitrile (1.18 mL, 18.0 mmol). The reaction mixture was stirred for 3 h at 55 °C and then cooled to room temperature. The crystallized product was filtered by suction, washed with diethyl ether and dried under vacuum to afford **30** as a light yellow powder. Yield: 71%. Anal. Calcd for C₁₄H₁₈N₄O₃: C, 57.92; H, 6.25; and N, 19.30. Found: C, 57.88; H, 6.29; and N, 19.22. Melting point: 210-211 °C (decomp). IR (KBr): 3035, 2952, 2250, 1604, 1569, 1512, 1483, 1446, 1337, 1251, 1236, 1090, 1013 cm⁻¹. ¹H NMR (500 MHz, CDCl₃): δ = 2.57 (t, 2H, J = 6.7 Hz, -CH₂CN), 2.67 (br. s, 4H, -CH₂NCH₂-), 2.76 (t, 2H, J = 6.7 Hz, -CH₂N), 3.42 (br. s, 4H, -CH₂NCH₂-), 3.95 (s, 3H, -OCH₃), 6.33 (d, 1H, 3.1 Hz, Ar-H), 6.38 (dd, 1H, J = 2.1, 9.2 Hz, Ar-H), 7.96 (d, 1H, J = 9.3 Hz, Ar-H). ¹³C NMR (125 MHz, CDCl₃): δ = 16.06, 47.03, 52.14, 53.08, 56.20, 97.22, 105.57, 118.49, 128.75, 129.76, 155.44, 156.21.

4.3.20. Synthesis of 3-(4-(3-(Methoxymethoxy)-4-nitrophenyl) piperazin-1-yl)propanenitrile (31)



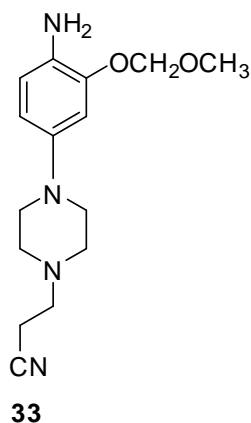
Following the same procedure adopted for the synthesis of **30**, the reaction of amine **29** with acrylonitrile afforded the title compound **31** as light yellow solid. Yield: 59%. Anal. Calcd for $C_{15}H_{20}N_4O_4$: C, 56.24; H, 6.29; and N, 17.49. Found: C, 56.19; H, 6.34; and N, 17.43. Melting point: 215-216 °C (decomp). IR (KBr): 3030, 2962, 2249, 1605, 1569, 1510, 1483, 1448, 1337, 1253, 1235, 1090, 1013 cm^{-1} . 1H NMR (500 MHz, $CDCl_3$): δ = 2.49 (t, 2H, J = 6.7 Hz, $-CH_2CN$), 2.58 (m, 4H, $-CH_2NCH_2-$), 2.68 (t, 2H, J = 6.7 Hz, $-CH_2N$), 3.33 (m, 4H, $-CH_2NCH_2-$), 3.90 (s, 3H, $-OCH_3$), 5.22 (s, 2H, $-OCH_2O-$), 6.40 (d, 1H, 3.1 Hz, Ar-H), 6.56 (dd, 1H, J = 2.2, 9.2 Hz, Ar-H), 7.88 (d, 1H, J = 9.4 Hz, Ar-H). ^{13}C NMR (125 MHz, $CDCl_3$): δ = 16.02, 46.94, 52.11, 53.06, 56.67, 95.52, 101.21, 106.78, 128.30, 153.77, 155.13.

4.3.21. Synthesis of 3-(4-(4-Amino-3-methoxyphenyl)piperazin-1-yl)propanenitrile (32)



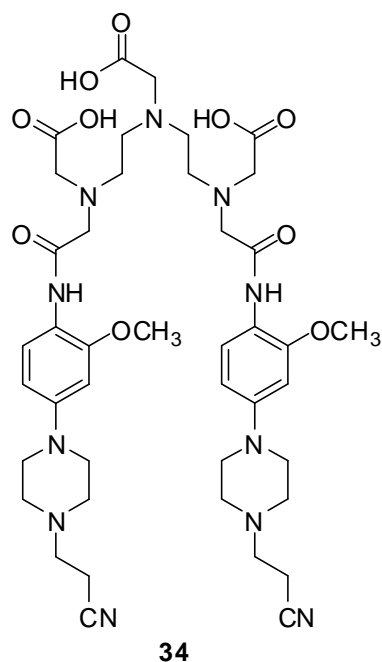
Following the same procedure adopted for the synthesis of **17**, the reduction of the nitro group of compound **30** (1.52 g, 5.24 mmol) afforded the title compound **32** as a light purple thick oil. Yield: 88%. Anal. Calcd for $C_{14}H_{20}N_4O$: C, 64.59; H, 7.74; and N, 21.52. Found: C, 64.53; H, 7.80; and N, 21.42. IR (KBr): 3407, 3303, 3013, 2940, 2248, 1592, 1515, 1449, 1424, 1377, 1341, 1139, 1098, 1033 cm^{-1} . 1H NMR (500 MHz, $CDCl_3$): δ = 2.49 (t, 2H, J = 7.0 Hz, $-CH_2CN$), 2.62 (t, 4H, J = 5.0 Hz, $-CH_2NCH_2-$), 2.69 (t, 2H, J = 7.0 Hz, $-CH_2N$), 3.02 (t, 4H, J = 5.0 Hz, $-CH_2NCH_2-$), 3.51 (br. s, 2H, NH_2), 3.83 (s, 3H, $-OCH_3$), 6.36 (dd, 1H, J = 2.4, 8.2 Hz, Ar-H), 6.46 (d, 1H, J = 2.4 Hz, Ar-H), 6.60 (d, 1H, J = 8.2 Hz, Ar-H). ^{13}C NMR (125 MHz, $CDCl_3$) δ : 15.38, 50.68, 52.40, 52.87, 55.11, 102.00, 109.19, 115.09, 118.54, 130.17, 144.20, 147.61, 165.47.

4.3.22. Synthesis of 3-(4-(4-amino-3-(methoxymethoxy)phenyl) piperazin-1-yl)propanenitrile (33)



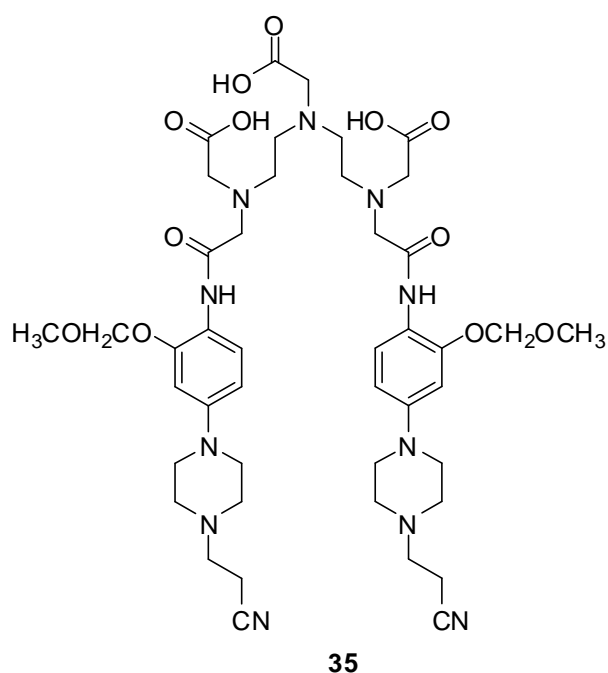
Following the same procedure adopted for the synthesis of **17**, the reduction of the nitro group of nitrile **31** afforded compound **33** as a light brown oil. Yield: 84%. Anal. Calcd for $C_{15}H_{22}N_4O_2$: C, 62.05; H, 7.64; and N, 19.30. Found: C, 62.00; H, 7.69; and N, 19.24. IR (KBr): 3443, 3359, 2949, 2249, 1591, 1517, 1454, 1378, 1337, 1241, 1215, 1174, 1075 cm^{-1} . 1H NMR (500 MHz, $CDCl_3$): δ = 2.46 (t, 2H, J = 6.7 Hz, $-CH_2CN$), 2.59 (br. s, 4H, $-CH_2NCH_2-$), 2.68 (t, 2H, J = 6.7 Hz, $-CH_2N$), 2.99 (br. s, 4H, $-CH_2NCH_2-$), 3.42 (s, 3H, $-OCH_3$), 4.54 (br. s, 2H, NH_2), 6.38 (dd, 1H, 2.4, 8.2 Hz, Ar-H), 6.59 (d, 1H, J = 8.2 Hz, Ar-H), 6.68 (d, 1H, J = 2.3 Hz, Ar-H). ^{13}C NMR (125 MHz, $CDCl_3$): δ = 15.69, 50.70, 52.67, 53.18, 56.02, 95.18, 105.94, 111.09, 115.93, 118.65, 126.98, 130.66, 144.48, 145.63, 166.77.

4.3.23. Synthesis of 2,2'-(2,2'-(carboxymethylazanediy)bis(ethane-2,1-diyl)bis((2-(4-(4-(2-cyanoethyl)piperazin-1-yl)-2-methoxyphenylamino)-2-oxoethyl)-azanediy))diacetic acid (34)



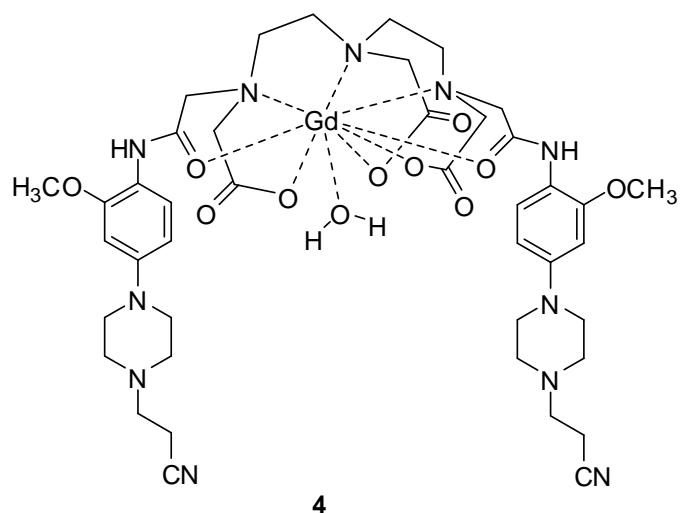
Following the same procedure adopted for the synthesis of **18**, condensation of compound **32** (0.26 g, 0.76 mmol) with DTPAA afforded compound **34** as a gray powder. Yield: 51%. Anal. Calcd for C₄₂H₅₉N₁₁O₁₀: C, 57.46; H, 6.77; and N, 17.55. Found: C, 57.39; H, 6.83; and N, 17.47. Melting point: 141-142 °C. IR (KBr): 3462, 2959, 2836, 2252, 1706, 1664, 1534, 1453, 1420, 1396, 1239, 1202, 1174, 1135, 1090, 1029 cm⁻¹. ¹H NMR (500 MHz, *d*₆-DMSO): δ = 2.55 (m, 4H), 2.62-2.68 (m, 8H), 2.71-2.81 (m, 12H), 3.02 (m, 8H), 3.21-3.33 (m, 12H), 3.77 (s, 6H, -OCH₃), 6.35 (d, 2H, J = 8.2 Hz, Ar-H), 6.52 (d, 2H, J = 2.4 Hz, Ar-H), 7.80 (dd, 2H, J = 2.5, 8.2 Hz, Ar-H), 9.32 (s, 2H). ¹³C NMR (125 MHz, *d*-DMSO): δ = 14.98, 30.70, 36.24, 48.70, 52.12, 52.36, 52.72, 54.81, 55.48, 55.69, 59.05, 99.95, 106.85, 120.06, 148.23, 149.66, 162.37, 168.40, 171.61, 172.40.

**4.3.24. Synthesis of 2,2'-(2,2'-(carboxymethylazanediy)bis
(ethane-2,1-diyl)bis((2-(4-(4-(2-cyanoethyl)piperazin-1-yl)-2-
(methoxymethoxy)phenylamino)-2-oxoethyl)azanediyl))diacetic
acid (35)**



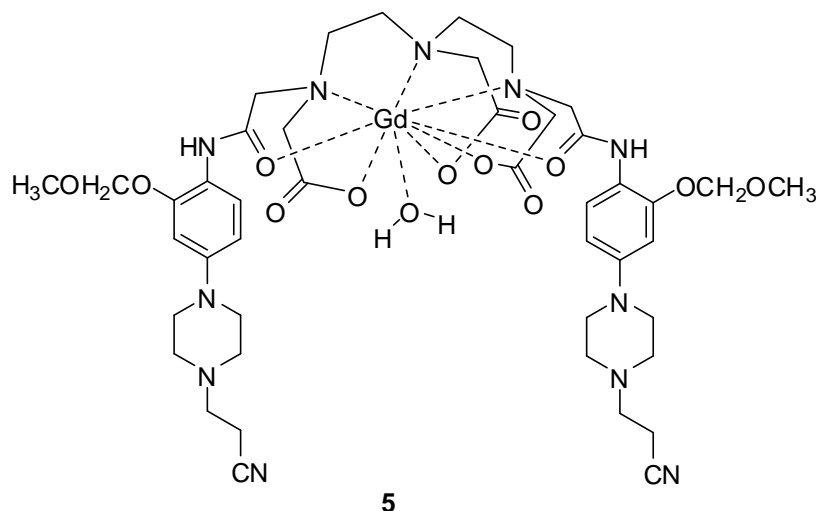
Following the same procedure adopted for the synthesis of **18**, condensation of compound **33** with DTPAA afforded compound **35** as a light purple powder. Yield: 63%. Anal. Calcd for $C_{44}H_{63}N_{11}O_{12}$: C, 56.34; H, 6.77; and N, 16.43. Found: C, 56.27; H, 6.85; and N, 16.36. Melting point: 156-157 °C. IR (KBr): 3503, 2964, 2256, 1729, 1530, 1396, 1219, 1079 cm^{-1} . 1H NMR (500 MHz, d_6 -DMSO): δ = 2.55 (m, 4H), 2.65-2.71 (m, 8H), 2.70-2.87 (m, 12H), 3.05 (m, 8H), 3.33-3.43 (m, 16H), 5.20 (s, 4H, -OCH₂O-), 6.52 (d, 2H, J = 8.1 Hz, Ar-H), 6.68 (d, 2H, J = 2.8 Hz, Ar-H), 7.46 (dd, 2H, J = 2.7, 8.1 Hz, Ar-H), 7.92 (s, 2H), 9.42 (s, 2H). ^{13}C NMR (125 MHz, d -DMSO): δ = 14.96, 30.72, 35.82, 48.62, 51.67, 52.05, 52.40, 52.67, 54.81, 54.98, 55.57, 55.90, 94.56, 103.09, 108.46, 120.02, 162.36, 168.47, 172.37, 172.60.

4.3.25. Synthesis of complex (4)



Following the same procedure adopted for the synthesis of complex **2**, condensation of ligand **34** (0.100 g, 0.114 mmol) with Gd₂O₃ (0.021 g, 0.057 mmol) afforded complex **4** as a light blue solid. Yield: 89%. Anal. Calcd for C₄₂H₅₆GdN₁₁O₁₀ • 4H₂O: C, 45.68; H, 5.84; and N, 13.95. Found: C, 45.62; H, 5.90; and N, 13.89. FAB-MS (*m/z*): calcd for C₄₂H₅₆GdN₁₁O₁₀, 1032.35 ([MH]⁺). Found: 1032.35 ([MH]⁺). Melting point: > 300 °C. IR (KBr): 3444, 3030, 2927, 2250, 1611, 1456, 1399, 1323, 1250, 1204, 1135, 1093 cm⁻¹.

4.3.26. Synthesis of complex (5)



Following the same procedure adopted for the synthesis of complex **2**, condensation of ligand **35** with Gd₂O₃ afforded complex **5** as light purple solid. Yield: 83%. Anal. Calcd for C₄₄H₆₀GdN₁₁O₁₂ · 4H₂O: C, 45.39; H, 5.89; and N, 13.23. Found: C, 45.32; H, 5.95; and N, 13.26. FAB-MS (*m/z*): calcd for C₄₄H₆₀GdN₁₁O₁₂, 1092.37 ([MH]⁺). Found: 1092.37 ([MH]⁺). Melting point: > 300 °C. IR (KBr): 3486, 3012, 2845, 2253, 1616, 1403, 1322, 1246, 1123, 1090, 990 cm⁻¹.

4.4. X-ray Photoelectron Spectroscopy

The experiment was performed in a Thermo Scientific Escalab 250Xi spectrometer equipped with a monochromated Al *K*_α (1486.6 eV) x-ray source. A low-energy electron flood gun was used for surface charge compensation. The spectrometer energy was calibrated by fixing Cu 2p_{3/2}, Ag 3d_{5/2} and Au 4f_{7/2} peaks at binding energies of 932.6, 368.2 and 83.9 eV, respectively [31]. The electron energy analyzer was operated in constant pass energy of 30 eV and the electron take off angle was 90⁰. The instrumental energy resolution was 0.5 eV with x-ray spot size of 650-μm diameter. The base pressure in the analysis chamber was 5.0×10⁻¹⁰ mbar. The spectra were

referenced with C-C 1s peak at 284.8 eV. Avantage software and OriginLab 9.0 was used for all data processing.

4.5. Cytotoxicity Study Assay

Toxicity for chelates (**2-5**) was analyzed on adherent 3T3 mouse embryonic fibroblastic cells by MTT assay following Mesaik et al. [32] with some modification. In brief cells were incubated at $6 \times 10^4 \text{ ml}^{-1}$ concentration in 96 well flat bottom plate in 5% CO₂ and 37 °C for 24 h. After adherence of cells, compounds were added at concentration 10 µg/ml for further 48 h incubation. On day 3 tetrazolium dye MTT was added. After 4 h of incubation media was removed and organic solvent DMSO was added to dissolve insoluble purple formazan. Absorbance was taken at 540 nm using spectrophotometer and the % viability of cells was calculated.

CHAPTER 5

CONCLUSION AND FUTURE WORK

In conclusion, four new Gd(III) complexes **2-5** of the type $[\text{Gd}(\text{L})\text{H}_2\text{O}] \cdot n\text{H}_2\text{O}$ have been synthesized. Complexes **2** and **3** are water insoluble whereas **4** and **5** are water soluble. The relaxivity of **2** and **3** were slightly lower compare to Omniscan®, a commercially available MRI contrast agent. The lower relaxivity of **2** and **3** was attributed to their lower solubility in water. The water solubility of these complexes may be increased by incorporating polar functions in the aromatic ring, which in turn, may improve their relaxivity. On the other hand, **4** and **5** gave a higher relaxivity compare to Omniscan®. The highest relaxivity of **5**, among the synthesized complexes, is attributed to the increase in solubility owing to the presence MOM function in the aromatic ring. The cytotoxicity studies of these complexes revealed that they are non-toxic which warrant their potential and physiological suitability as MRI contrast agents. For the future work, following studies on these complexes are recommended:

1. Stability constant determination to know stability of these complexes in the human body. Stability in the human body is one of the key factors that should be considered in the process of designing drugs and pharmaceuticals.
2. In vivo toxicity studies to determine the maximum dosage that can be administered without causing harm to the patient.
3. In vivo MRI studies to determine the activity of these complexes under MR machine in a living subject such as mice.

References

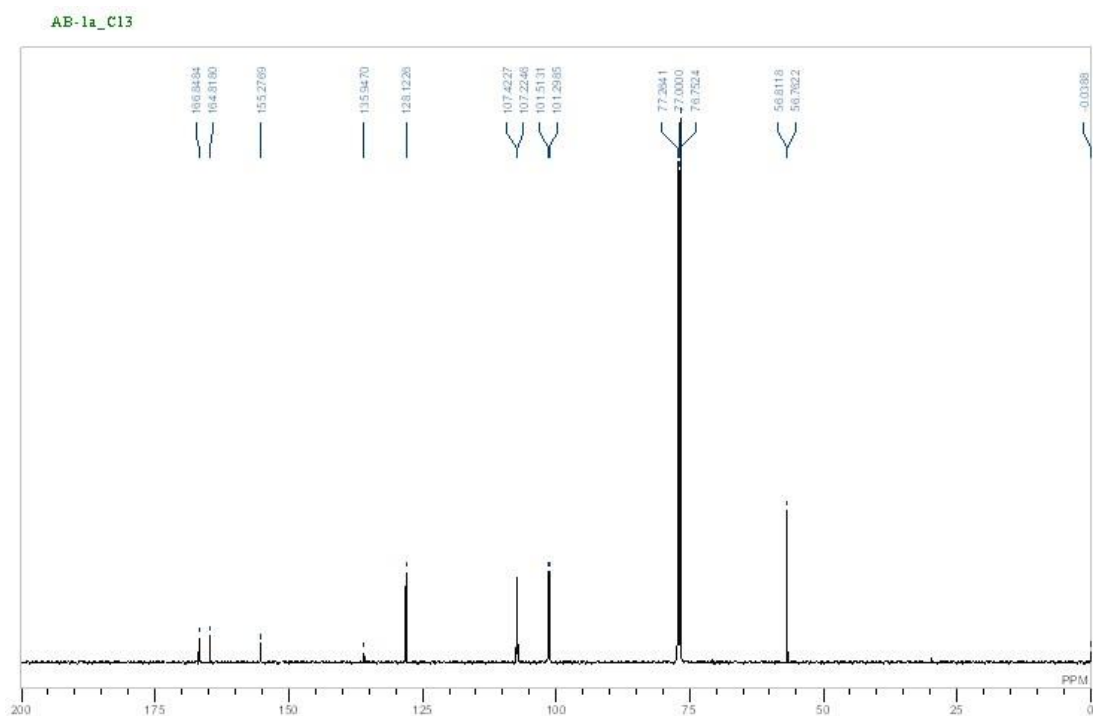
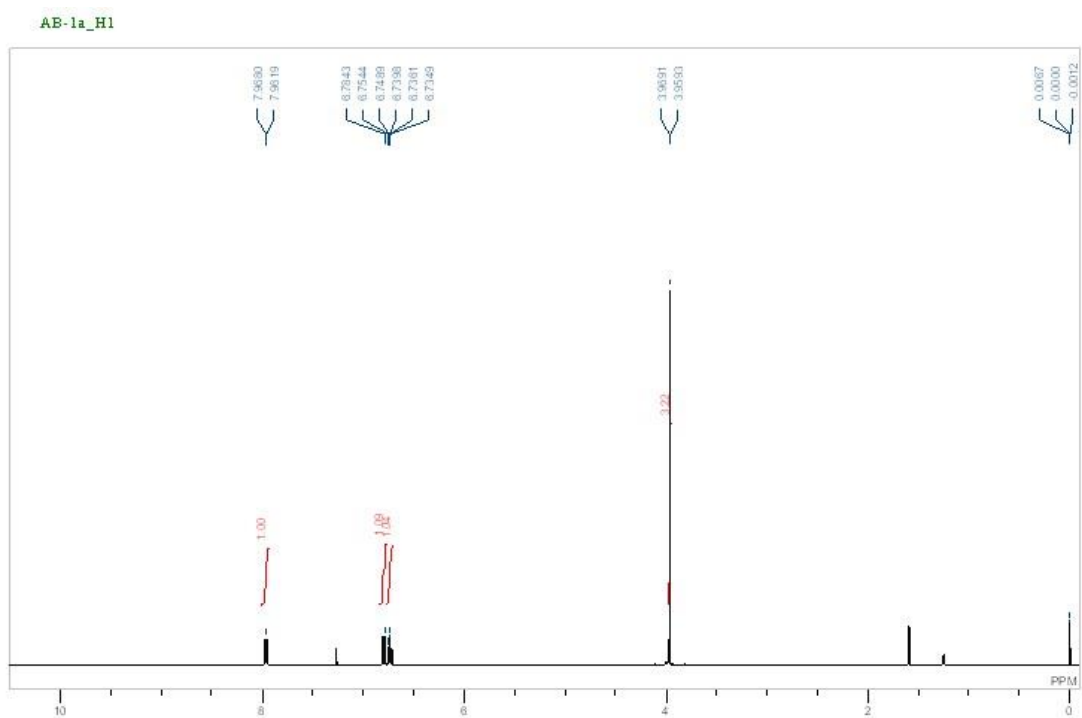
1. Bloch, F. *Phys. Rev.* (1946), 70, 460.
2. Purcell, E.M; Torrey, H.C; Pound, R.V. *Phys. Rev.* (1946), 69, 37.
3. Smith, H.J, *Tidsskr Nor Laegeforen.* (2003), 123(23), 3352.
4. Runge V.M, Clanton J.A, Lukehart C.M, Partain C.L, James A.E.: *Am. J. Roentgenol.* (1983), 141, 1209.
5. Sarka L., Burai L., Brucher E.: *Chem. Eur. J.*, (2000), 6, 719.
6. Caillie J.M, Lemanceau B, Bonnemain B.: *Am. J. Neuroradiol.* (1983), 4, 1041.
7. Bousequet J.C., Saini S., Stark D., Halm P.: *Radiology*, (1998), 166, 693.
8. Shellock, F. G.; Kanal, E. *J. Magn. Reson. Imaging* (1999), 10, 477.
9. G. M. Lanza, P. M. Winter, S. D. Caruthers et al., *J. Nucl. Cardiol.*, (2004), 11(6), 733–743.
10. A. E. Merbach and É. Tóth, in *The Chemistry of Contrast Agents in Medical Magnetic Resonance Imaging Ed 2nd*, John Wiley & Sons, Chichester, 2013.
11. Elemento, Elisa (2008) *New gadolinium contrast agents for MRI*, Durham theses, Durham University.
12. J. Peters, J. Huskens and D. J. Raber, *Prog. Nucl. Magn. Reson. Spectrosc.*, (1996), 28, 283-350.
13. I. Solomon and N. Bloembergen, *J. Chem. Phys.*, (1956), 25, 261-266.
14. Caravan, P; Ellison, J.J; McMurry, T.J; Lauffer, R.B. *Chem Rev.* (1999), 99(9), 2293.
15. Evans, C. *Biochemistry of the Lanthanides*; Plenum Press: New York, (1990).
16. Tweedle M.F., Hagan J.J., Kumar K., Mentha S., Chang C.A.: *Magn. Reson. Imaging*, (1991), 9, 409.
17. Chang, C. *InVest. Radiol.* (1993), 28, 521.

18. Palasz A., Czekaj P. *Acta Biochim. Pol.*, (2000), *47*, 1107.
19. Loncin J.F, Desreux J.F, Merciny E. *Inorg. Chem.*, (1986), *25*, 2644.
20. Ching-Hui H., Kido N., Al Zaki A., Brechbiel M. W., Tsourkas A. *ACS NANO*, (2012), *6*, 9416-9424.
21. Zhang D., Zhang X., Lin Z., Zhang H., Chen Y., He S. *Inorg. Chem. Commun.*, (2014), *40*, 66–68.
22. Dutta, S.; Kim, S.-K.; Patel, D. B.; Kim, T.-J.; Chang, Y. *Polyhedron* 2007, *26*, 3799.
23. Nisar Ullah, *Medicinal Chemistry*, (2014), *10*, 484-496.
24. D.J. Hnatowich, W.W. Layne, R.L. Childs, *Appl. Radiat. Isot.*, (1982), *33*, 327-332.
25. Chun Han, Ledong Wan, Hongbin Ji, Ke Ding, Zhangjian Huang, Yisheng Lai, Sixun Peng, Yihua Zhang, *Eur. J. Med. Chem.*, (2014), *77*, 75-83.
26. Major Gooyit, Mijoon Lee, Valerie A. Schroeder, Masahiro Ikejiri, Mark A. Suckow, Shahriar Mobashery, Mayland Chang, *J. Med. Chem.*, (2011), *54* (19), 6676–6690.
27. J.F. Moulder, W.F. Stickle, P.E. Sobol, K.D. Bomben, *Handbook of XPS*, Perkin-Elmer Corp, Eden Prairie, MN, (1992).
28. Ki-Hye Jung, Hee-Kyung Kim, Gang Ho Lee, Duk-Sik Kang, Ji-Ae Park, Kyeong Min Kim, Yongmin Chang, Tae-Jeong Kim, *J. Med. Chem.*, (2011), *54*, 5385–5394.
29. Sanjeev K. Verma, B. N. Acharya, and M. P. Kaushik, *Org. Lett.*, (2010), *12*, 4232-4235.
30. Debroye, E., Eliseeva, S. V., Laurent, S., Vander Elst, L., Petoud, S., Muller, R. N., Parac-Vogt, T. N. *Eur. J. Inorg. Chem.*, (2013), 2629-2639.

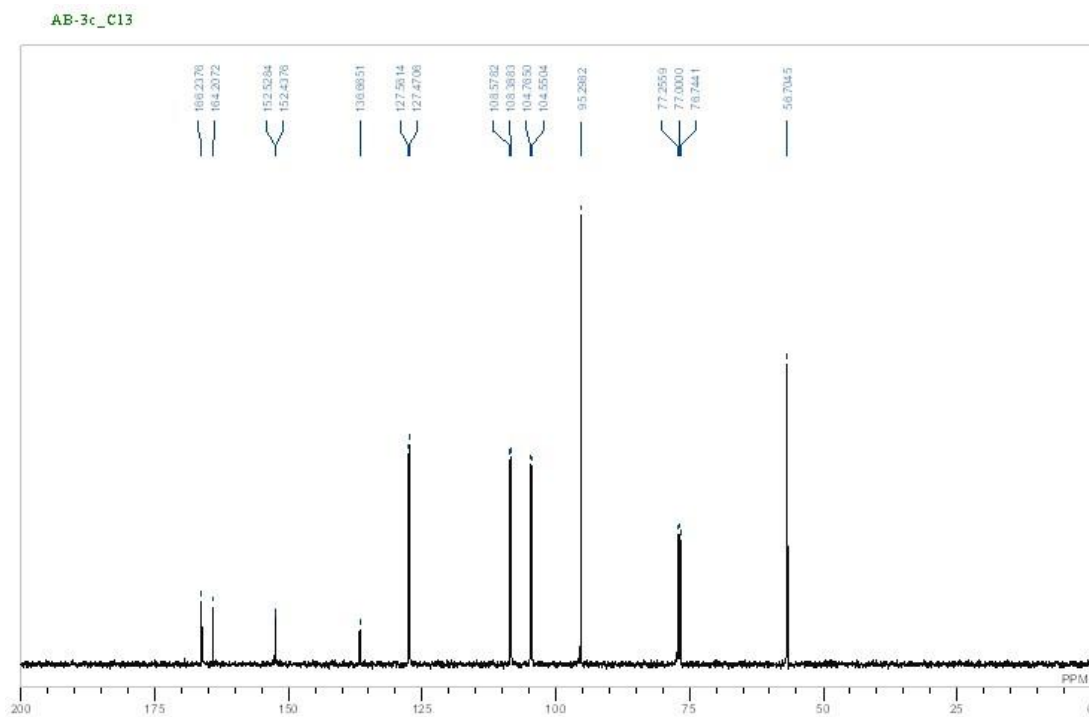
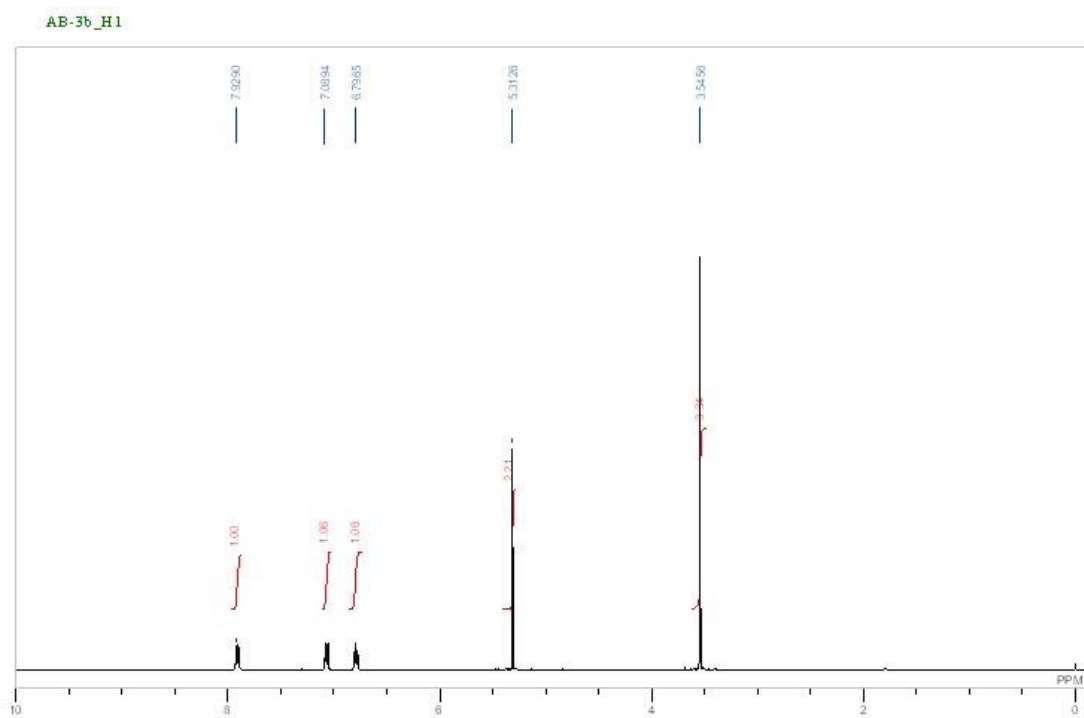
31. Briggs D, Seah MP, *Practical Surface Analysis* vol. 1 (2nd ed.), Wiley: New York, (1990).
32. M.A. Mesaik, Z. Haq, S. Murad, Z. Ismail, N.R. Abdullah, H.K. Gill, A. Rahman, M. Yousaf, R.A. Siddiqui, A. Ahmad and M.I. Choudhary, *Molecular Immunol.* 43 (2006), 1855–1863.

Appendices

Appendix A (4-fluoro-2-methoxy-1-nitrobenzene):

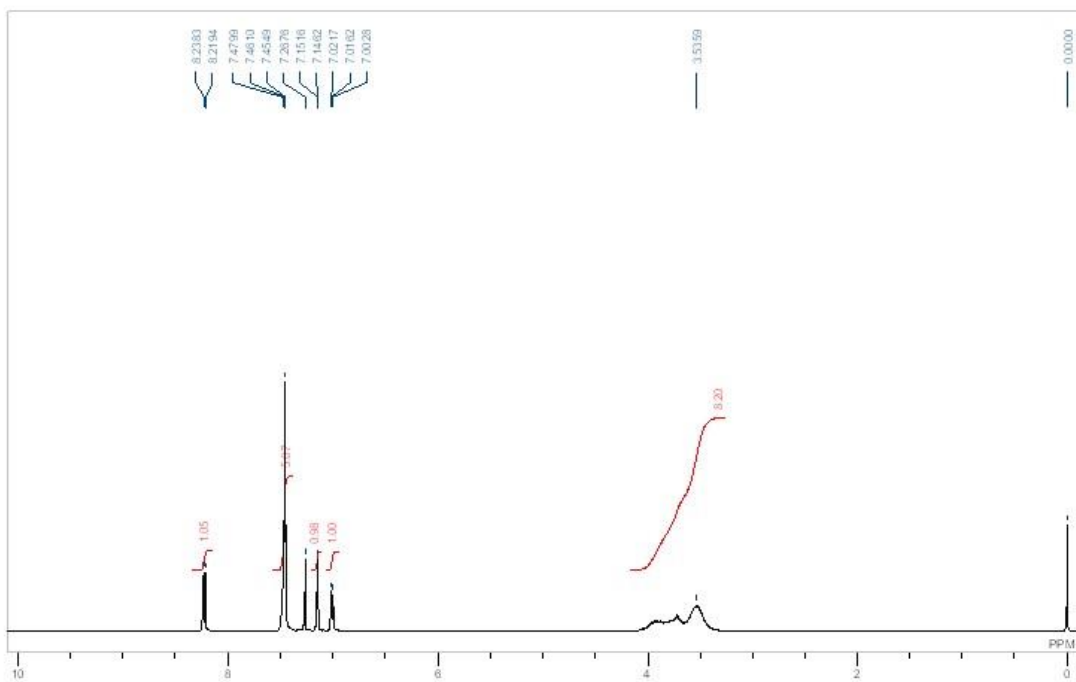


Appendix B (4-fluoro-2-(methoxymethoxy)-1-nitrobenzene):

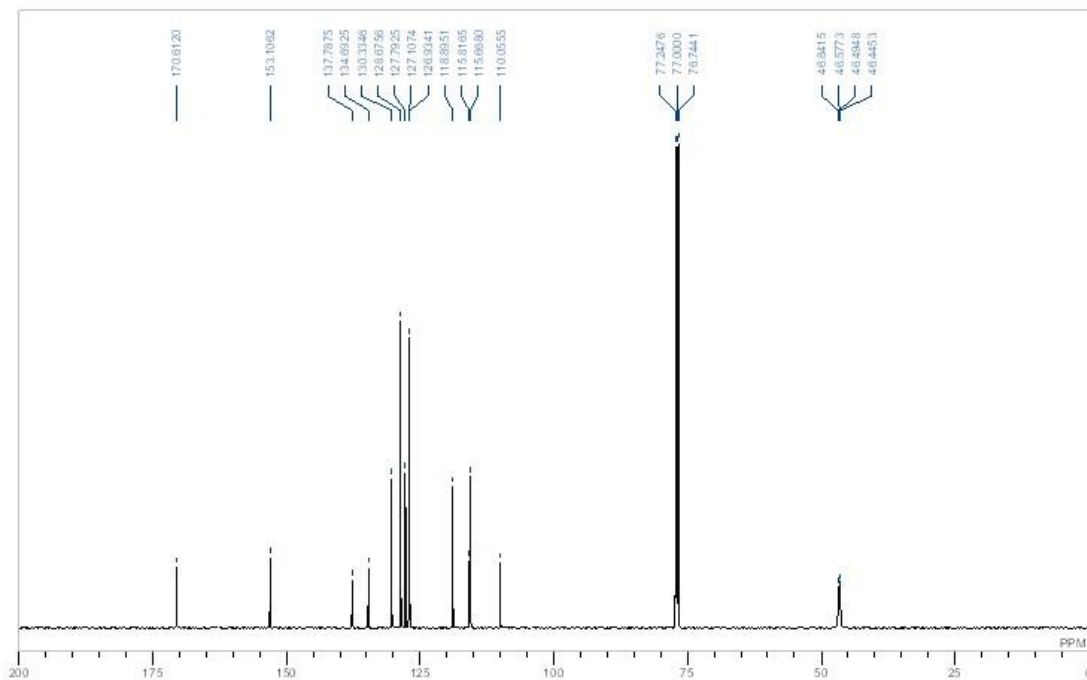


Appendix C (4-(4-benzoylpiperazin-1-yl)-2-nitrobenzonitrile):

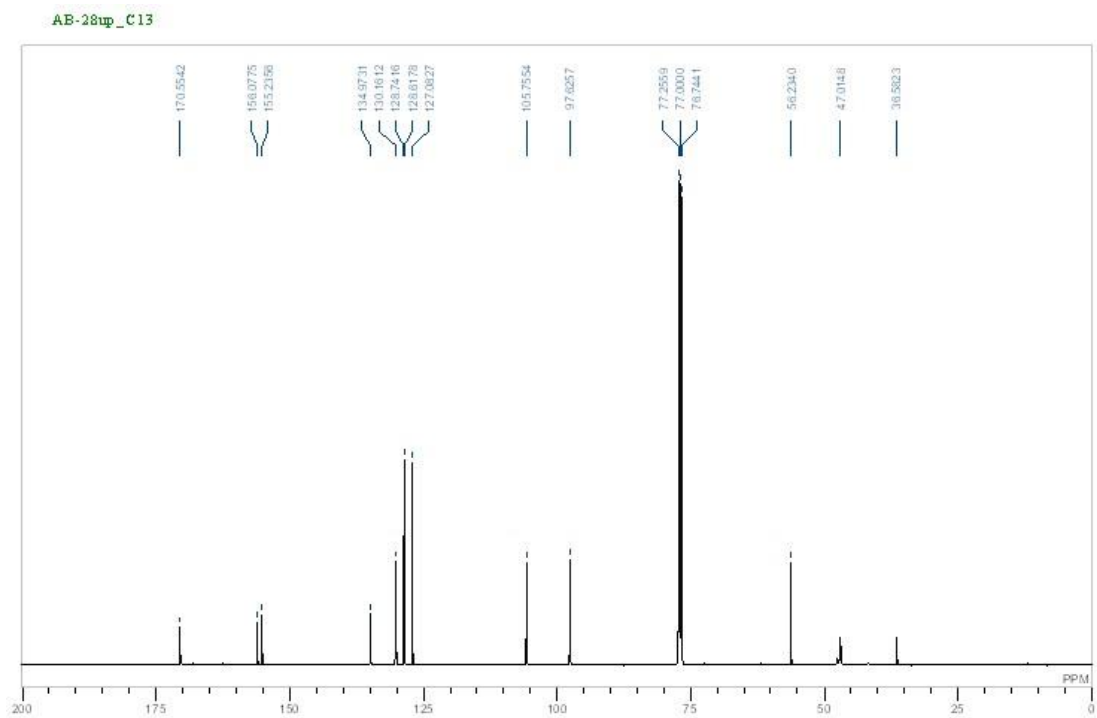
AB-27b_H1



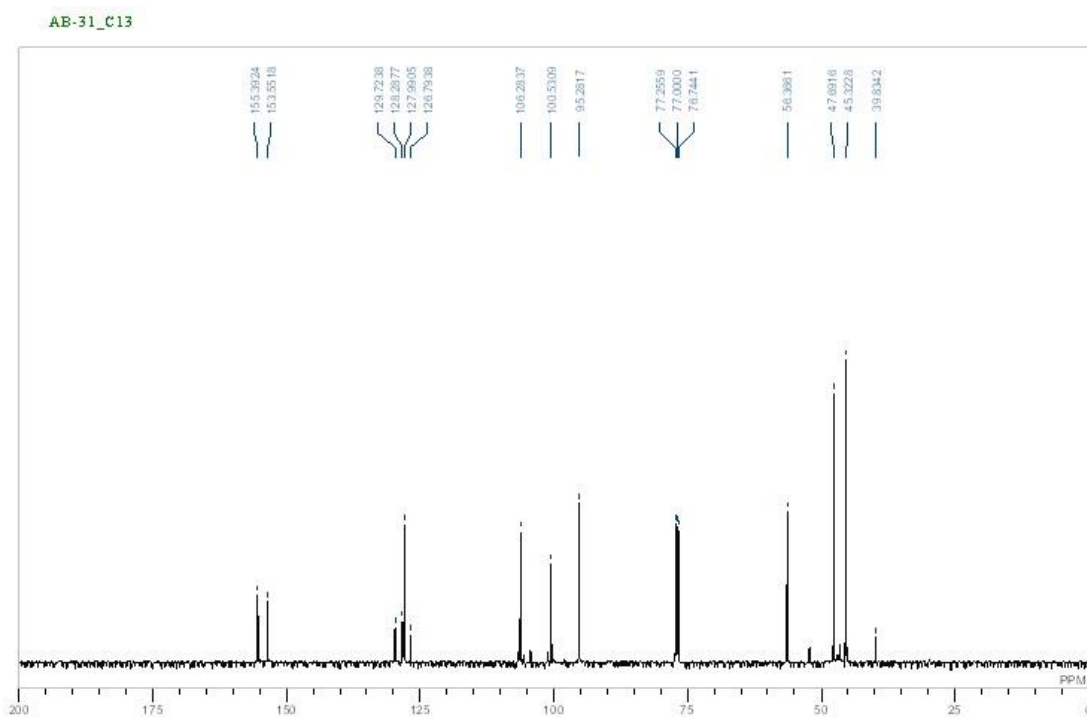
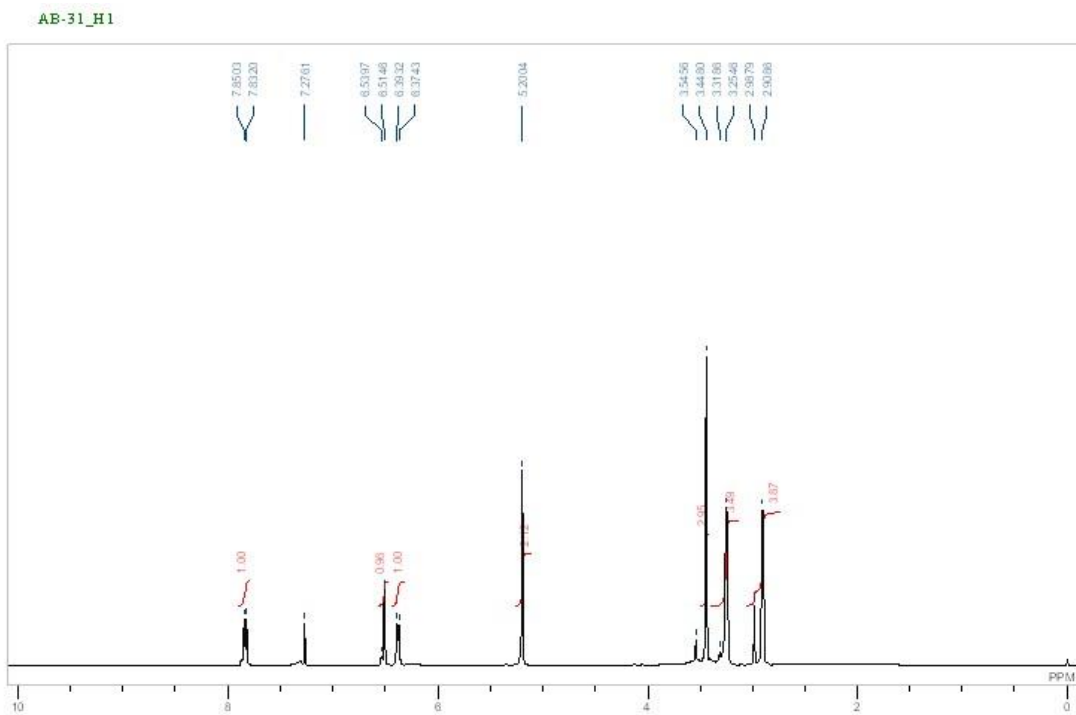
AB-27c_C13



Appendix D (4-(3-methoxy-4-nitrophenyl)piperazin-1-yl)(phenyl)methanone):

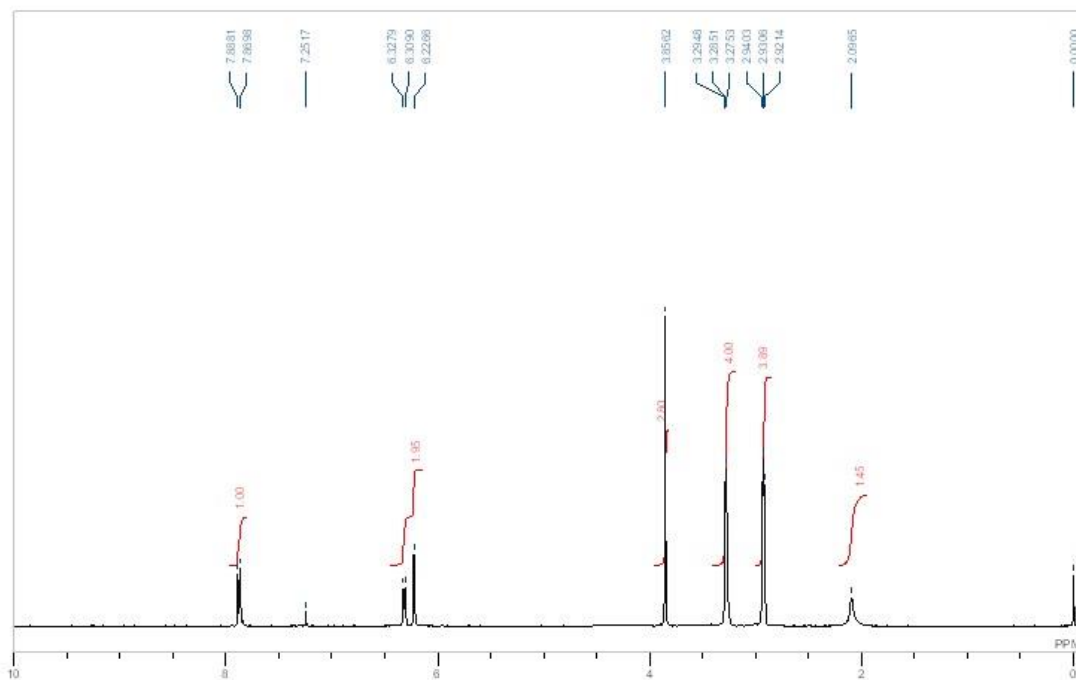


Appendix E (4-(3-(methoxymethoxy)-4-nitrophenyl)piperazin-1-yl)(phenyl)methanone):

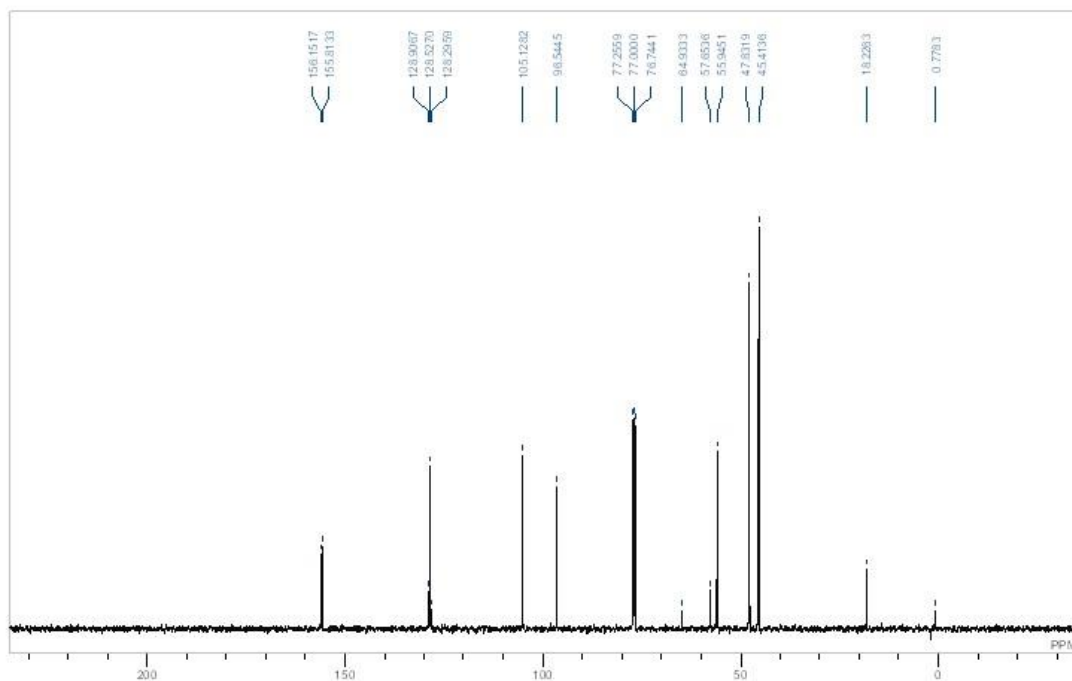


Appendix F (1-(3-methoxy-4-nitrophenyl)piperazine):

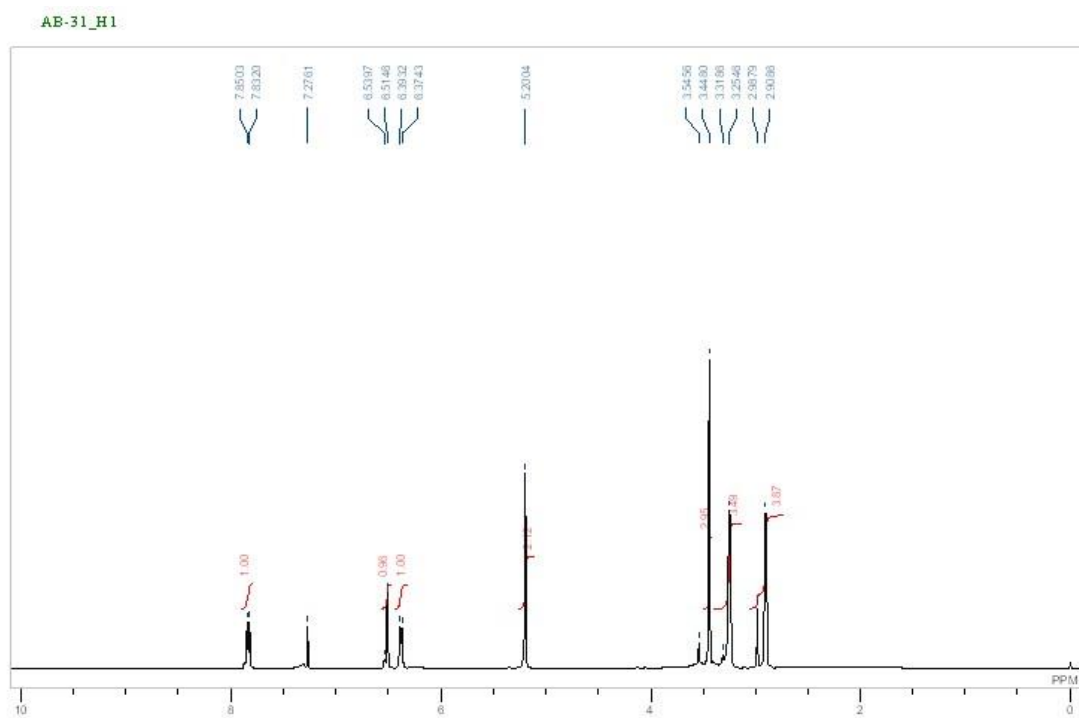
AB-29_H1



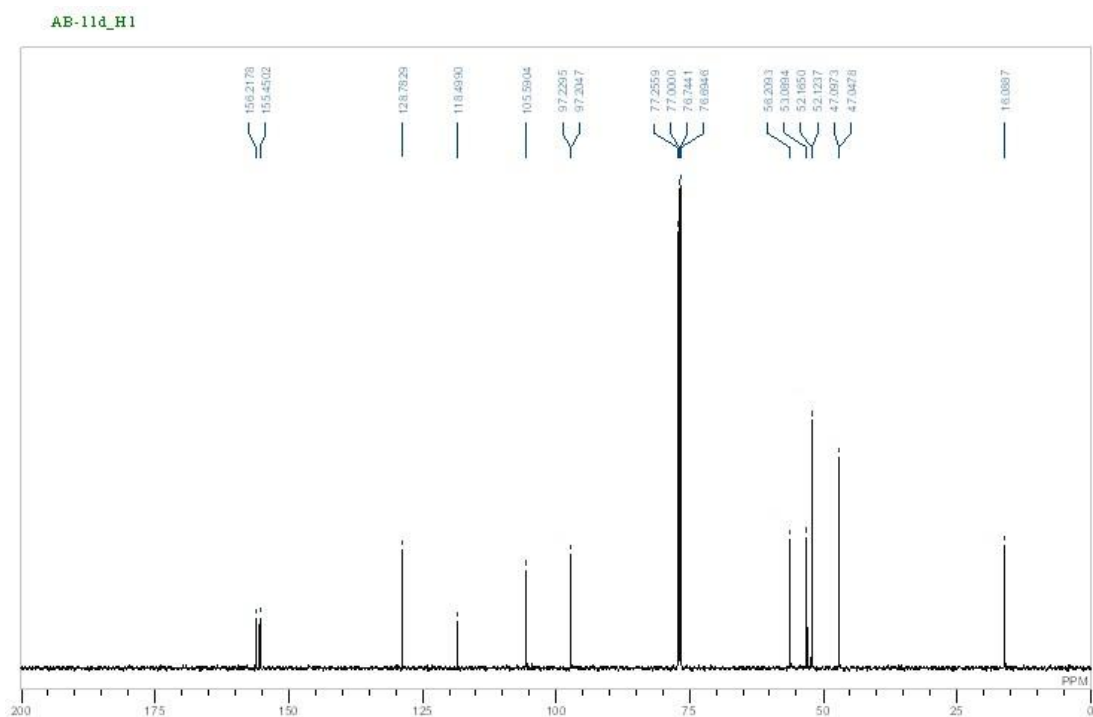
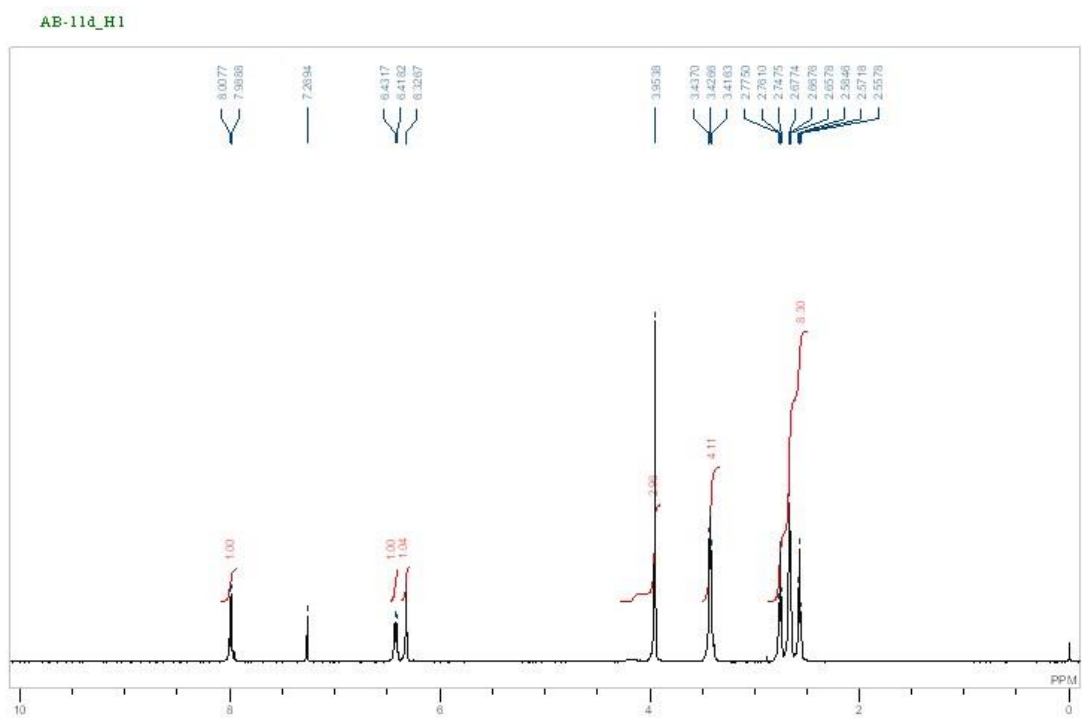
AB-29_C13



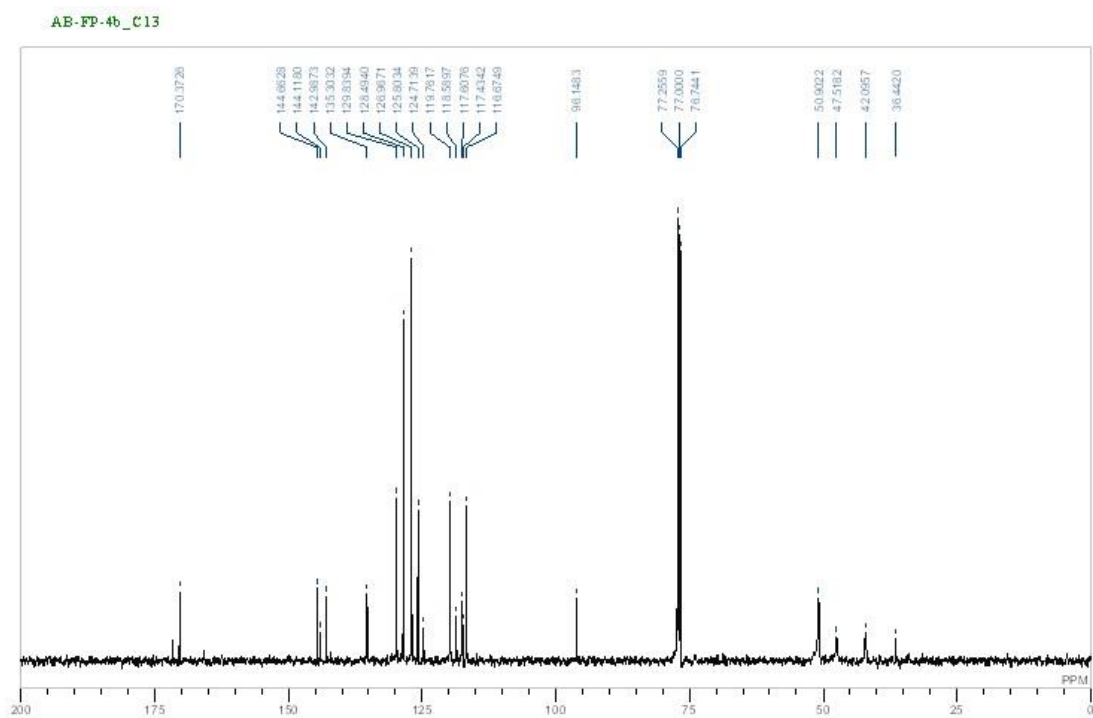
Appendix G (1-(3-(methoxymethoxy)-4-nitrophenyl)piperazine):



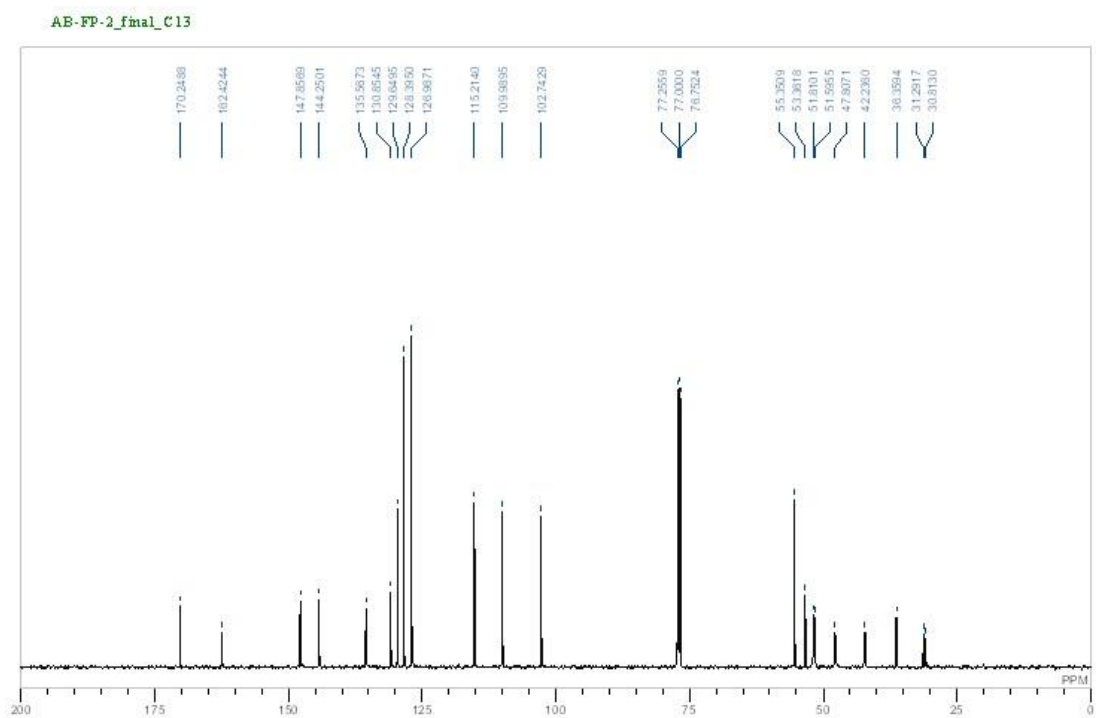
Appendix H (1-(3-(methoxymethoxy)-4-nitrophenyl)piperazine):



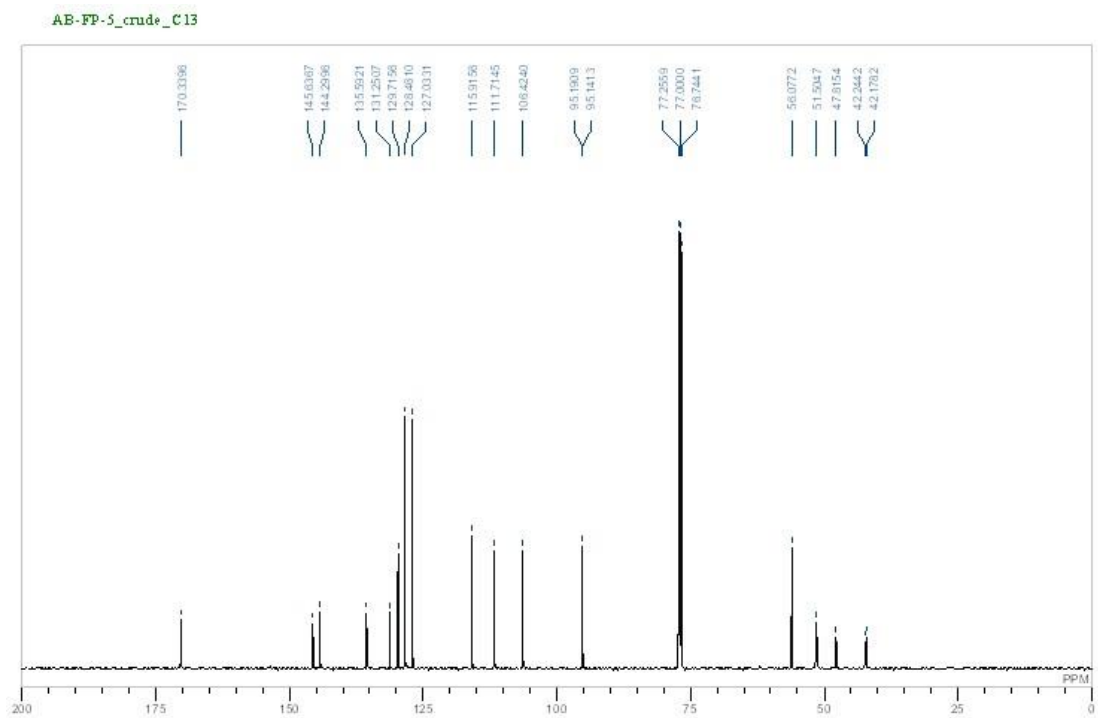
Appendix J (2-amino-4-(4-benzoylpiperazin-1-yl)benzotrile):



Appendix K ((4-(4-amino-3-methoxyphenyl)piperazin-1-yl)(phenyl)methanone):

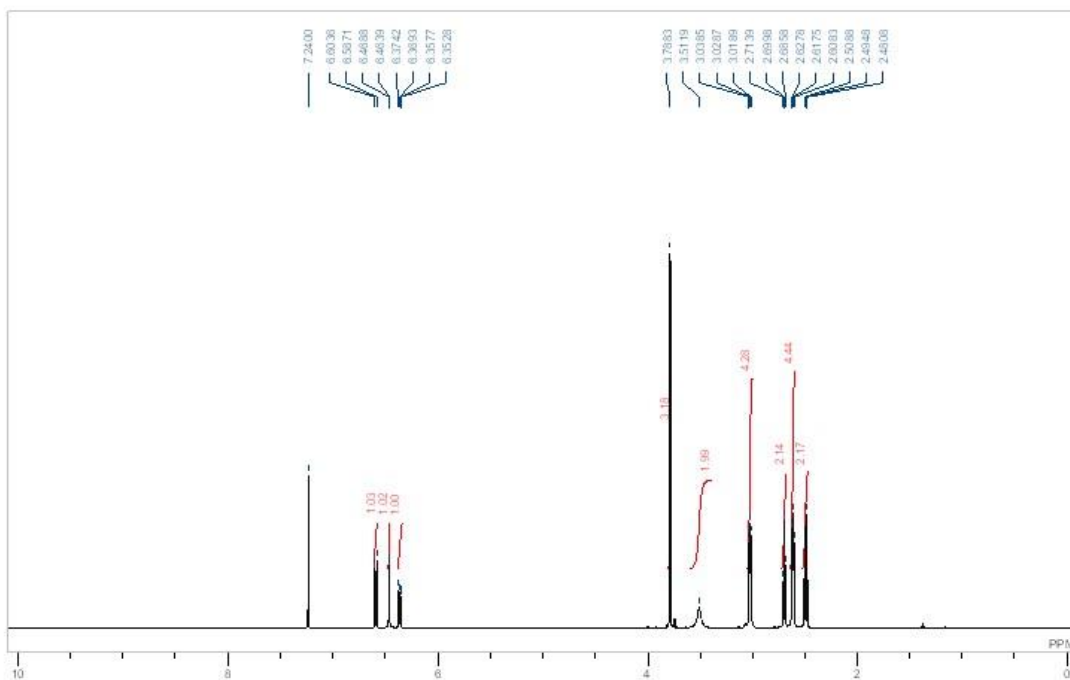


Appendix L ((4-(4-amino-3-(methoxymethoxy)phenyl)piperazin-1-yl)(phenyl)methanone):

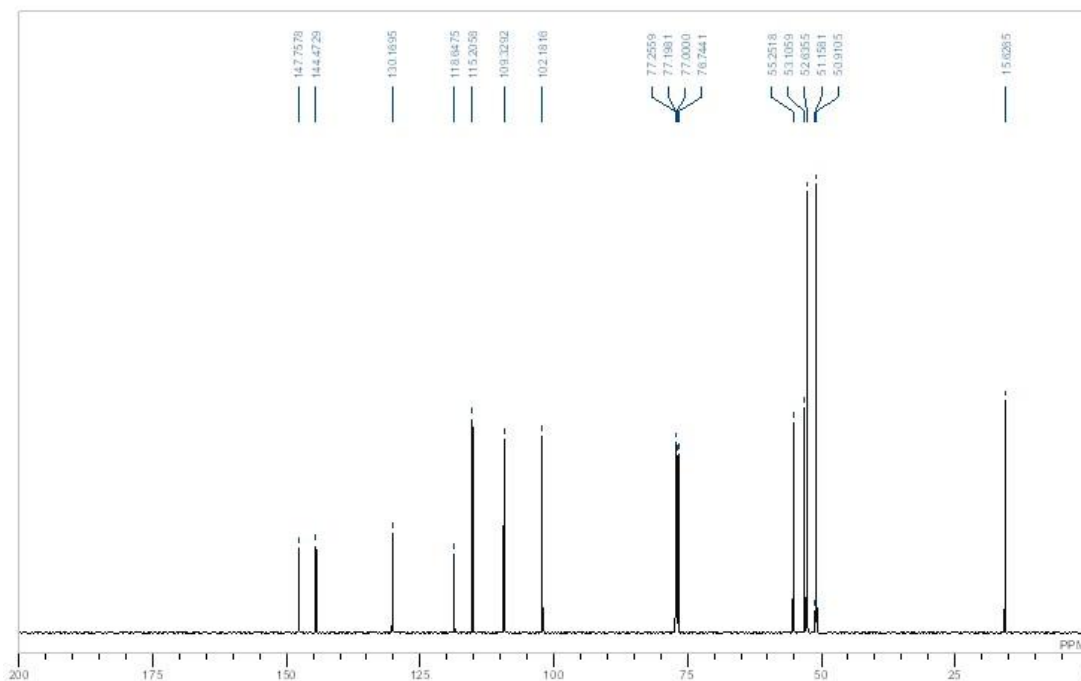


Appendix M (3-(4-(4-amino-3-methoxyphenyl)piperazin-1-yl)propanenitrile):

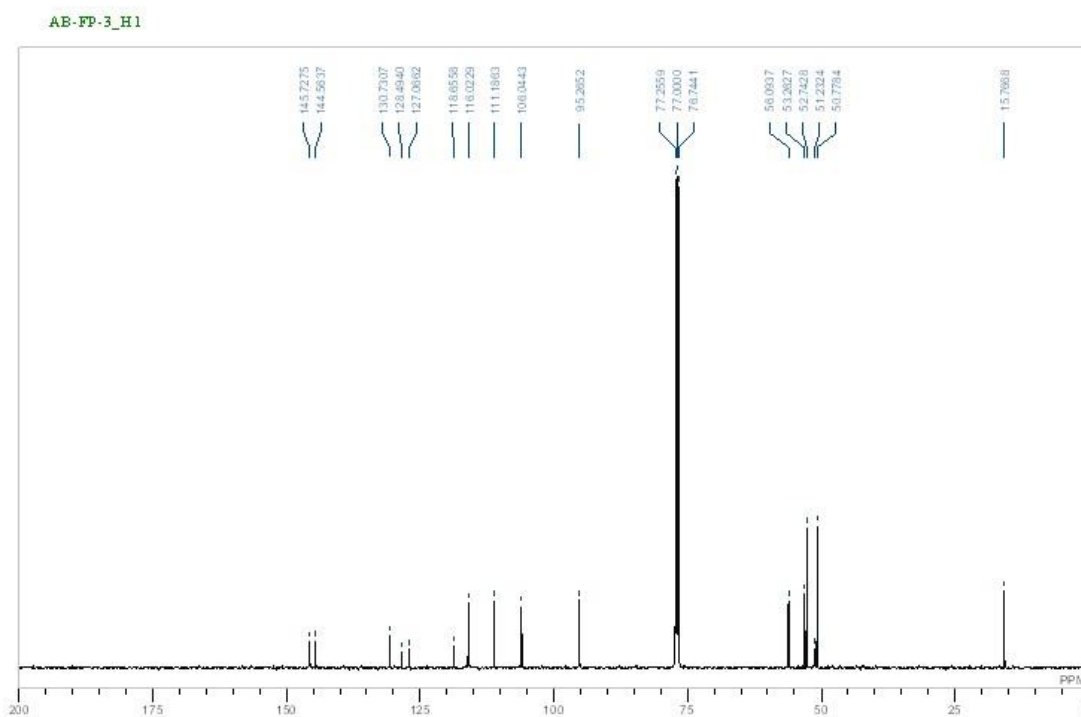
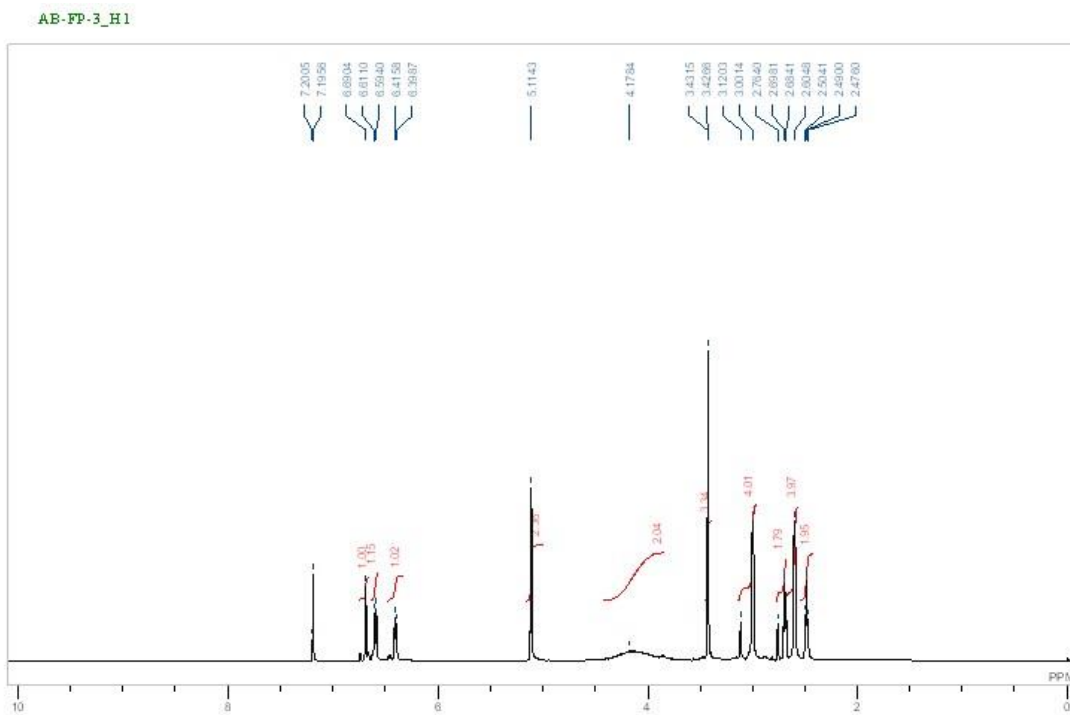
AB-FP-1_fm1_H1



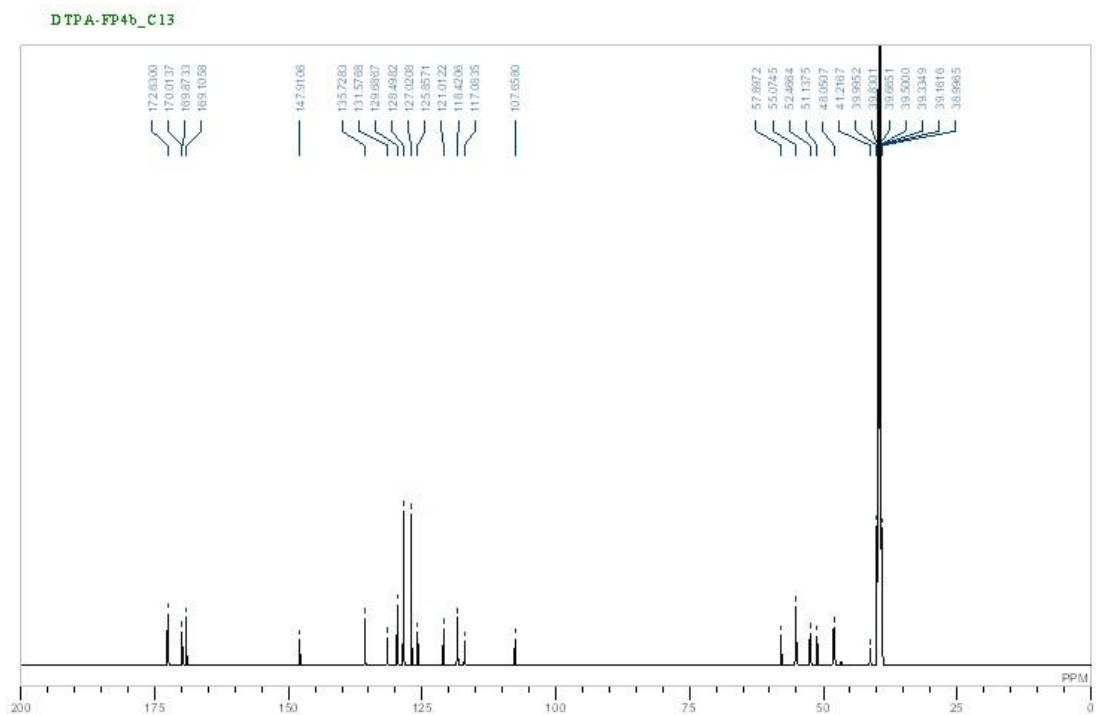
AB-FP-1_fm1_C13



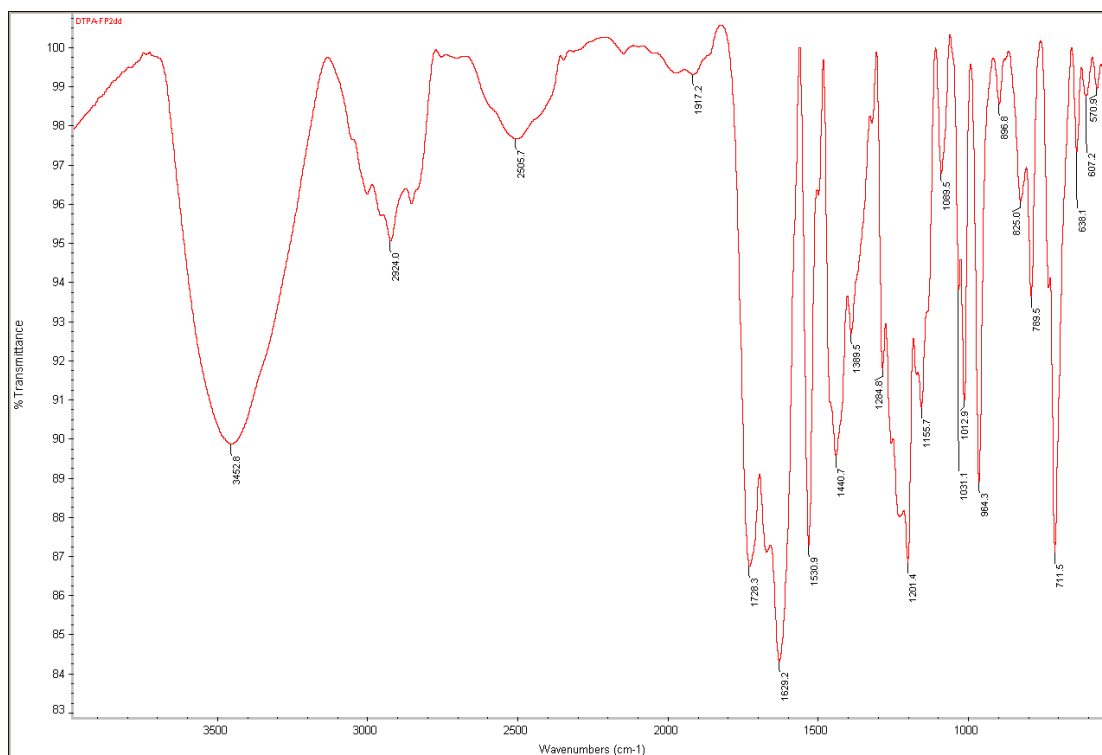
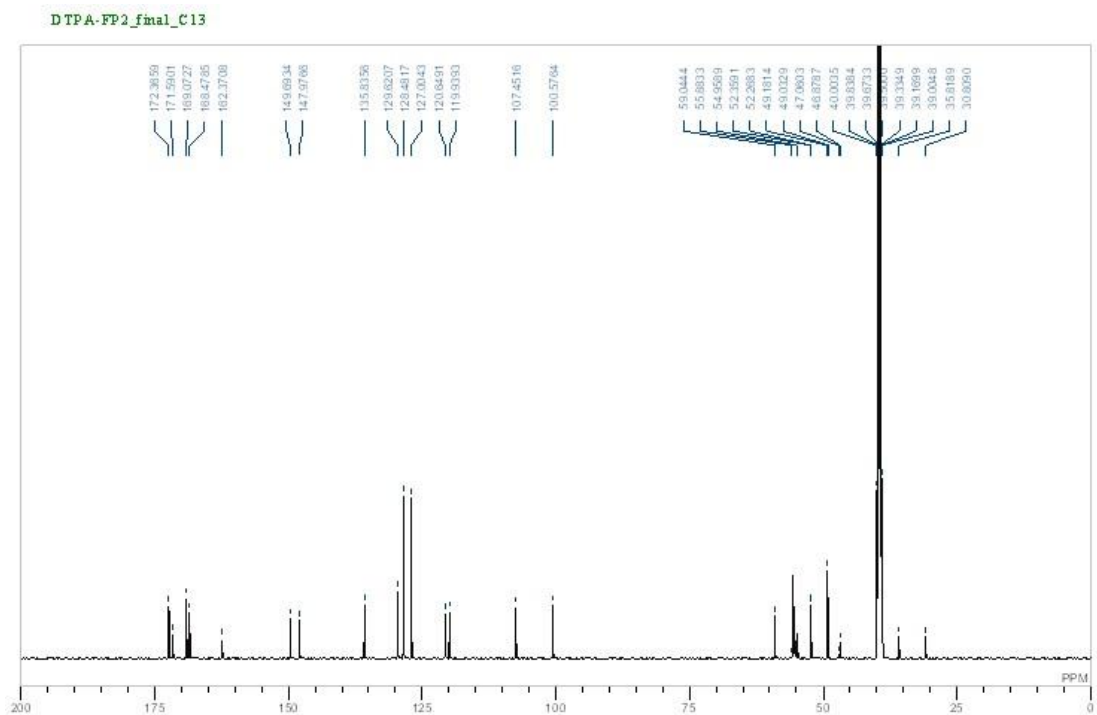
Appendix N (3-(4-(4-amino-3-(methoxymethoxy)phenyl)piperazin-1-yl)propanenitrile):



Appendix O (2,2'-((((carboxymethyl)azanediyl)bis(ethane-2,1-diyl))bis((2-((5-(4-benzoylpiperazin-1-yl)-2-cyanophenyl)amino)-2-oxoethyl)azanediyl))diacetic acid):



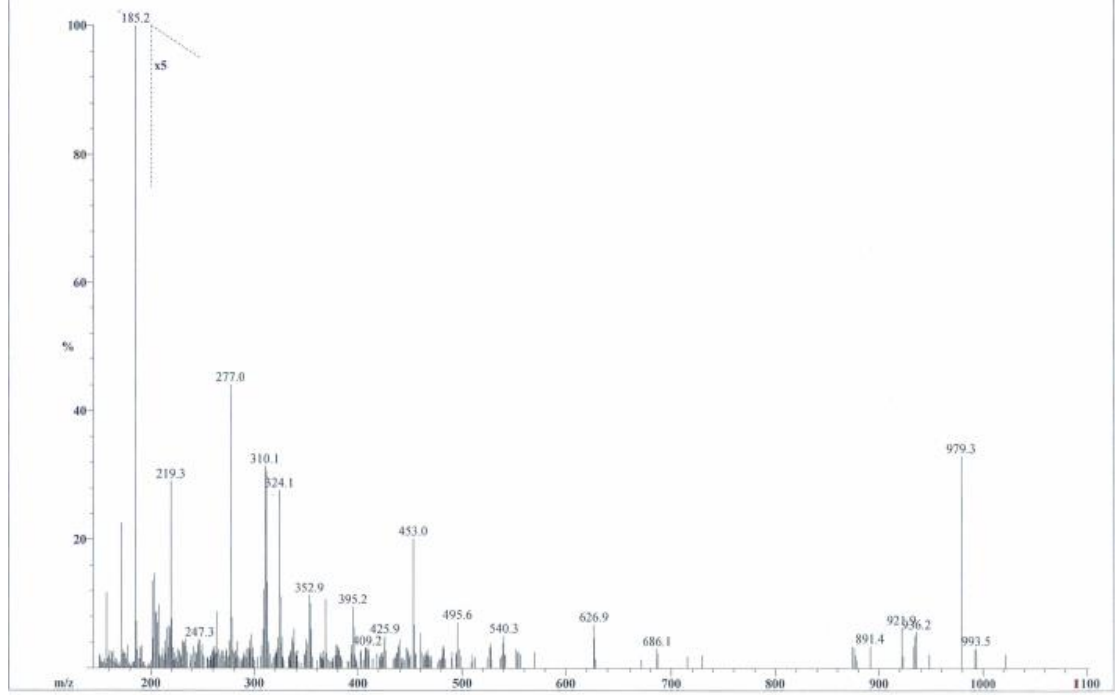
Appendix P (2,2'-((((carboxymethyl)azanediyl)bis(ethane-2,1-diyl))bis((2-((4-(4-benzoylpiperazin-1-yl)-2-methoxyphenyl)amino)-2-oxoethyl)azanediyl))diacetic acid):



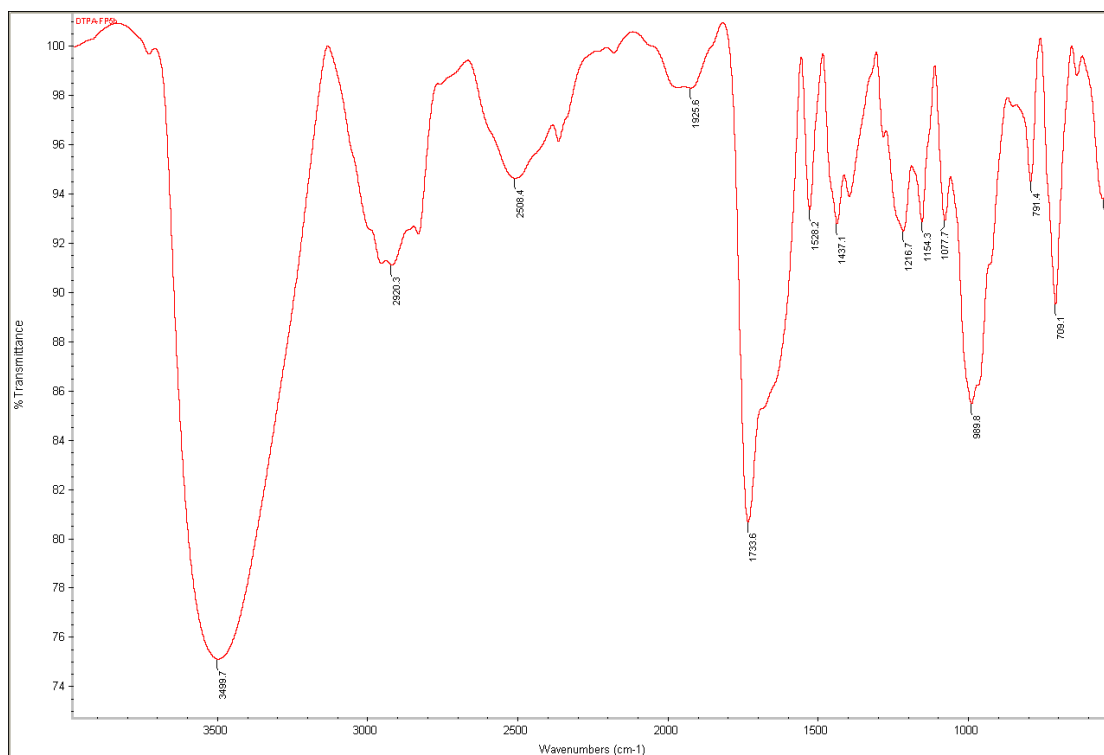
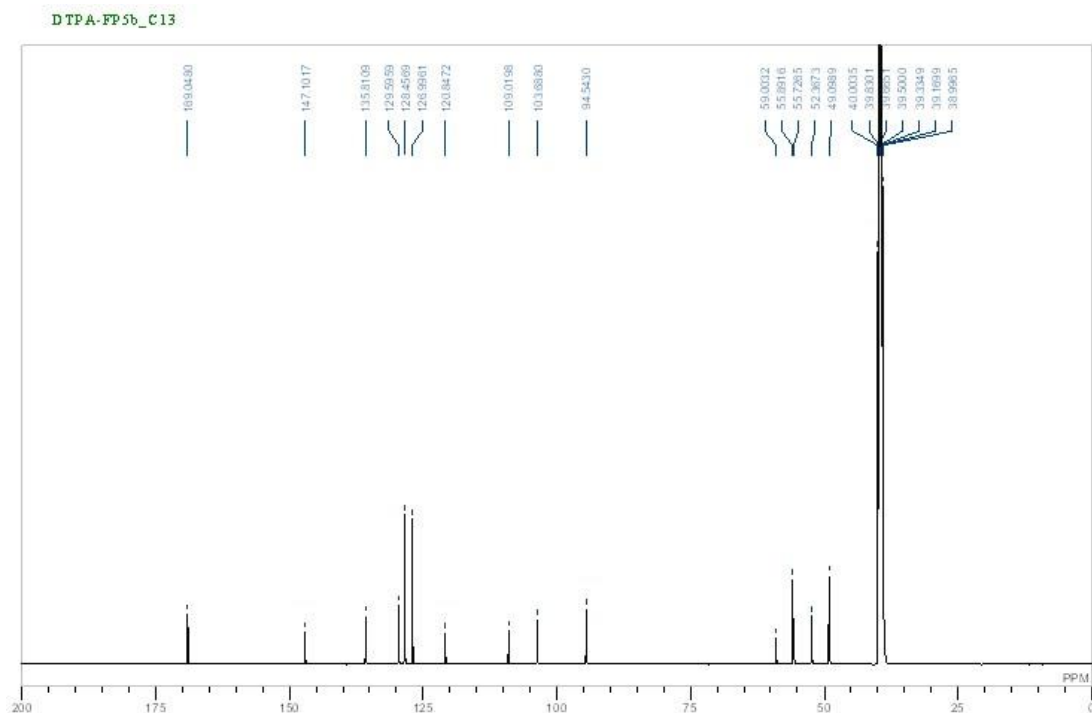
Scan: 20
Base: m/z 185; 10.9%FS TIC: 498936

R.T.: 1.75

#Ions: 376



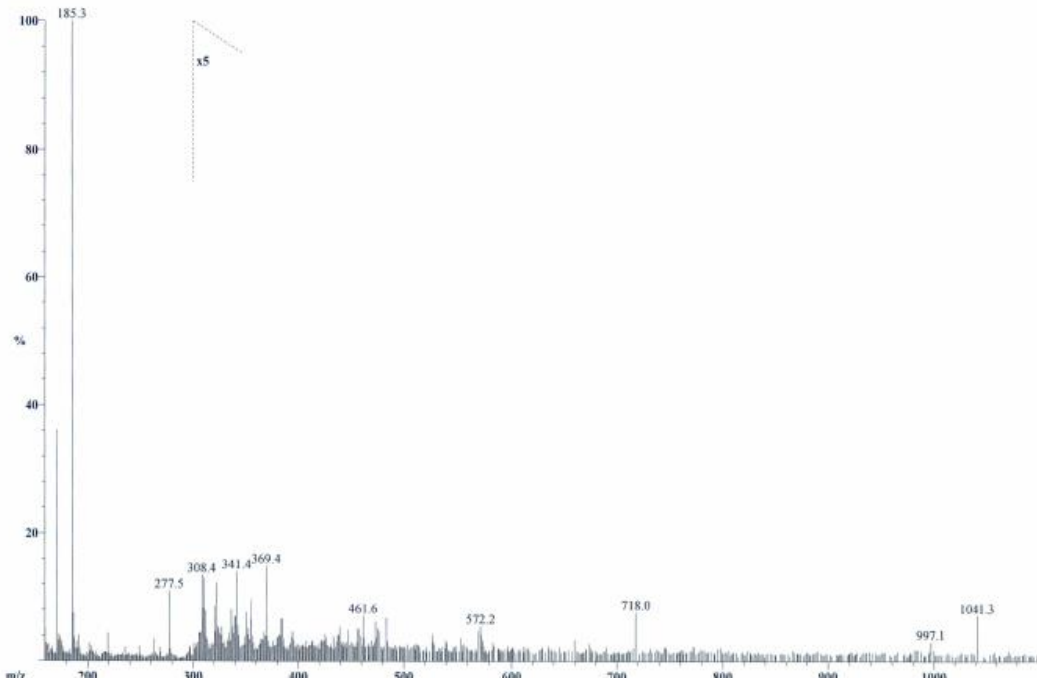
Appendix Q (2,2'-((((carboxymethyl)azanediyl)bis(ethane-2,1-diyl))bis((2-((4-(4-benzoylpiperazin-1-yl)-2-(methoxymethoxy)phenyl)amino)-2-oxoethyl)azanediyl))diacetic acid):



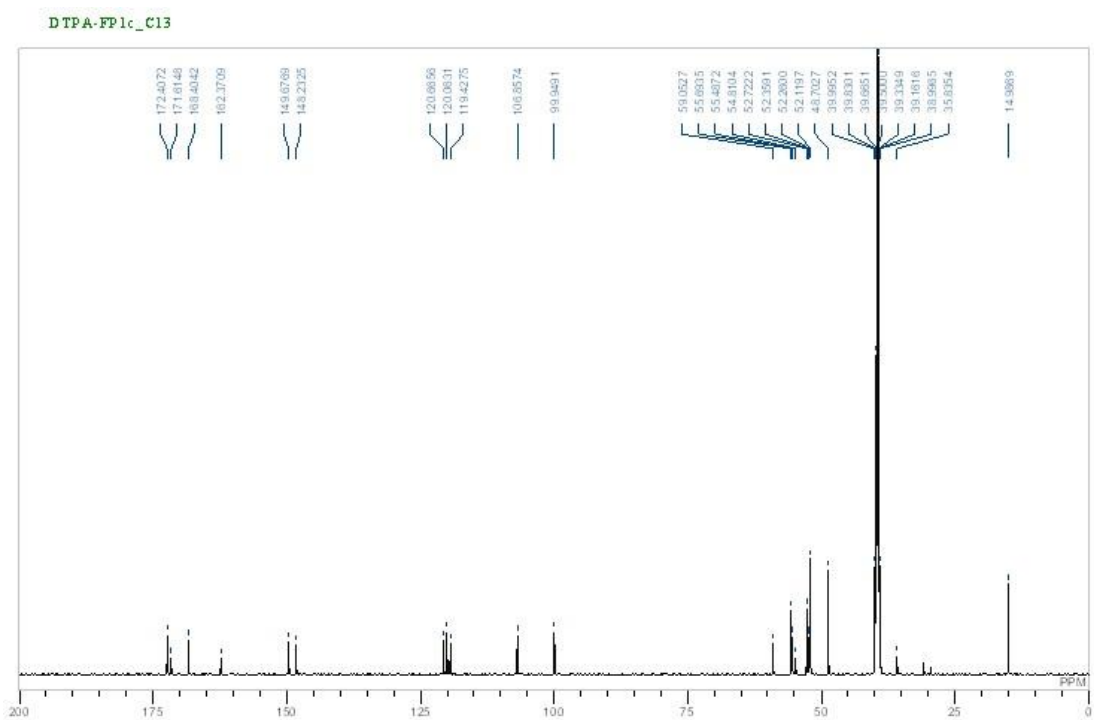
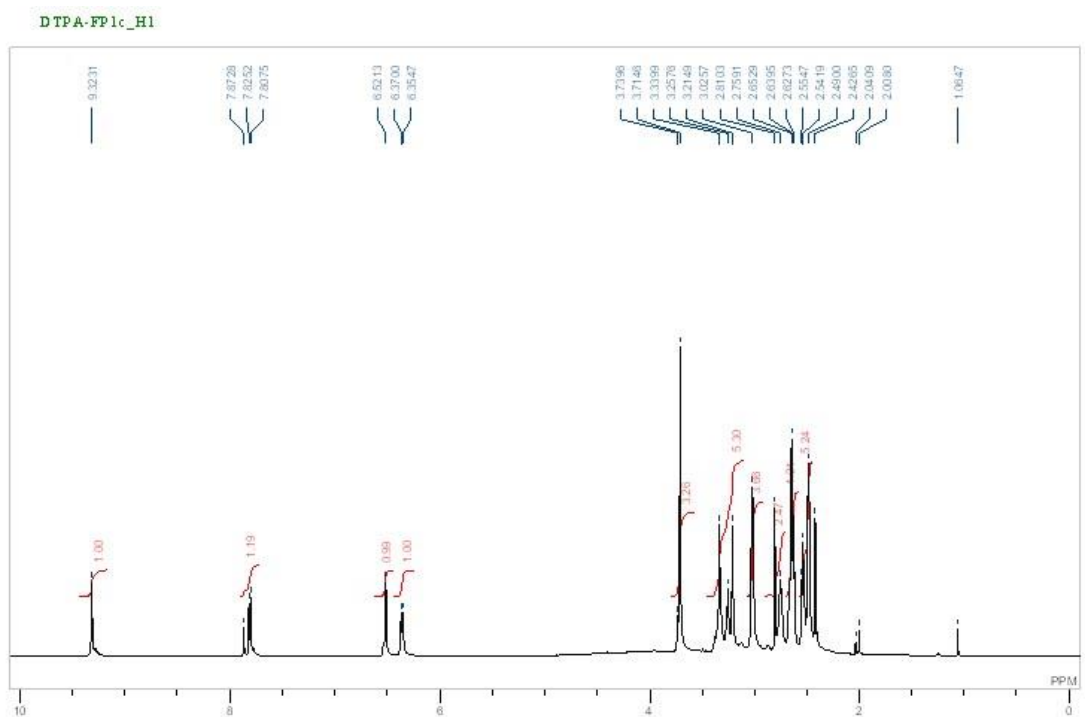
Scan: 9
Base: m/z 185; 35%FS TIC: 2449090

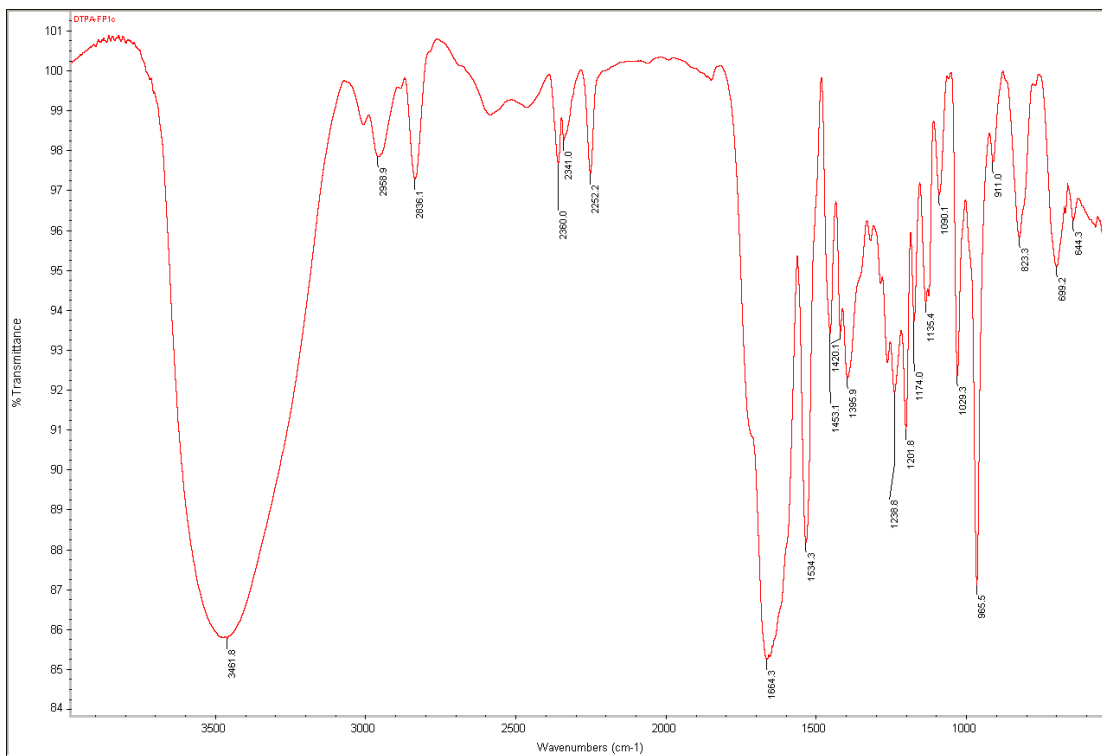
R.T.: .75

#Ions: 846

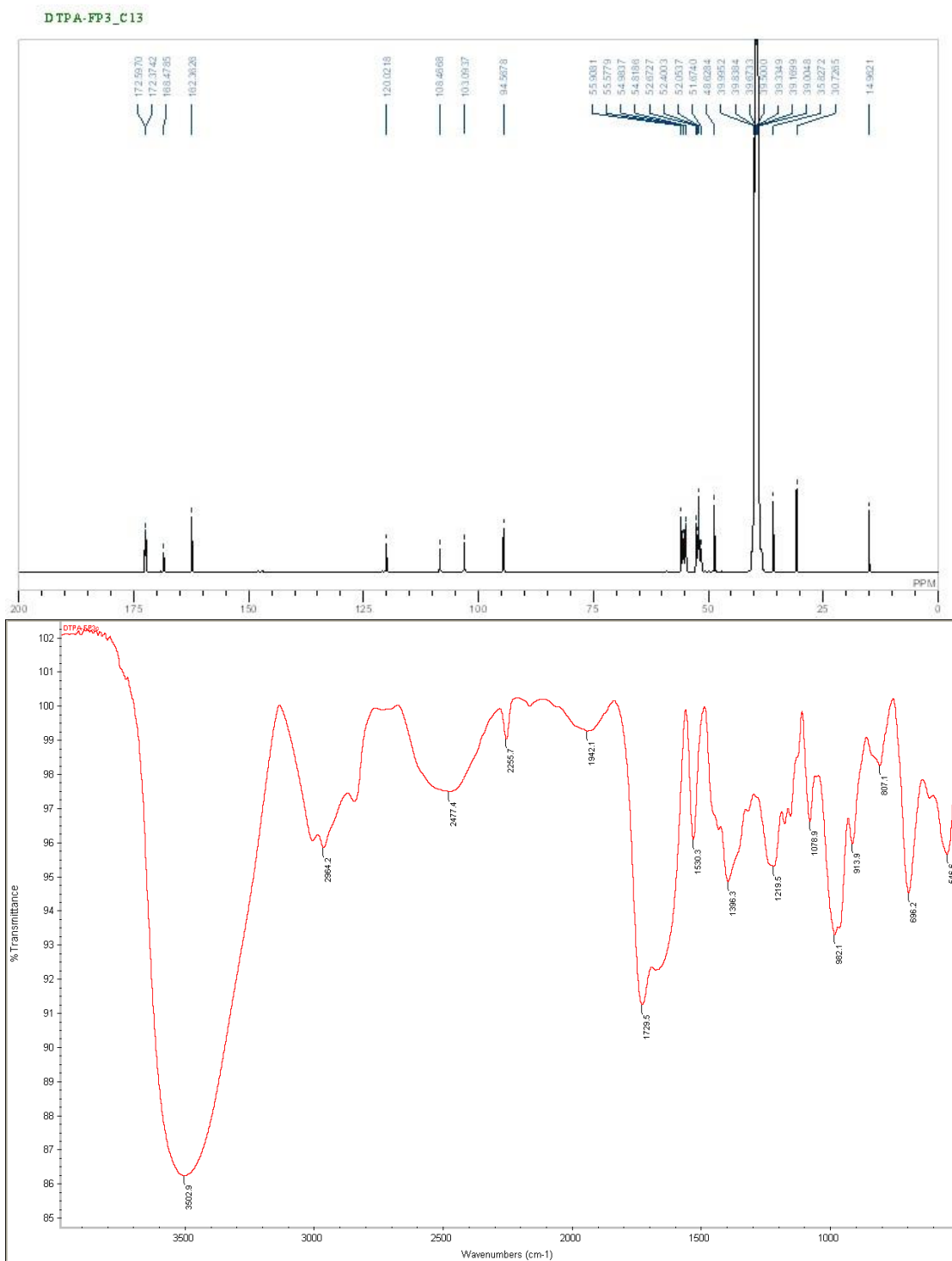


Appendix R (2,2'-((((carboxymethyl)azanediyl)bis(ethane-2,1-diyl))bis((2-((4-(4-(2-cyanoethyl)piperazin-1-yl)-2-methoxyphenyl)amino)-2-oxoethyl)azanediyl))diacetic acid):





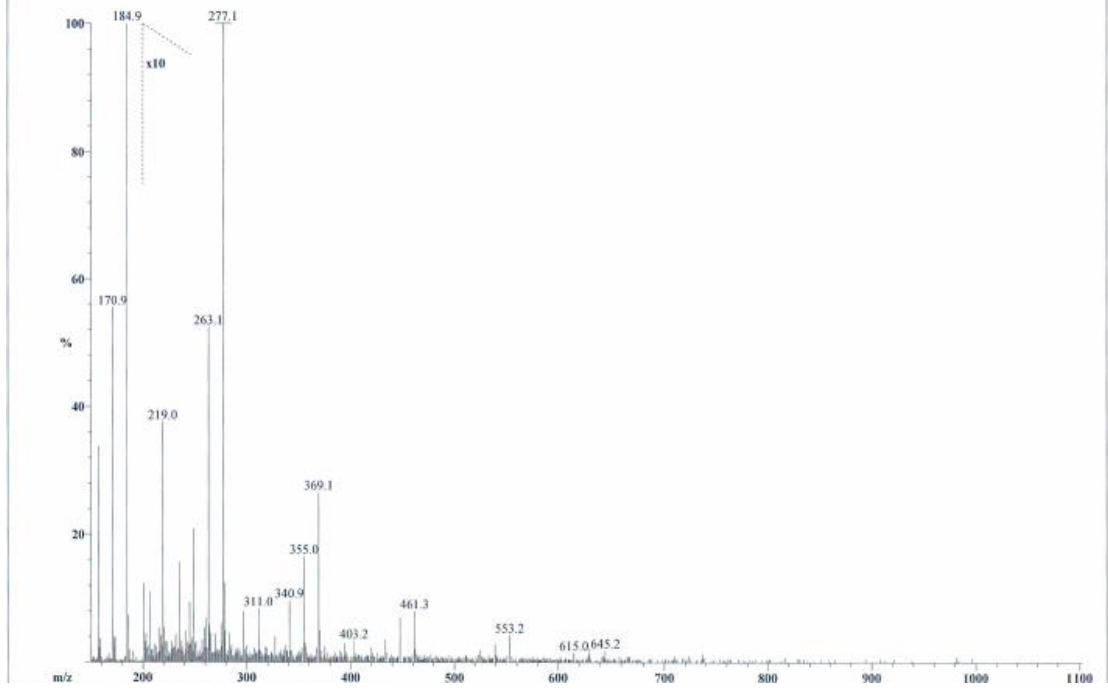
Appendix S (2,2'-((((carboxymethyl)azanediyl)bis(ethane-2,1-diyl))bis((2-((4-(4-benzoylpiperazin-1-yl)-2-(methoxymethoxy)phenyl)amino)-2-oxoethyl)azanediyl))diacetic acid):



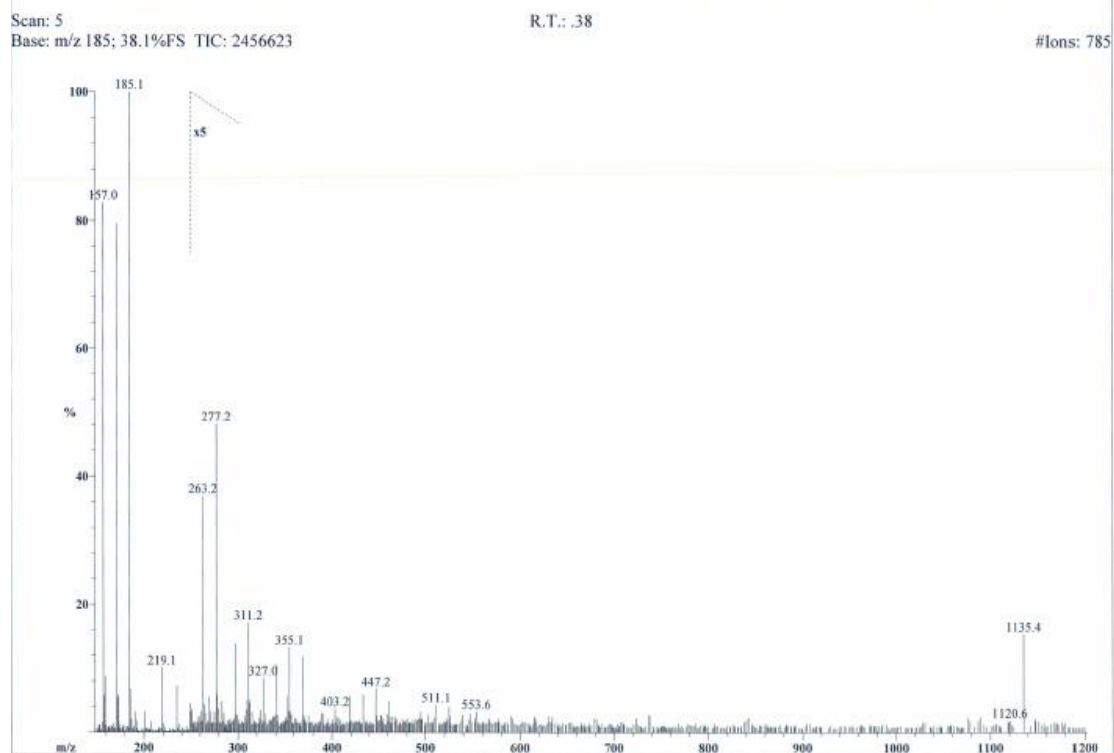
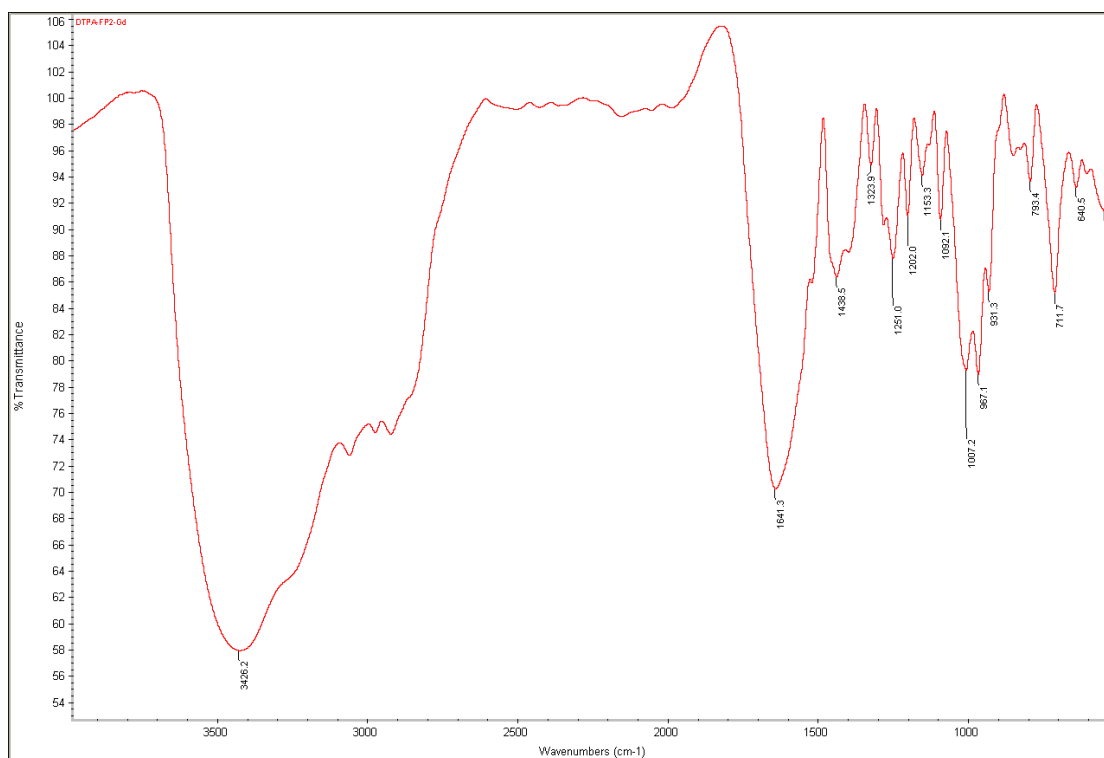
Scan: 6
Base: m/z 185; 87.5%FS TIC: 2995445

R.T.: .47

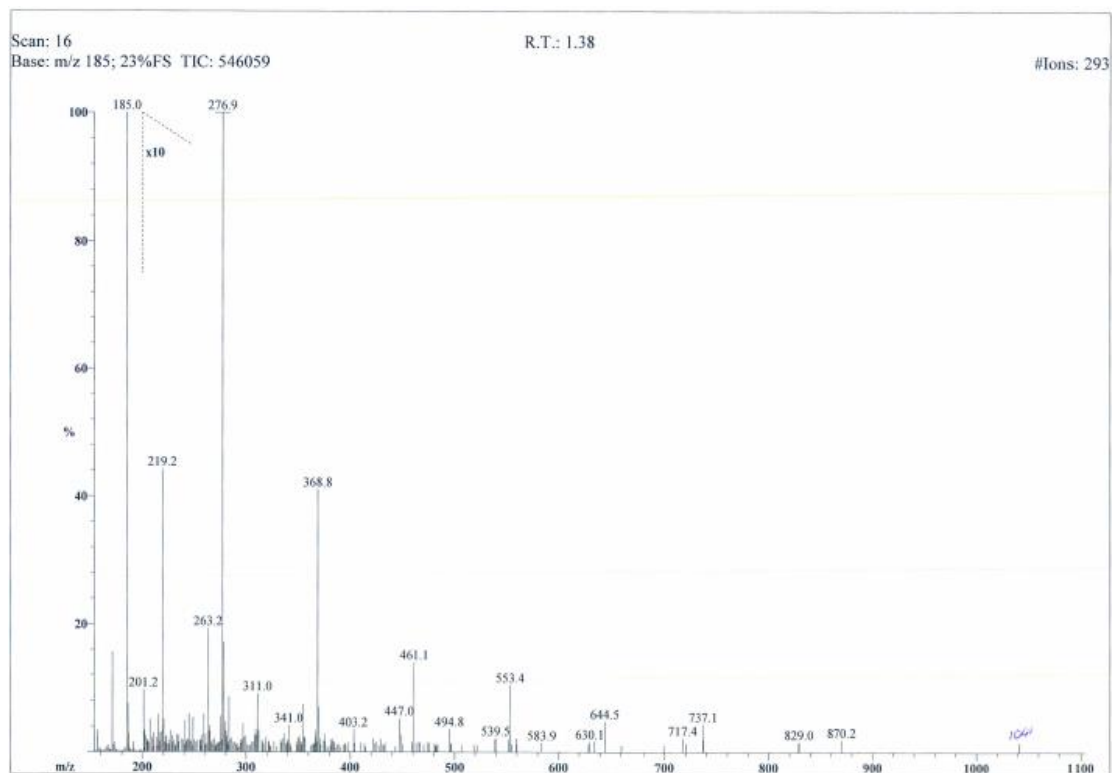
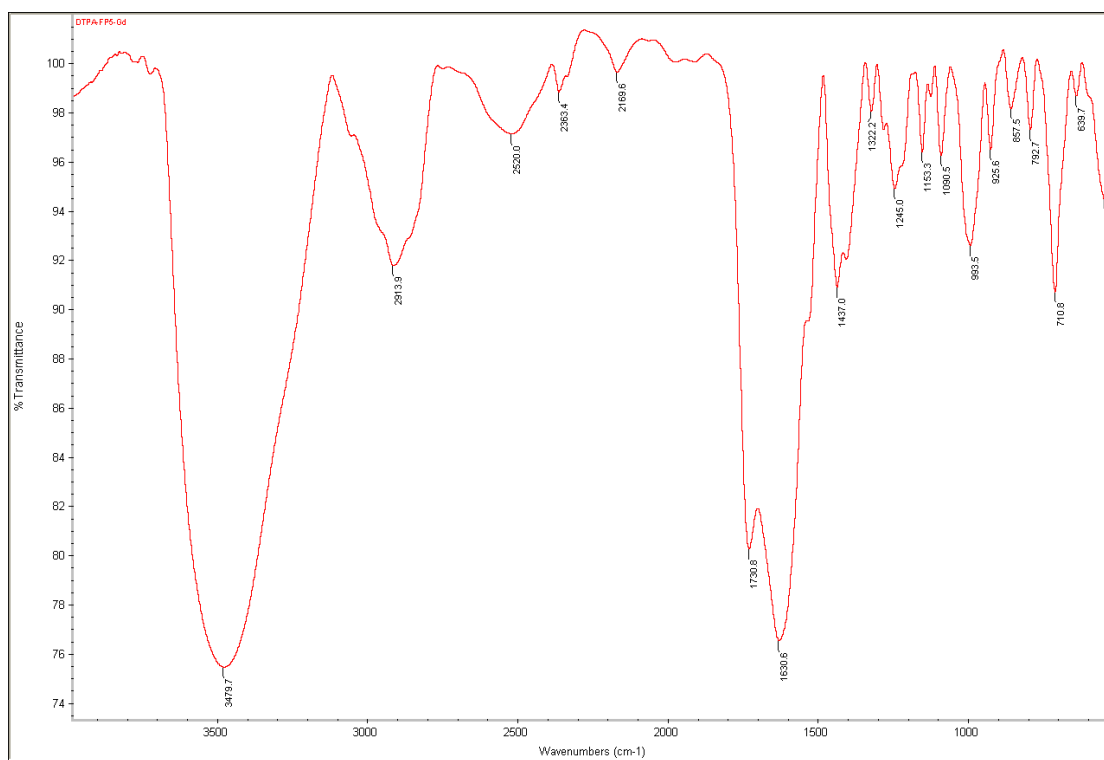
#Ions: 571



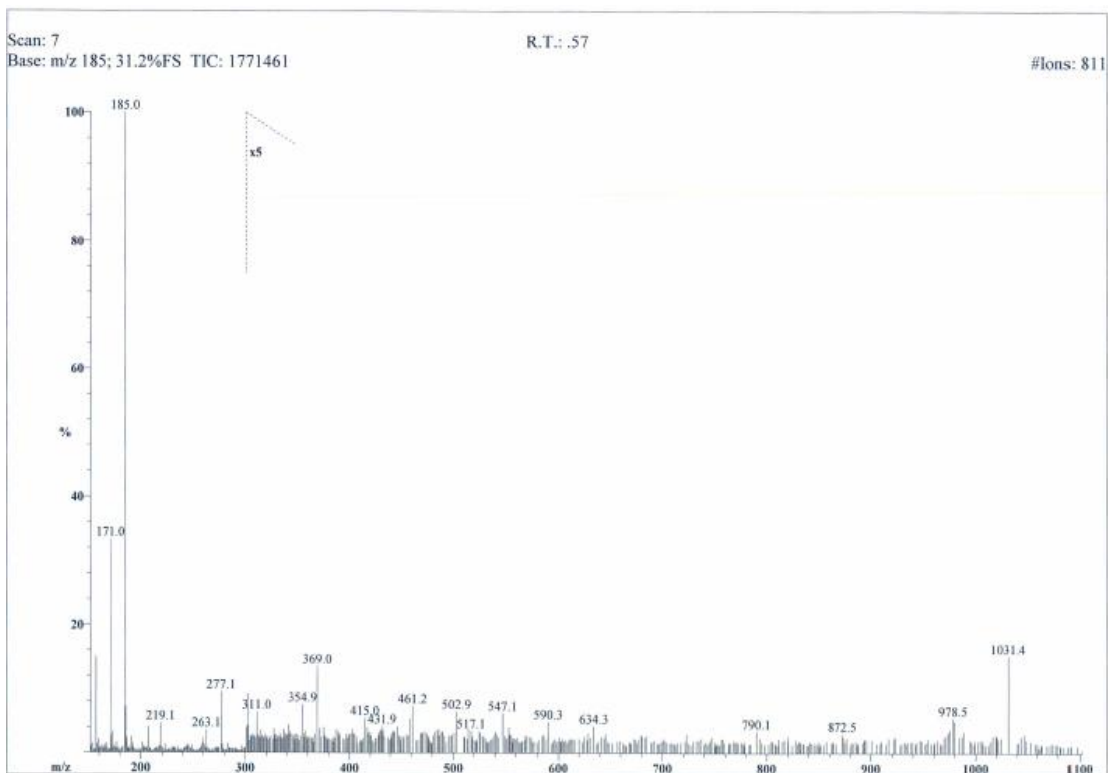
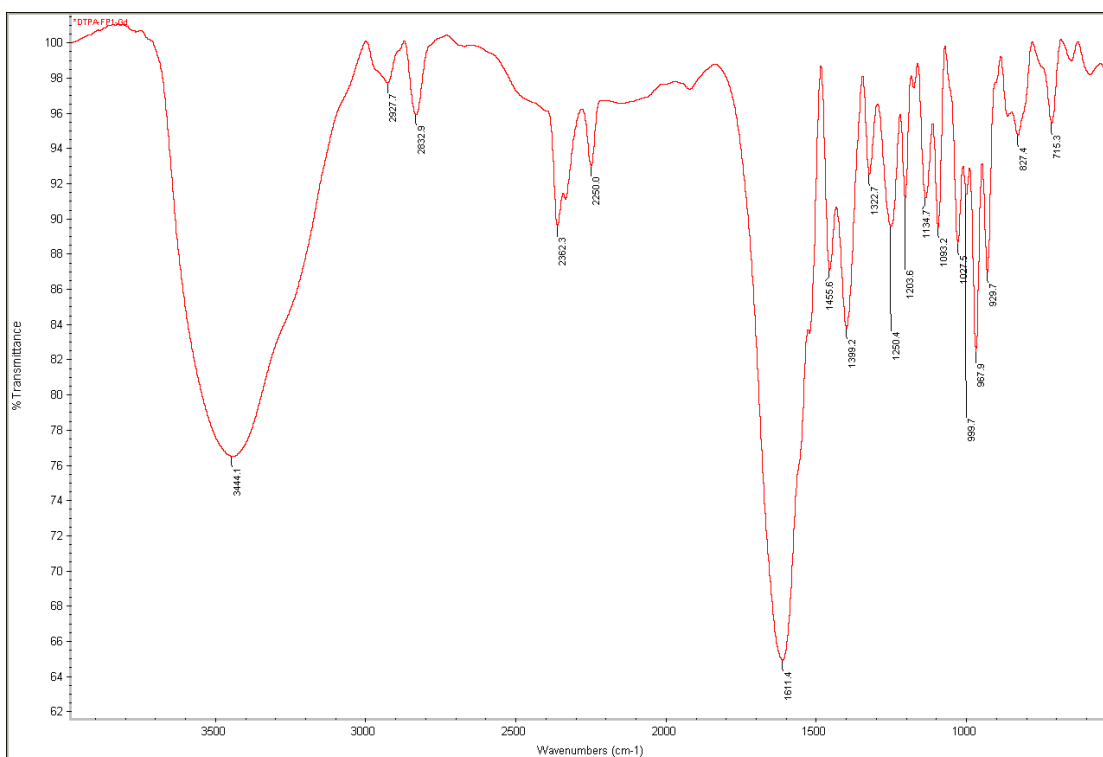
Appendix T (Chelate 2):



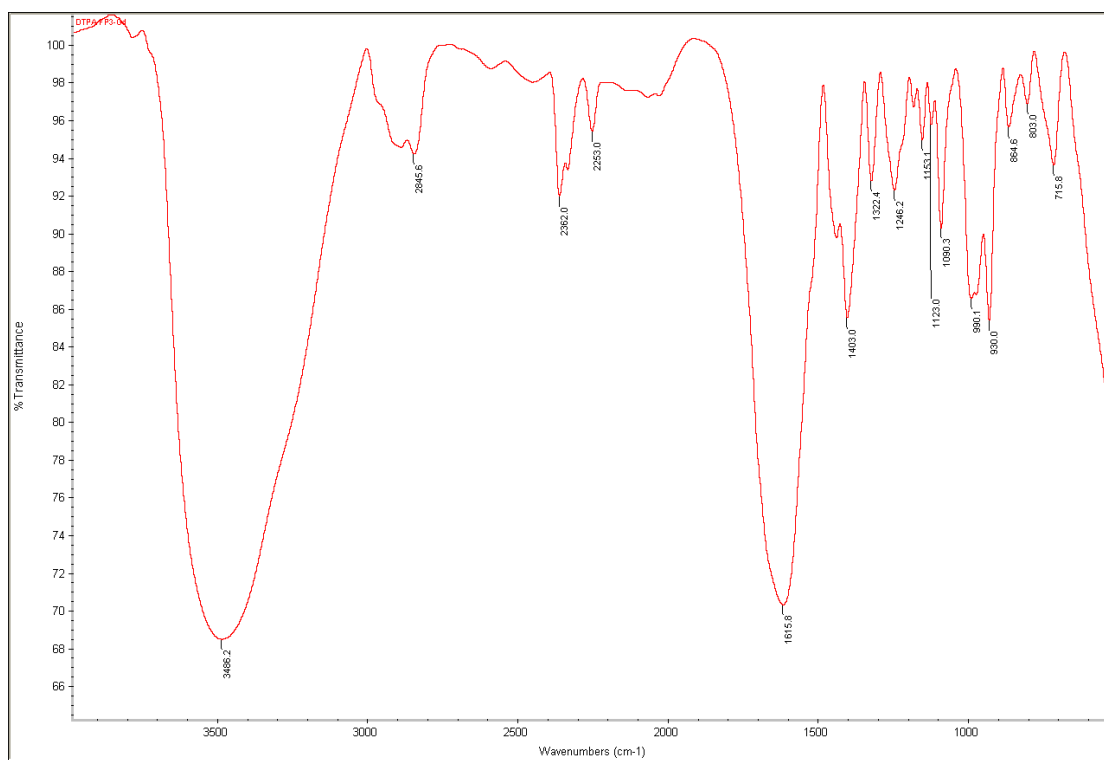
Appendix U (Chelate 3):



Appendix V (Chelate 4):



Appendix W (Chelate 5):



Vitae

Name	Abdullah Omer Obaid Ba-Salem
Nationality	Yemeni
Date of Birth	4-7-1987
E-mail	abdullahbasalem@gmail.com
Address	PO Box 20337, Alkhobar 31952
Academic Background	B.Sc. in industrial chemistry from KFUPM (2005-2010)